Investigation of Kinetic Hydrate Inhibitor Performance and the Mechanism of Inhibition

By Mr Gwyn Ardeshir Mali, for the qualification of Doctor of Philosophy, Heriot Watt University, Institute of Petroleum Engineering, January 2018.

Abstract

A number of light hydrocarbons are known to form hydrates with water at a combination of low temperature and high pressure. Under these conditions, it is not uncommon for hydrates to form and plug oil and gas pipelines and other equipment, resulting in shutdown, potential risk of explosion, and accidental release of hydrocarbons into the environment. Conventional chemical inhibitors such as methanol and ethylene glycol are the most frequently used tool in hydrate prevention strategies, however, they can result in significant capital and operational costs as well as health, safety and environmental concerns. An alternative to conventional inhibitors are Low Dosage Hydrate Inhibitors (LDHI), of which Kinetic Hydrate Inhibitors (KHIs) are the more frequently used. KHIs are water soluble polymers, which prevent or delay hydrates nucleation and/or growth. Over the last two decades, much has been learnt about the mechanism of KHI; however, gaps still remain in the knowledge surrounding the mechanism of inhibition. The research described in this thesis seeks to increase the understanding of KHI performance and was carried out from 2003 to 2008 and was a part of the Joint Industrial Project (JIP) titled "Micro and Macro-Scale Evaluation of Low Dosage Hydrate Inhibitors" conducted by the Centre for Gas Hydrate Research at Heriot Watt University.

The research involved a series of laboratory tests using stirred autoclave reactors that qualitatively demonstrated that the presence of ethanol, methanol and alkanes have a negative impact on the performance of KHI, while salts and synergist 2-Butoxyethanol have a positive impact. The effect of methanol was supplemented with molecular dynamic simulation that demonstrated that the methanol preferentially adheres to the polymer structures.

A multi test tube rocking cell was used to generate large volumes of data to investigate the stochastic behaviour of hydrate formation with and without KHI. The results showed that the commencement of hydrate growth is logarithmically related to subcooling, and higher pressures resulted in higher induction at comparative subcooling and driving force.

The information gathered improves the understanding of factors that impact the performance of KHI, improves the understanding in the designing of appropriate testing of KHI, and enhances knowledge of kinetics of hydrate nucleation and growth.

Dedicated to my father
for his heartfelt encouragement and endless support
You are missed!

Acknowledgements

I would like to express my sincere gratitude and appreciation to Professor Bahman Tohidi and Dr. Robin Westacott for their excellent supervision, invaluable guidance, patience, and continuous support and encouragement during the last few years. I also owe many thanks to Dr. Mossayeb (Jahan) Arjmandi, Dr. Antonin Chapoy, Dr. Jeerachada (Pui) Tanchawanich, Dr. Joanna Lachwa, Miss Annabelle Molliet and Mr Rod Burgass for their guidance and assistance in the work.

I feel that I am privileged to be have spent this time at the Centre for Gas Hydrate Research and the Institute of Petroleum Engineering, and have made lifelong friends with many of the members of the group.

I would also like to thank the financial support from the Engineering and Physical Sciences and Research Council (EPSRC) and the Centre for Gas Hydrates Research.

Last but not least, I would like to thank the support of my parents, my friends, and other members of my family; without their love and support, this degree would have been impossible to finish.

ACADEMIC REGISTRY
Research Thesis Submission

Name*:*	Gwyn Ardeshir Mali		
School:	School of Energy, Geoscience, Infrastructure and Society		
Version: *(i.e. First, Resubmission, Final)*	Final	Degree Sought (Award **and** Subject area)	PhD, Petroleum Engineering

Declaration

In accordance with the appropriate regulations I hereby submit my thesis and I declare that:

1) the thesis embodies the results of my own work and has been composed by myself
2) where appropriate, I have made acknowledgement of the work of others and have made reference to work carried out in collaboration with other persons
3) the thesis is the correct version of the thesis for submission and is the same version as any electronic versions submitted*.
4) my thesis for the award referred to, deposited in the Heriot-Watt University Library, should be made available for loan or photocopying and be available via the Institutional Repository, subject to such conditions as the Librarian may require
5) I understand that as a student of the University I am required to abide by the Regulations of the University and to conform to its discipline.

* *Please note that it is the responsibility of the candidate to ensure that the correct version of the thesis is submitted.*

Signature of Candidate*:*		Date:	

Submission

Submitted By *(name in capitals):*	
Signature of Individual Submitting:	
Date Submitted:	

For Completion in the Student Service Centre (SSC)

Received in the SSC by *(name in capitals):*			
Method of Submission *(Handed in to SSC; posted through internal/external mail):*			
E-thesis Submitted (mandatory for final theses)			
Signature:		Date:	

Contents Table

Chapter 1: Introduction to Gas Hydrates and Kinetic Hydrate Inhibitors

1.1 Gas Hydrates and Their Structures

Gas hydrates or clathrate hydrates are crystalline solids composed of polyhedra of hydrogen bonded water molecules, which act as a cage that contains a guest molecule. These guest molecules stabilise the hydrate structure by Van der Waals forces between themselves and the water cage, which makes these structures more stable than ice under elevated pressure conditions.

Different hydrate structures exist depending on the guest species present, and the pressure and temperature conditions. There are three classes of natural gas hydrate structures that are of interest, which are called structure I (sI), structure II (sII), and structure H (sH). The different hydrate structures are shown in Figure 1.1.

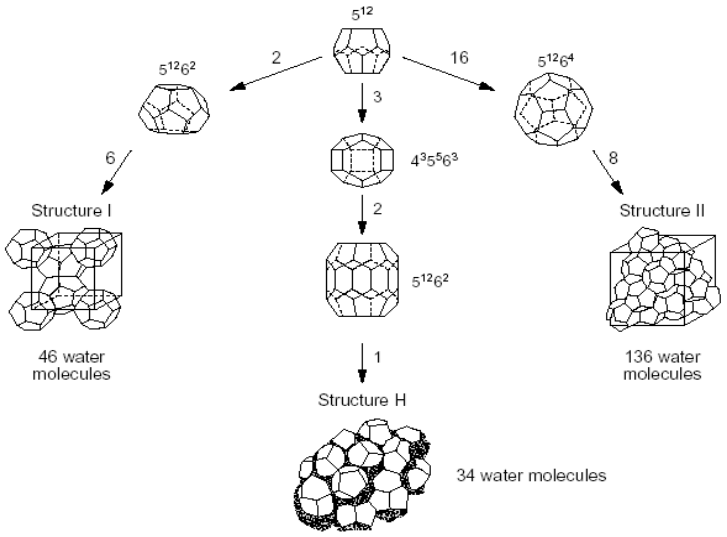

Figure 1.1 Various hydrate structures (Sloan 1998)

The sI hydrate consists of two different cage structures, i.e. large cages with 12 pentagonal and 2 hexagonal faces ($5^{12}6^2$) and small cages with 12 pentagonal faces (5^{12}). The repeating crystal cell has 2 small and 6 large cages, and consists of 46 water molecules and fits into 12Å cube. The sII hydrate also consists of two different cage

structures, i.e. large cages with 12 pentagonal and 4 hexagonal faces ($5^{12}6^4$) and smaller cages with 12 pentagonal faces (5^{12}). The repeating crystal cell has 16 small and 8 large cages, it consists of 136 water molecules, and fits into a 17.3 Å cube.

sH are not deemed to be important to the petroleum industry and are considered to be a scientific curiosity as they form in the presence of cyclic alkane groups such as methylcyclohexane and methylcyclopentane and alkane such as isopentane, which are only found in laboratories in sufficient quantities to form this structure. The sH structure consists of three different cage structures, i.e. small cages with 12 pentagonal faces (5^{12}), large cages with 3 square, 6 pentagonal and 3 hexagonal faces ($4^3 5^6 6^3$), and an extra large cage with 12 pentagonal and 8 hexagonal faces ($5^{12}6^8$). The repeating cell has 3 small, 2 large and 1 extra large cages in the repeating structure, and consists of 34 water molecules.

The suitability of a molecule to be a guest depends on its size in comparison to the cage structure, and, although more than one molecule can fit inside the hydrate cage structure, this is rare. sI hydrates' large cages ($5^{12}6^2$) are large enough to hold molecules up to 6.0 Å, which include the natural gas components, ethane and carbon dioxide. sII hydrates' large cages ($5^{12}6^4$) are large enough to hold molecules up to 7.1 Å, which include the natural gas components, propane, iso- and normal -butane. For sII hydrate, a guest molecule is required to fill the large cage to stabilise the hydrate structure whereas the small cage may be filled or be empty. Certain sII hydrate forming molecules such as n-butane require small help gases in the small cages to stabilise the hydrate structure, as they cannot form hydrates on their own (due to their large molecular sizes).

In the context of the oil and gas industry, sII is considered to be the most relevant hydrate structure, as it is the hydrate which tends to be more prevalent in pipelines due to the presence of the propane and butane in most produced natural gases. However, sI may occur in highly lean gases that exclusively contain methane and ethane.

1.2 Hydrate Inhibition

Hydrates are of most interest to petroleum scientists and engineers because they can form in, and block oil and gas pipelines. There are two broad approaches to overcome or control the hydrocarbon hydrate problem, namely the thermodynamic approach and the Low Dosage Hydrate Inhibitor (LDHI) approach.

The thermodynamic approach generally attempts to alter the physical conditions or the chemical composition of a system, so that the hydrate state is thermodynamically unfavourable. These include: water removal, increasing temperature, decreasing pressure, addition of "antifreeze" (methanol, ethanol, ethylene glycol) to the fluid, or via a combination of these. From an engineering standpoint, maintaining temperature and/or pressure outside hydrate formation conditions requires design and equipment modifications, such as insulated or jacketed piping. Such modifications are often unfeasible or costly to implement and maintain. The most common approach used by operators to mitigate hydrate problems in pipelines is the use of “antifreeze” or thermodynamic inhibitors, which changes the hydrate stability curve and allows the system to operate in conditions where hydrates cannot form.

Figure 1.2 illustrates the impact of thermodynamic inhibitor on hydrate phase boundary. Thermodynamic inhibitors work by moving the hydrate stability curve to the left, which reduces the temperature and/or increase the pressures where hydrates are stable (hydrates are stable on the left-hand side of the curve). The process operating conditions line indicative of the pressure and temperatures of an offshore pipeline system that may require some sort of hydrate inhibition. The requirement for inhibition is seen where the operating conditions enter hydrate forming zone, whereas the addition of thermodynamic inhibitor moves the conditions that hydrate forms and prevents the operating conditions entering the hydrate forming zone.

The amount of thermodynamic inhibitor required to prevent hydrate blockages is typically between 20% and 40% by weight of the water present in the oil or gas stream (Urdahl et al. 1995). Consequently, several thousand gallons per day of such solvents are usually required. Such quantities present handling, storage, recovery and safety (toxicity/flash point) issues. Separation issues associated with the thermodynamic

inhibitor recovery can also result in the contamination of the oil and gas product or treated water, which can impact both the hydrocarbon refining process and the disposal of the water respectively.

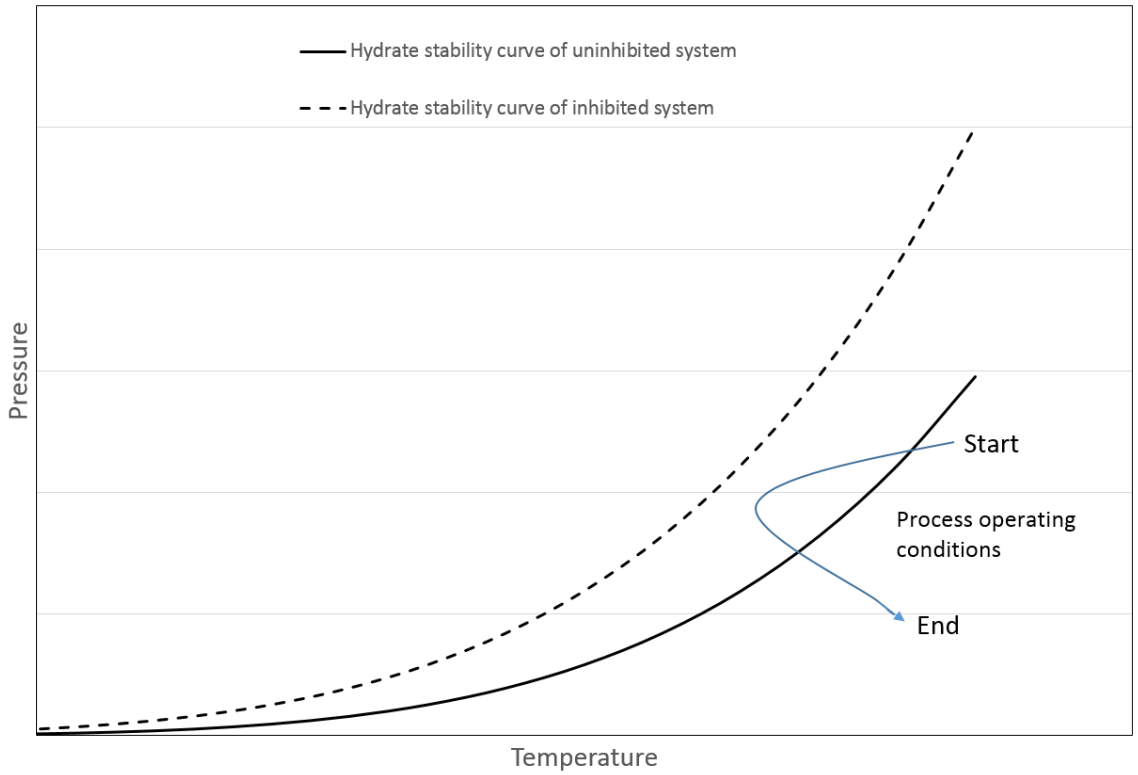

Figure 1.2 Impact of thermodynamic inhibitor on hydrate phase boundary

Attempts are being made to replace thermodynamic inhibitors with Low Dosage Hydrate Inhibitors (LDHI) for certain applications. LDHI are additives (amount used <2%), which either delay the gas hydrate formation (kinetic inhibitors) or keep the gas hydrate agglomerates small and therefore pumpable so that they can be transported through the pipeline (anti-agglomerants). In short, these inhibitors either prevent the nucleation and/or the growth of the gas hydrate particles or modify the hydrate growth in such a way that smaller hydrate particles result. LDHI are an attractive alternative to thermodynamic inhibitors as they can be: cost effective (Frostman *et al.* 2003, Mehta *et al.* 2002) and much easier to engineer as they do not require recovery of the inhibitors, whereas thermodynamic inhibitors require recovery to be cost effective, which can be costly and difficult to manage.

1.3. Kinetic Hydrate Inhibitors

Kinetic Hydrate Inhibitors (KHIs) or threshold hydrate inhibitors (THIs) are water-soluble polymers, which prevent or delay hydrates nucleation and/or growth. KHIs function by increasing the time required for the nucleation and subsequent mass growth of crystals; this time is defined as the induction time. A good overview of kinetic hydrate inhibitor technology can be found in Kelland (2006).

The earliest usage of a KHI was of poly (N-vinylpyrrolidine) (PVP) which was first used as a kinetic ice inhibitor and was applied for many years as a cryoprotectant against ice formation. The first article to appear describing true kinetic hydrate inhibition was a patent from Duncum et al. (1994) at BP, UK on tyrosine and some of its derivatives, including polymers, although no polymer examples were given. Soon afterwards Sloan (1995) filed a patent covering polymers containing monomers consisting of five, six, or seven membered amide rings as kinetic hydrate inhibitors. These include polymers of N-vinyl pyrrolidine (5-ring), the saccharides (6-ring), and N-vinylcaprolcatam (7-ring). Examples quoted are polyvinylcaprolatam (PVCap), PVP, hydroxyethylcellulose (HEC) and the terpolymer product Gaffix VC-713. Lederhos et al. (1996) carried out a screening study (as part of the patent) of around 1500 commercially available water-soluble polymers by the use of tetrahydrofuran (THF) tests, and discovered the use of PVP, PVCap and the terpolymer product Gaffix VC-713 as effective hydrate inhibitors. PVCap and PVP are the most widely used and discussed inhibitors in published academic work, where industrial research mostly remains confidential. Since this initial work, numerous other polymeric inhibitors have been discovered, which are mostly polymeric amide based species, as either homopolymers or copolymers. The discoveries are comprehensively described in Kelland (2006). Notable examples of non-amide based polymers include: a zwitterionic molecule described in Storr et al. (2004), and a liquid oligomer described in Pakulski et al. (1998).

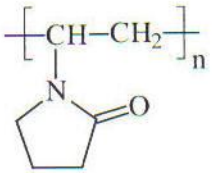

PVP

PVCap

Figure 1.3. PVP and PVCap monomers

The key parameters used to evaluate the performance of KHI are subcooling/driving force and the induction time (Arjmandi et al. 2005). The degree of subcooling is the temperature difference between the hydrate stability and fluid conditions and the induction time is the time until hydrate growth is evident at the conditions. The currently available KHI are reported to have an ability to prevent hydrates at around 12-15 ^{o}C, and the best performing inhibitor to date inhibited hydrate formation to 24.1 ^{o}C subcooling (Colle et al. 2005).

The performance of KHI vary by the type of hydrate crystal being inhibited, whether sI or sII crystals. It has been found that the available KHI are not as effective at sI inhibition than sII inhibition, which is possibly due to the lack of sI inhibitor application in the oil and gas industry. It is proposed that the failure mechanism of KHI in sII forming systems could be attributed to uninhibited sI hydrate formation. It is proposed that sII KHI performance could be improved by combining sI and sII KHI to inhibit both crystal types.

The stochastic nature of the nucleation and growth process that KHIs mitigate requires multiple tests to determine the efficacy of the polymers for benchmarking and application. Field application also requires the creation of representative pipeline conditions in a lab or flow loop, which is inherently challenging and expensive. A method described in Anderson et al. (2011) and Glenat et al. (2011) has offered a practical solution to the testing of KHI inhibition with a stirred autoclave reactor, which involves cooling the vessel to form hydrates, bringing the system to melt all but 1% of the hydrates, then stepwise cooling to monitor hydrate growth. This technique eliminates the stochasticity associated with hydrate formation and focuses on hydrate growth, and the

results of the tests were discovered to be highly repeatable. The work also enabled the identification of different crystal growth inhibition regions, including: complete inhibition region where no hydrates can be formed, slow growth region where hydrates form at a reduced rate, and the rapid growth region where massive crystal growth will occur. The crystal growth regions are useful performance markers for KHI field application.

Descriptions of numerous successful field trials and applications of KHI have been published (Bloys and Lacey 1995, Corrigan et al. 1996, Notz et al. 1996, Leporcher et al. 1998, Pakulski et al. 1998, Phillips and Grainger 1998, Argo et al. 1999, Talley and Mitchell 1999, Mitchell and Talley 1999, Fu et al. 2001, Lovell and Pakulski 2002, Boyne et al. 2003, Budd et al. 2004, Glénat et al. 2004, Rithauddeen and Al-Adel 2014), and application of LDHI has increased over recent years and it is estimated that there were around 40-50 applications worldwide by 2006 (Kelland 2006).

Although KHIs are not as toxic as their AA counterparts, there is still a requirement by many corporate and governmental bodies to attain a much higher level of biodegradability than is currently available and this has restricted the use of KHI in certain locations. This is most apparent in Norway where biodegradability is required to be greater than 60% for all new oilfield chemistry, which means that currently no LDHI can be used. This has led to many fields not being able to use the technology e.g., ExxonMobil's Ringhorn field. The British government also requires biodegradability of 20+%, which has meant that PVCap by itself cannot be used and other alternatives have to be sought. As a result of these policies, service companies have attempted to develop more environmentally friendly inhibitors or "green inhibitors" (Fu et al. (2005)). Recent research has also sought to investigate removal of KHI from produced water using a range of various techniques (Adham et al. 2014)

In drilling, where the temperatures vary significantly from 40-50 °C to sea bed temperature, and highly saline solutions are used, it was believed that the cloud point was a major issue in the use of KHI such as PVCap. The issue was believed to be to the polymers cloud point where they fall out of solution and solidify at the higher temperature conditions associated with injection and then be unable to perform as KHI at the lower temperatures. Work by Fu et al (2001) showed that the cloud point was not such a restrictive issue, because at conditions above the cloud point, the solidified KHI polymers

remained inside the solvent droplets within the aqueous phase, and then later dissolved at conditions below the cloud point. However, it is possible that injection lines at high temperatures could result in lack of inhibition due to a blockage of injection nozzles, which is an element of design that needs to be considered when applying KHI.

Another separate issue, specific to drilling, is that some KHI polymers adsorb onto the clay particles in the drilling fluid and this needs to be considered in the selection and testing of the drilling fluid and hydrate inhibitor (Dzialowski et al. (2001)).

1.4. KHI Research

Since the initial discovery of KHI, the research has been focused on: the development of new inhibitors, enhancing the performance of existing inhibitors, and investigating into the underlying mechanisms of kinetic inhibition.

The research on KHI employs both a micro-scale simulation approach and a macro-scale approach. The macro-scale study can range in simplicity from a "throw it in a rig and see" approach to more complex laboratory equipment such as neutron diffraction, and a wide spectrum of complexity between the two. The micro-scale studies involve the simulation of the molecules at an atomic level, which include both the Monte Carlo (MC) probabilistic approach and the Molecular Dynamic Simulation (MDS) deterministic approach. The macro-scale experiments have been used to: understand the nature of inhibition, test inhibitors for application, and investigate the parameters that affect inhibition. The micro-scale studies are particularly useful to this field of study as it can give insight into the mechanisms involved, and thus aid in developing new and improving existing inhibitors.

The above fields of research will be discussed in two parts: investigation to understand the inhibition mechanism, and then investigation into the effect of physical and chemical parameters on inhibition performance. The development of new inhibitors is dominated by industrial research where the results are generally kept confidential.

1.5 Research into Understanding the Inhibition Mechanism of KHI

After the discovery of KHIs, researchers proceeded to investigate the inhibition mechanism of the inhibitors to get a better understanding of the science and facilitate the progression of the technology.

It is widely agreed by researchers that a key element of kinetic hydrate inhibition is associated with adsorption of the polymer aggregates onto the hydrate crystal structure to prevent growth. This has been experimentally proven with Neutron Scattering that demonstrates that KHI polymers aggregate on hydrate structures (Hutter et al. 2000, King et al. 2000). Additionally, adsorption is also used to explain various other experimental

studies that attribute adsorption on the impact of morphology on hydrate growth in the presence of KHI (Larsen et al. 1998, Zeng et al. 2005). The adsorption mechanism has also been supported by a series of molecular modelling work by several researchers that demonstrated that the KHI monomers preferentially adsorb onto hydrate surfaces (Carver et al. 1995, Carver et al. 1996, Kvamme et al 1997, Storr and Rodger 2000, Carver et al. 2000, Freer and Sloan 2000, Kvamme 2001, Makogon and Sloan 2002, Souza and Freitas (2002), Moon et al. 2003, Moon et al. 2005, Kvamme et al. 2005). Molecular simulation using the same adsorption mechanism theory was then used to develop an LDHI (Storr et al. 2004)

Zeng et al. (2005) claims that an additional mechanism exists, which involves the mitigation of hydrate nucleation. Experimental work by Koh et al. (2002) using differential scanning calorimetry and laser turbidimetry techniques suggests that the nucleation inhibition mechanism is present. The confirmation of KHI having both anti-nucleation and anti-growth inhibition mechanisms was once again suggested by Yang and Tohidi (2010) who used ultrasonic technique to identify the onset of hydrate nucleation.

The research suggests that there are two mechanisms of KHI inhibition: nucleation and growth inhibition. However, the investigative technique described by Anderson et al. (2011) and Glenat et al. (2011) demonstrate that hydrate growth prevention is the primary mechanism for kinetic hydrate inhibition.

1.6. Research into Understanding KHI Performance

The parameters that affect the performance of an inhibitor can be categorised into either the chemistry of the KHI, and the composition of the oilfield fluids and physical conditions in which it is applied to; these will be discussed separately.

1.6.1 Impact of Inhibitor Chemistry on KHI Performance

The chemical species involved in the polymer has a significant effect on hydrate inhibition. However, the monomer is not the only parameter involved in the design and selection of a polymer. It has been shown that co-polymerisation with other non-inhibiting and inhibiting monomers and altering the polymer backbone have led to substantial increases in inhibition performance (Colle et al. 1996). It has been hypothesized by Koh et al. (2002) that these effects can be explained by the non-inhibitor species altering the configuration of the polymer and preventing the polymer from self-interacting, thus ensuring more of the polymer is in contact with the solution. This can be achieved via either by altering the backbone to make it more rigid, or by being different species and thus making the polymers self-associate to a lesser extent.

Varying polymer concentration also has a pronounced effect on the performance of the inhibitor. This can be seen in data by Sloan et al. (1998), where they showed that increasing concentration improves the inhibitory properties of the solution. This is considered to be less of an issue for researchers due to the costs involved associated with increasing polymer concentration.

The length of the polymer also plays an important part in optimising the performance of KHI, it has been shown that there is an optimum length of polymer, for PVCap it was shown that a polymer with a molecular weight of 900 daltons or 6 monomers was better than longer lengths (Sloan et al. (1998)). This thesis proposes to explain this theory by hypothesizing that the larger the polymer, the more immobile they become and the more the polymer self-associate with themselves, both of which lead to a weakening in performance. However, as the polymer gets too small they are not able to sterically hinder the hydrate from growing due to their size and/or their inability to form aggregates. This is supported by the improvement in performance of copolymers such as

Gaffix VC-713 that should self-associate to a lesser degree than equivalent homopolymers.

A bimodal distribution of the polymer weight has also been shown to substantially increase polymer performance i.e. a mixture of polymers with two different lengths (Colle et al. (2005)). It is hypothesized that this happens due to the more mobile smaller polymers moving faster in solution and are more likely to meet the growing surface of the hydrate nuclei, thus giving more time for the larger polymers to arrive, which are better able to prevent further growth via larger aggregates to sterically prevent further hydrate growth.

All KHI require an aqueous solvent as a carrier fluid for the polymers. In some cases, synergists exist that improve the performance of KHI and are often used as the carrier fluid to transport the KHI polymers, of which the most notable are the quaternary ammonium salts and the glycol ethers (Cohen et al. 1998), which tend to be weak anti-growth inhibitors themselves, and have been shown to adsorb onto the surface of the hydrate structure (Kelland (2006)). Work by Lee & Englezos (2005) shows that the addition of non-active polymers such as polyethylene oxide can also improve the performance of KHI. There are three proposed hypotheses to explain the phenomenon of synergy: The first involves the synergist acting as a solvent so that the polymer self-associates to a lesser extent, and thus having a larger contact area with the solution, thus improving performance. The second involves a theory similar to that explained for the benefit of bimodal distribution of polymers, where the smaller more mobile synergists will quickly get to the growth site where they can inhibit growth and thus give time for the larger more effective polymer to reach the hydrate growth site. The third theory is specific to the synergistic benefit of the inert polymers, and this involves the inert polymers helping to form aggregates with the active polymers and sterically hindering water getting to hydrate growth sites.

1.6.2. Impact of Oilfield Fluids and Physical Conditions on KHI Performance

Several factors impact the performance of KHI when applying the technology to the field. The various parameters are discussed separately.

Pressure and Temperature

The effect of subcooling on induction time has historically been the primary method to evaluate the performance of KHI. Arjmandi et al. (2005) demonstrated that this term can be used for comparative purposes at most conditions apart from at pressures 4-20 MPa. Similar work conducted by Svartaas et al. (2006) confirmed this phenomenon. For field application it is important to test the system at actual conditions and not rely on subcooling as an indicator in itself. This phenomenon is explored in Chapter 7.

Hydrodynamics

The system hydrodynamics is believed to have a significant impact on the kinetics of hydrate formation, and growth morphology. As expected it also impacts the performance of KHI; this is well described in Matthews et al. (2002). For real world application, inhibitors need to be empirically tested at conditions close to those experienced in the field (and using a similar gas composition), and autoclave and rocking cells are the most commonly used equipment for this process.

Hydrocarbon Phase

Certain oils have tendencies to naturally inhibit hydrate blockages via an anti agglomerant effect. This has been attributed to the maltene fraction and asphaltene components of the oil. It is known that some oils have a negative effect on the performance of KHI. The impact of oils and in particular condensates will be discussed in further detail in Chapter 5.

Salts

Sloan et al. (1998) showed that sea salt had a negative performance at concentrations less than 6 mass%, and a positive effect at greater concentrations. Experiments conducted as part of this thesis are in agreement with Sloan et al. (1998) and test a variety of different salt types. The results will be discussed in more detail in Chapter 3.

Thermodynamic Inhibitors and Oilfield Chemicals

At low temperatures and high levels of subcooling it may be desirable to blend LDHI with thermodynamic inhibitors. Applications of this technology already exist, such as in the Gulf of Mexico where a thermodynamic inhibitor, a KHI and an AA were combined for use in a packer fluid (Pakulski et al. (2005), Szymczak et al. (2005)).

For high levels of subcooling, it may be desirable to look at combining thermodynamic inhibitors with LDHI. From the thermodynamic inhibitors, it is known that methanol has a negative or antagonistic effect on KHI (Sloan et al. (1998)) whereas ethylene glycol has a slight synergistic effect (Arjmandi (2005), Kim et al. (2014)). This will be discussed in more detail in Chapter 2.

The compatibility of KHI with other oilfield chemicals and reservoir fluids have been indirectly researched through the KHI field applications previously discussed. The application studies were carried to ensure KHI efficacy and other compatibility issues were mitigated prior to use in the field. A good description of the necessary steps required for application can be found in Phillips and Grainger (1998).

Solids

No work has been done to evaluate the impact that solids may have on hydrate formation, however the presence of reservoir fines and sand may have a negative impact on the

nucleation of hydrates and the performance of KHI as the solids could promote nucleation by behaving as seed for nucleation.

1.7. Thesis Overview

This thesis is an investigation into the nature of kinetic hydrate inhibitors, with a focus on understanding the effect that some oilfield components have on the performance of the inhibitors. The work described in the thesis involves a series of experimental work and molecular simulation used to investigate factors affecting the performance of KHI.

The experimental work involved a series of laboratory testing to investigate the effect of alcohols, salts, condensate, and synergists, have on the performance of KHI. The results are supplemented with use of molecular dynamic simulation to understand the impact to performance due to the presence of methanol. The final chapter then involves a study looking at the impact of pressure has on KHI performance and describes a novel experimental setup to enhance testing of KHI.

Chapter 2: The Effect of Alcohols on the Performance of KHI

Hydrate problems are encountered in severe locations where it may be desirable to inject both KHI and traditional thermodynamic inhibitors. In such conditions, the degree of subcooling is too high for KHIs to work alone and thermodynamic inhibitors can be combined to reduce the subcooling to a point where KHIs can be used. The effect of these thermodynamic inhibitors on the performance of kinetic inhibitors needs to be investigated if they are to be used together. At the time of this work, methanol has been tested with PVCap (Subramanian et al. 1998) and showed to have an antagonistic effect on the performance of PVCap. Ethylene glycol however demonstrated to have a slight synergistic effect on KHI including PVCap (Arjmandi (2005), Kim et al. (2014)).

The primary objective of this work is to: investigate the antagonistic nature of methanol on the performance of KHI, investigate the impact of ethanol, and to develop an understanding of the phenomenon. The work carried out consists of several experimental studies, including:

- Investigating the effect of methanol and ethanol on PVCap performance using stirred autoclave reactors (Section 2.1);

- The effect of methanol on the performance of commercially available inhibitors using stirred autoclave reactors (Section 2.2);

2.1. The Effect of Methanol and Ethanol on the Performance of PVCap

This study was carried out to investigate the effect of ethanol and methanol on the performance of PVCap. The experimental work involved the use of kinetic or stirred autoclave vessels to evaluate the effect of various concentrations of ethanol and methanol on the performance of PVCap.

2.1.1 Methodology

A 500 ml stirred autoclave reactor was used in the experiments (Figure 2.1). The reactor consists of a testing vessel (700 bar rated), a magnetic stirrer, and a temperature control system. The torque applied to the stirrer shaft is estimated from the electric current input to the electric driving motor.

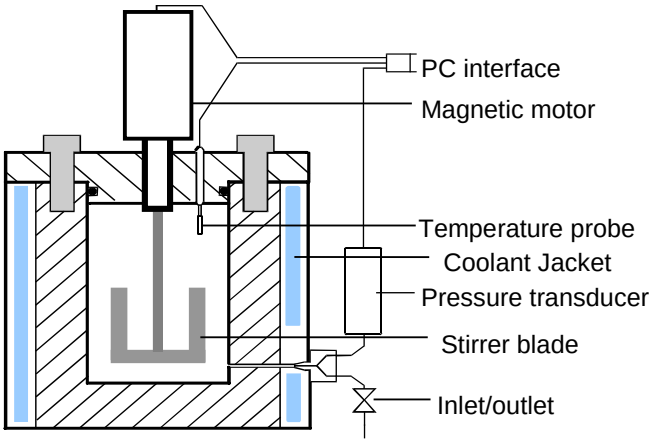

Figure 2.1. Schematic diagram of a typical Stirred Autoclave Reactor

In the experiments, 200 ml of the test liquid was loaded into the vessel, and then a natural gas was charged into the cell up to the required pressure (90-100 bar at test conditions). To form hydrates, the system was cooled down to a temperature set point, with a stirring rate of ~600 rpm. The system was then left to form hydrates. The temperature, pressure and torque profiles from the reactor are stored via computer using LabView software.

The chemicals tested included aqueous solutions of 2.5 mass% Luvicap (BASF), which gives a composition of 1 mass% PVCap (2000-8000 Daltons) and 1.5 mass% ethylene glycol. Tests were then run with an addition of 5 mass%, 10 mass%, 20 mass% and 30 mass% methanol and 6.875 mass% (almost equivalent to 5 mass% MeOH on the hydrate phase diagram), 20 mass % and 30 mass% ethanol in the above solution.

For each solution, the autoclave temperature was reduced to the desired subcooling and held for a period of 10 hours. The concept of subcooling is illustrated in Figure 2.2 and it

is the temperature difference between the hydrate phase stability line and the current process conditions.

If hydrate growth was evident within an 8 hour range, indicated by a drop in pressure of 2 bar or more, the experiment was stopped, however if there was no hydrate present, the autoclave test temperature was increased to 40 °C for more than 20 hours to remove water memory. Subsequent to the heating phase, the test temperature was decreased by approximately 2 °C to the previous temperature and the test repeated. After the initial failure of the inhibitor at a certain temperature for the inhibitor solution, the test temperature was then increased stepwise to determine at what level of subcooling the inhibitor solution could prevent hydrates for the 8 hour period.

The overall purpose was to determine what level of subcooling the KHI failed to prevent hydrate growth. All tests involved keeping the pressures within 90-100 barg to eliminate the impact of pressure on the tests.

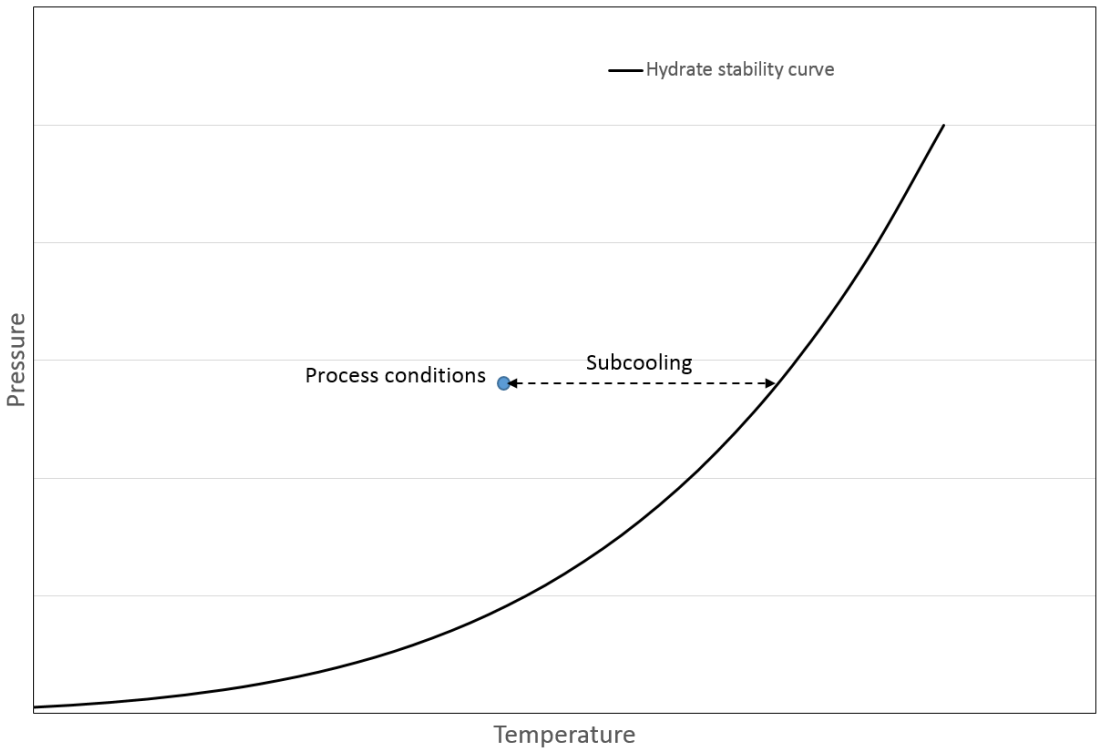

Figure 2.2. Schematic to describe subcooling concept.

The calculation of the phase boundaries for the natural gas and inhibitor solution tested was achieved by using HWHYD software, which is a software developed by the Centre for Gas Hydrates at Heriot-Watt University, Edinburgh. The HWHYD software has been developed via extensive testing and the matching to a series of different empirical models.

Time to formation or induction times in experiments were determined as the period between the initial time, t_i, when system begins to settle at the testing temperature, and the time where hydrate formation is first observed, t_f, from a drop in system pressure (ΔP), as illustrated in Figure 2.3.

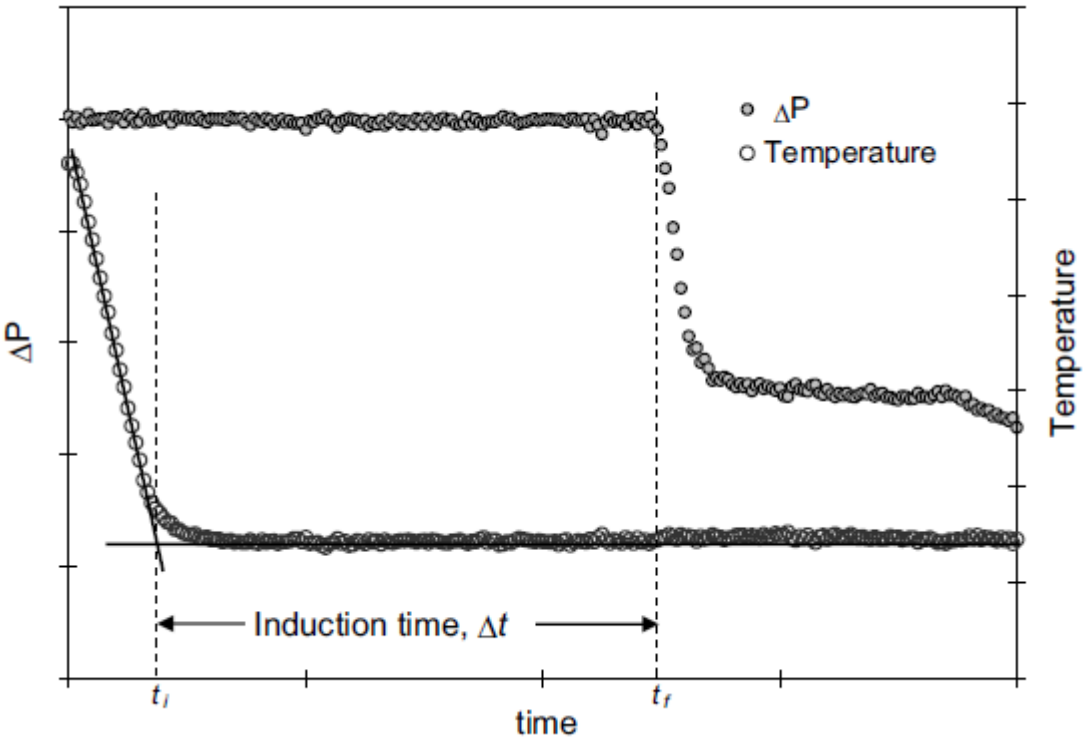

Figure 2.3 Illustration of typical temperature, pressure change, ΔP (from linear liquid+gas *PT* relationship) associated with hydrate formation, for an experiment showing the method used to determine induction time (Δt).

2.1.2 Results

Tables 2.1 and 2.2 are a summary of the results, which represent the subcooling associated to inhibitor failure rate. The range of subcooling where the inhibitor failed to prevent hydrate growth for 8 hours is presented in the tables. A test is considered a failure if it cannot prevent a reduction in pressure of 2 bar for a minimum of 8 hours, which indicated hydrate growth. All the subcoolings take into account the effect of the alcohol on the phase boundary. The pressures were all in the range of 90-100 barg to minimize the impact of pressure.

Table 2.1. Summary of the Stirred Autoclave Reactor Results for Methanol.

MeOH Concentration (mass%)	Adjusted subcooling range which hydrates are not formed for at least 8 hrs (°C)
0	11.1-11.9
5	9.1-11.5
10	10.3-10.4
30	6.9-7.1

Table 2.2. Summary of the Stirred Autoclave Reactor Results for Ethanol.

EtOH Concentration (mass%)	Subcooling range which hydrates are not formed for at least 8 hrs (°C)
0	11.1-11.9
6.875	10.4-10.9
20	6.9-7.2
30	5.8-6.3

Figures 2.4 and 2.5 illustrate the effect of the varying molar concentration on the subcooling at which 1 mass% PVCap can prevent a drop in pressure of 2 bar for more than 8 hours of methanol and ethanol, respectively. The figure has the extrapolated values and the error boundaries are represented.

Figure 2.6 represents a comparison in molar terms of varying methanol/ethanol concentration on the maximum subcooling at which 2.5 mass% Luvicap prevents catastrophic growth for more than 8 hrs.

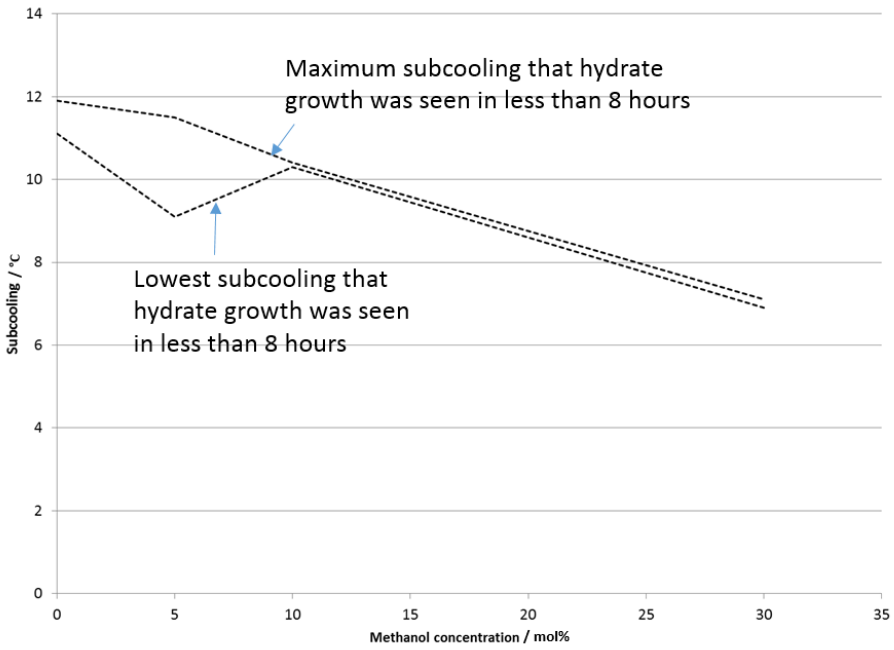

Figure 2.4 Effect of varying methanol concentration on the maximum subcooling at which 2.5 mass% Luvicap prevents catastrophic growth for more than 8 hrs (constant pressure of 90-100 bar)

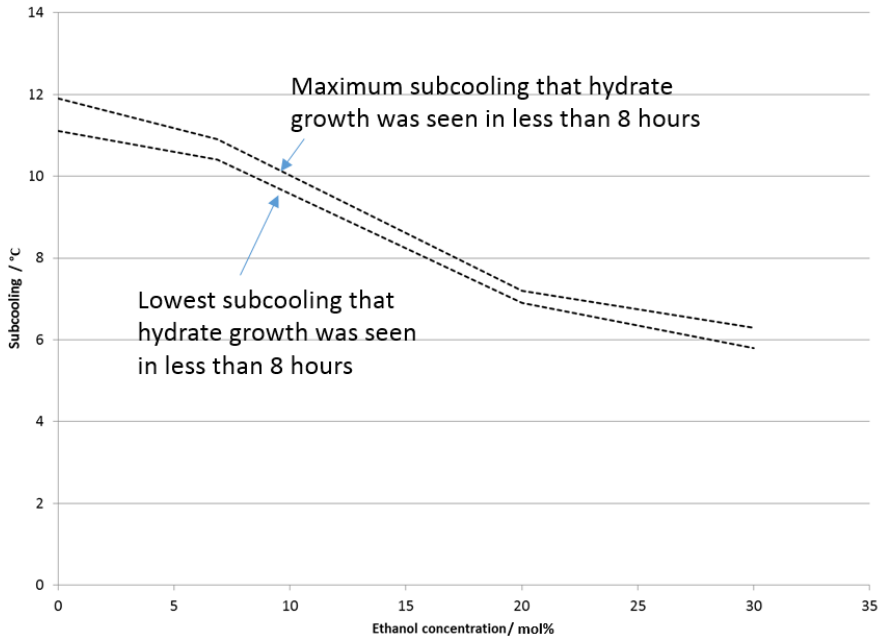

Figure 2.5 Effect of varying ethanol concentration on the maximum subcooling at which 2.5 mass% Luvicap prevents catastrophic growth for more than 8 hrs. (constant pressure of 90-100 bar)

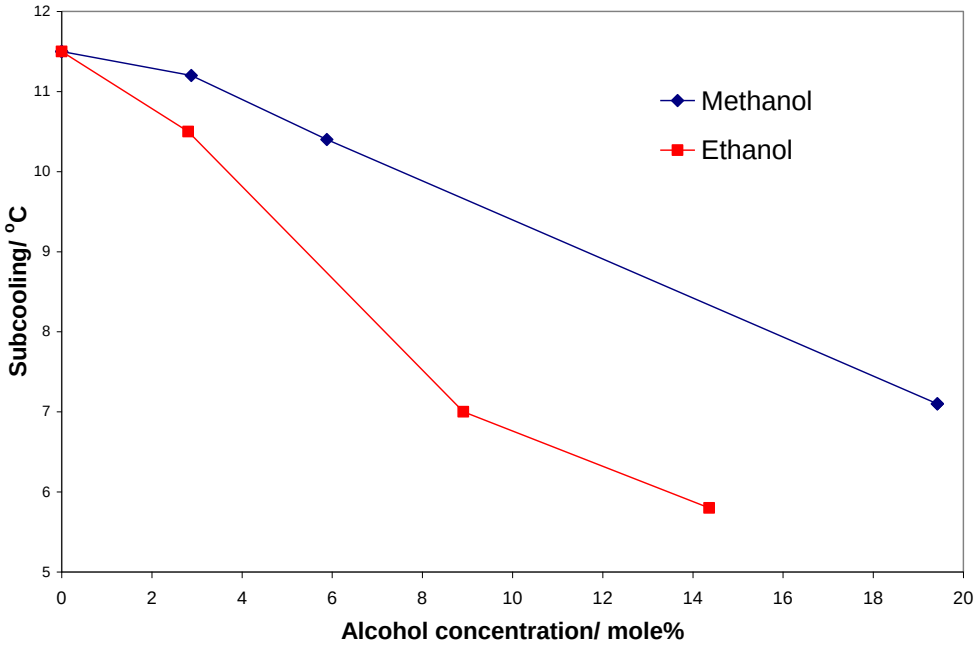

Figure 2.6. Comparison in molar terms of varying methanol/ethanol concentration on the maximum subcooling at which 2.5 mass% Luvicap prevents catastrophic growth for more than 8 hrs. (constant pressure of 90-100 bar)

Figures 2.4 to 2.6 show that ethanol and methanol both have an adverse effect on the kinetic inhibition performance of PVCap. The results show that ethanol has a more significant effect than methanol on a molar basis. The results also suggest that the nature of the negative effect of methanol and ethanol on PVCap performance are very similar.

The results from previous work by Subramanian et al. (1998) can be seen in Figure 2.7. The published work shows a linear relationship with increasing methanol concentration, which is similar to the results gathered in the tests conducted.

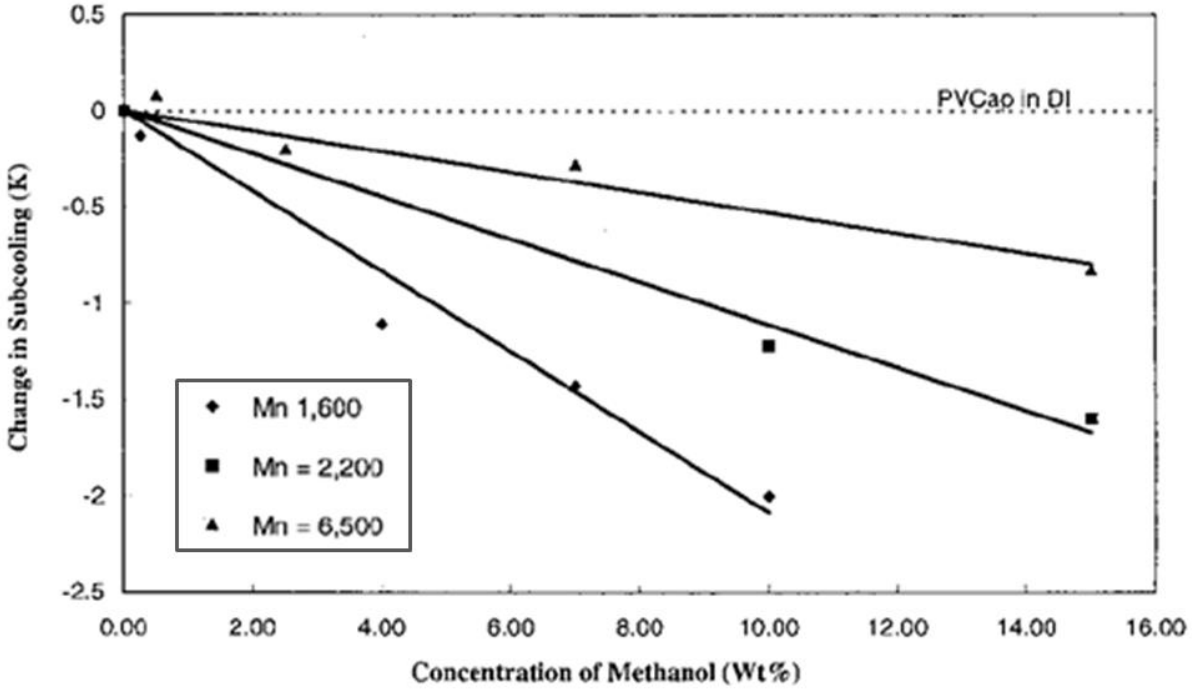

Figure 2.7 Effect of methanol on 0.5 wt % PVCap on subcooling. Mn=molecular weight of polymer (Subramanian et al. (1998))

2.2 Investigation into the Effect of Methanol on Commercial Inhibitors using Stirred Autoclave Reactors.

In the previous section it was demonstrated that ethanol had a negative impact on the performance of PVCap, similar to methanol which was reported by other researchers. This section involves a series of tests to investigate the effect that methanol has on the performance of commercial kinetic inhibitors.

2.2.1 Experimental Methodology

The same experimental set-up used for Section 2.1 was used for this work. The chemicals tested included: a commercial inhibitor (KHI 1); and a VP/VCap copolymer (KHI 2).

For both inhibitors, a series of blank test were carried out in order to find a reasonable induction time for comparison purposes (at 4 °C). Tests were then conducted with 5 mass% methanol and constant subcooling. Firstly, a test was conducted using constant temperature and modifying the pressure to attain similar subcooling, to investigate if pressure conditions have an effect on the conclusions. Secondly, the system was tested in a different stirred autoclave reactor of 300 ml volume at a fixed temperature, to investigate if the experimental set-up used had any effect on the conclusions.

2.2.2 Results

KHI 1

Table 2.3 presents the conditions for the tests carried out with KHI 1 in the 500 ml reactor, including the temperature, pressure, the associated dissociation temperature, subcooling and induction time. Table 2.4 presents the conditions for the tests carried out with KHI 1 conducted in the 300 ml reactor, including the temperature, pressure, the associated dissociation temperature, subcooling and induction time. All the subcoolings take into account the effect of the alcohol on the phase boundary.

Table 2.3. Stirred autoclave reactor results for the effect of methanol on the performance of KHI 1 (500 ml vessel). All the subcoolings take into account the effect of the alcohol on the phase boundary.

Run	T (°C)	P (bar)	Dissociation Point (°C)	Ti (hours)	Subcooling (°C)
1	4.3	59	14.4	12	10.1
2	4.3	59	14.2	12	9.9

5 vol.% KHI aqueous solution.

Run	T (°C)	P (bar)	Dissociation Point (°C)	Ti (hours)	Subcooling (°C)
1	4.3	79	14.3	16	10.0
2	4.3	79	14.3	7	10.0
3	4.2	79	14.3	6	10.1

5 mass% MeOH and 5 vol.% KHI 1 aqueous solution (constant temperature)

Run	T (°C)	P (bar)	Dissociation Point (°C)	Ti (hours)	Subcooling (°C)
1	2.5	57	12.1	5	9.6
2	2.1	57	12.1	3	10.0

5 mass% MeOH and 5 vol.% KHI 1 aqueous solution (constant pressure)

Table 2.4 Stirred autoclave reactor results for the effect of methanol on the performance of KHI 1 (300 ml vessel). All the subcoolings take into account the effect of the alcohol on the phase boundary.

Run	T (°C)	P (bar)	Dissociation Point (°C)	Ti (hours)	Subcooling (°C)
1	4.9	61	15.4	4	10.5
2	4.9	61	15.4	1	10.5
3	4.9	61	15.4	2	10.5
4	4.9	61	15.4	1	10.5

5 vol.% KHI 1 aqueous solution.

Run	T (°C)	P (bar)	Dissociation Point (°C)	Ti (hours)	Subcooling (°C)
1	4.8	81	15.2	1	10.4
2	4.8	81	15.2	1	10.4

5 mass% MeOH and 5 vol.% KHI 1 aqueous solution (Constant T.)

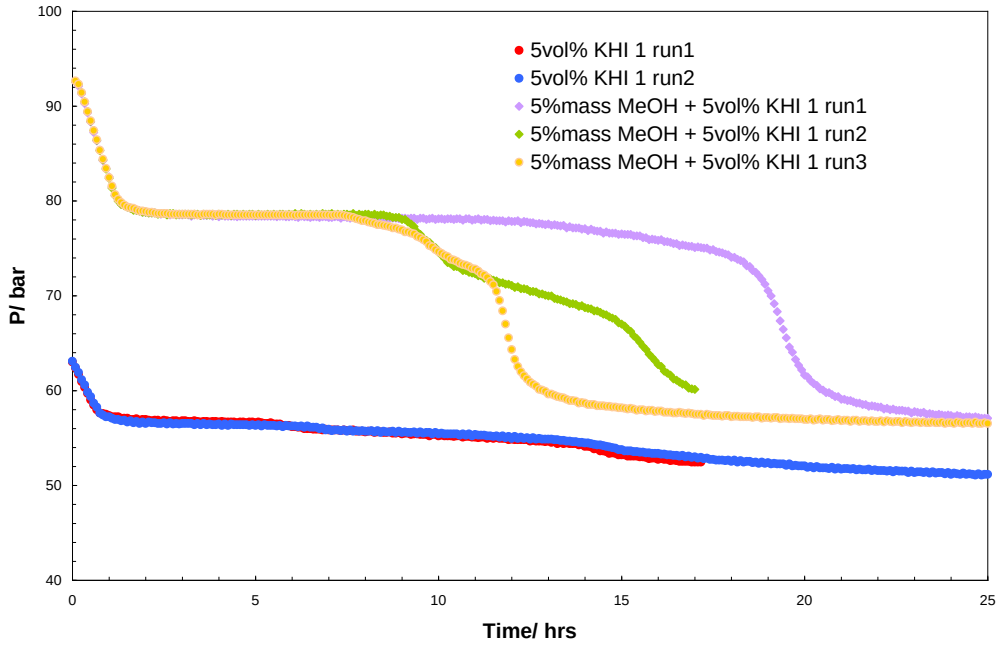

Figure 2.8 Effect of 5 mass% methanol on KHI 1 at constant temperature and modifying subcooling by adjusting pressure (500 ml vessel)

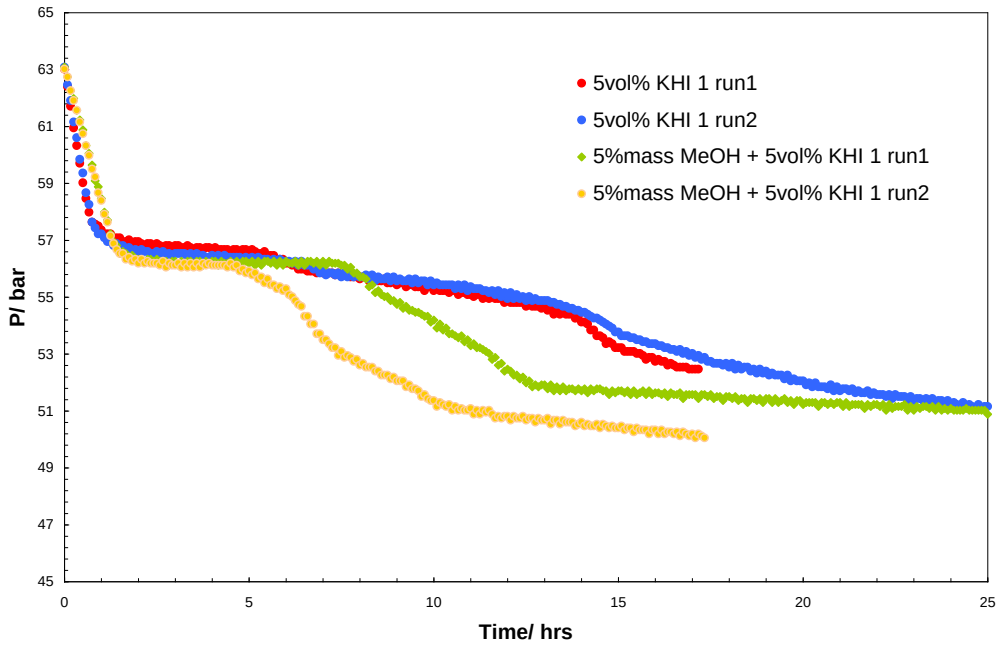

Figure 2.9 Effect of 5 mass% methanol on KHI 1 at constant pressure and subcooling (500 ml vessel)

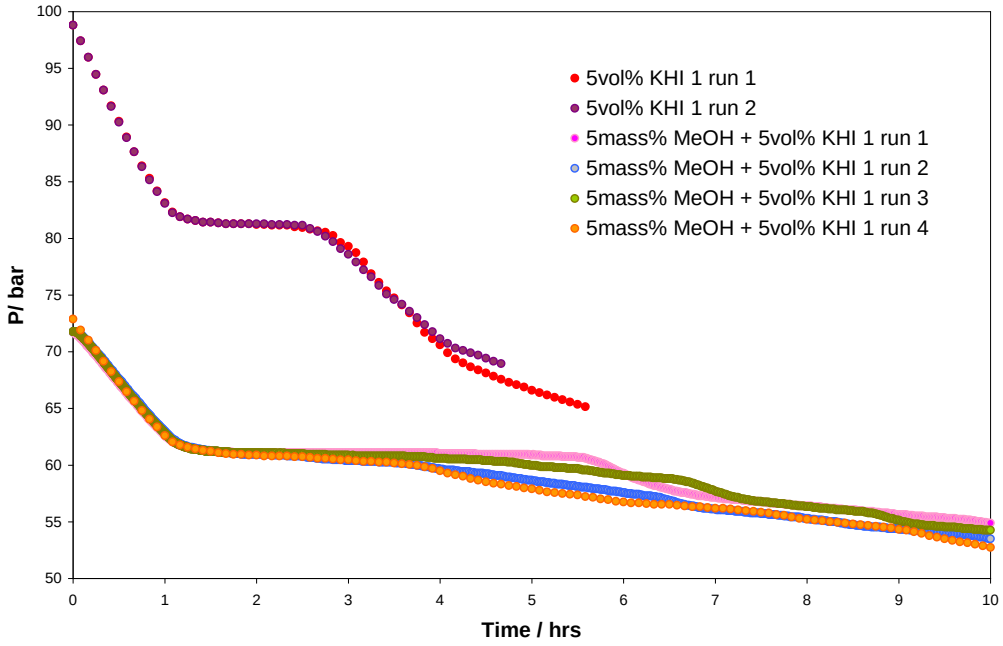

Figure 2.10 Effect of 5 mass% methanol on KHI 1 at constant temperature and subcooling (300 ml vessel).

The results of the tests conducted in the 500 ml stirred autoclave reactor can be seen in Figures 2.8 and 2.9, and the results for the tests conducted in the 300 ml stirred autoclave reactor are presented in Figure 2.10. Figure 2.8 and 2.10 present the results at constant temperature (modifying pressure for same subcooling), and the results in Figure 2.9 are at constant pressure (modifying temperature for same subcooling).

The addition of methanol reduces the performance of the KHI resulting in shorter induction times. This appears to be true for both the constant temperature (higher pressure) and constant pressure (lower temperature), and is true for the tests in both reactors.

KHI 2

Table 2.5 presents the conditions for the tests carried out, including the temperature, pressure, the associated dissociation temperature, subcooling and induction time for the tests carried out with KHI 2.

Table 2.5 Stirred autoclave reactor test results for the effect of methanol on the performance of KHI 2.

4 mass% KHI 2 aqueous solution.

Run	T (°C)	P (bar)	Dissociation Point (°C)	Ti (hours)	Subcooling (°C)
1	4.0	76	16.9	5	12.9
2	4.0	76	16.9	5	12.9

5 mass% MeOH and 4 mass% KHI 2 aqueous solution (Constant T.)

Run	T (°C)	P (bar)	Dissociation Point (°C)	Ti (hours)	Subcooling (°C)
1	2.1	76	14.8	0	12.8
2	2.1	76	14.8	0	12.8

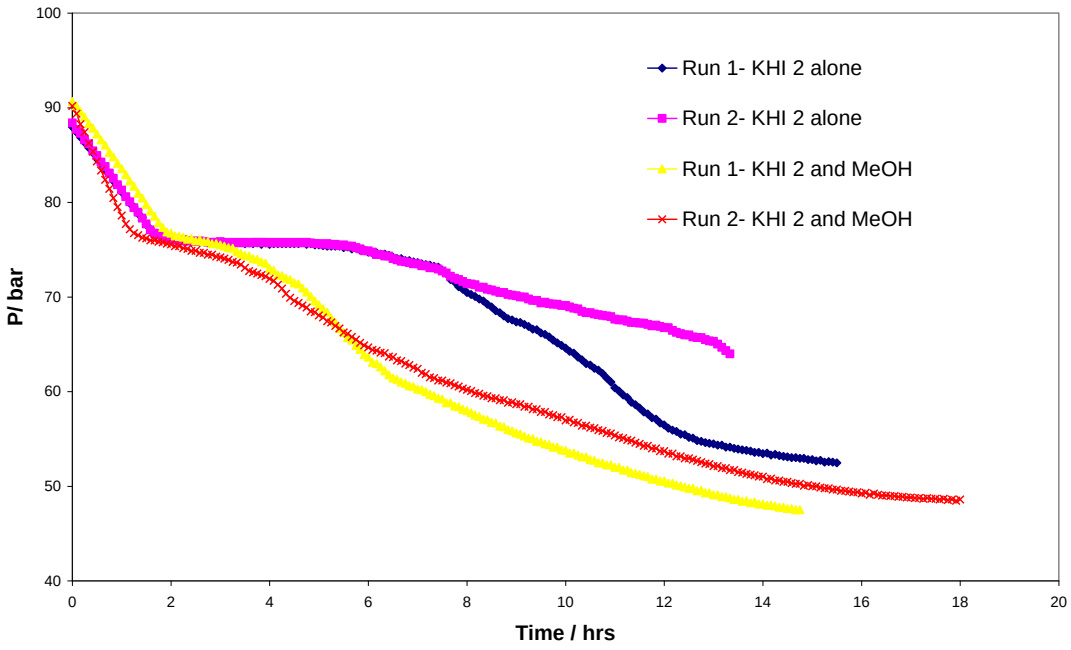

Figure 2.11 Effect of 5 mass% methanol on KHI 2 at constant pressure and subcooling.

The results shown in Figure 2.11 shows that methanol has a negative effect on the performance of KHI 2 for both nucleation prevention and prevention of catastrophic growth. This is demonstrated by smaller induction time and quicker growth of hydrate.

2.3 Results and Discussion

The experiments with the stirred autoclave reactors showed that both methanol and ethanol had a negative effect on the performance of all the KHI tested. Out of the two, ethanol had the more adverse effect on the performance of PVCap.

The actual antagonistic nature of alcohol on the performance of PVCap remained unclear after the stirred autoclave reactor investigation. However, an investigation by Yang et al. (2005) using an ultrasonic method to identify hydrate nucleation and growth was conducted to understand the mechanism of inhibition of PVCap alone, and PVCap in the presence of methanol. The results of this work demonstrated that PVCap is able to delay nucleation and inhibit hydrate growth in the presence and absence of methanol, however, the presence of methanol intensified growth once it started, and thus significantly damaged the role of PVCap in preventing growth.

The previously proposed theories to explain the role ethanol and methanol have on the reduced performance of the inhibitors are discussed:

- It is proposed that alcohols can associate with the polymers and affect the inhibitive properties of the KHI. It is possible that such interactions would change the conformation or shape of the polymer in solution, effectively changing its mobility; or that the alcohols may associate with the active sites of the KHI. To investigate the behaviour of methanol in aqueous PVCap solution, Molecular Dynamic Simulation was conducted, which is detailed in Chapter 6.

- The addition of the alcohols may increase the mass transfer of hydrocarbon gases into aqueous solutions by changing the polarity of the aqueous solution. This is supported by Wise et al. (2016) who demonstrates that the presence of methanol or ethanol increase the solubility of methane in water. This increase in concentration of natural gas hydrate formers in solution could result in more guest molecules to form hydrate nuclei, and/or increase the amount of hydrate formers in solution for when hydrate growth starts. Ethanol also has a larger impact on alkane solubility than methanol, which may explain why ethanol has a larger impact on KHI performance.

- It has been proposed that the alcohols may behave as a guest molecule to form hydrates. Ethanol and methanol are known to be able to act as a guest molecule in hydrates at certain conditions. However, the work described by Yang et al. (2011) suggests that methanol did not impact nucleation in PVCap solution but hydrate growth discredits this hypothesis.

Ethylene glycol has demonstrated to have a synergistic impact in both Arjmandi (2005) and Kim et al. (2014). The synergistic effects of ethylene glycol is not explained by any of the hypotheses described above and it is proposed that it could be un-associated with the antagonistic effects of methanol and ethanol. It is proposed that the synergistic effect of ethylene glycol is either due to the impact it has on the structure of the polymer or that there is an additional mechanism at play associated with combining different types of inhibitors, such as seen when having bimodal distributions of polymer lengths (Colle et al. (2005)).

Chapter 3: The Effect of Salts on the Performance of PVCap

3.1 Introduction

Produced water from oilfield operations contains various salt types which are present at a wide variety of different concentrations. Salts increase the water activity of a system and behave like a thermodynamic inhibitor, and thus have an impact on the hydrate phase boundary.

Unlike methanol and ethanol described in Chapter 2, the presence of salts increase the polarity of an aqueous solution and reduce the solubility of hydrate forming components in the aqueous phase, which should reduce the nucleation and growth of hydrates in the presence of KHI. The change in polarity of an aqueous solution may also change the conformation of the KHI polymer, and it is likely that the increase in polarity should increase self-agglomeration of a polymer like PVCap due to its predominantly non-ionic nature.

Previous work by Sloan et al. (1998) show that sea salt had negligible impact at low concentrations and positive impact at high concentrations. This chapter describes experimental work that investigates the impact of several common salt types have on the performance of PVCap, including: NaCl, NaBr, KCl, $CaCl_2$ and $MgCl_2$. The experimentation also tries to understand the impact that the ionic strength of a solution has on the performance of the KHI.

3.2 Experimental Methods and Equipment

Experiments were carried out using a mixed autoclave cell, a schematic of which is provided in Figure 3.1. The set-up consists of a 300 ml titanium cylindrical pressure vessel, surrounding coolant jacket with associated cryostat bath, magnetic stirrer, platinum resistance thermometer (PRT) and pressure transducer. Both temperature and pressure were recorded by computer using *LabView* software.

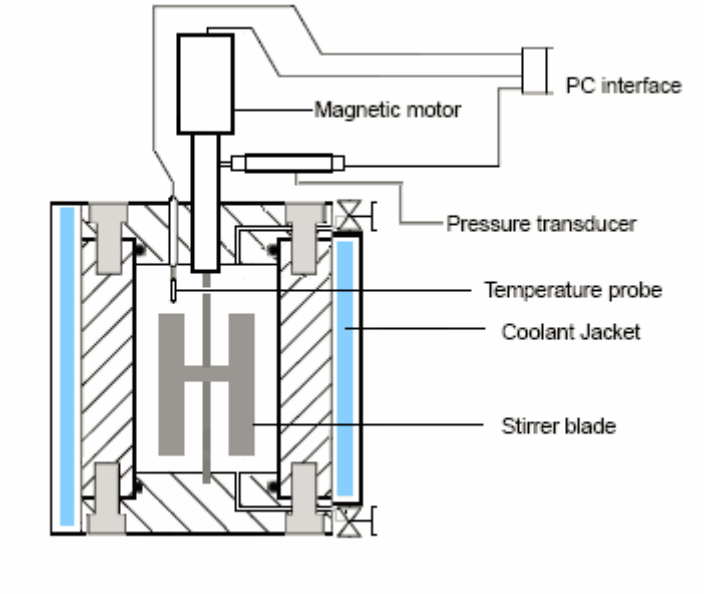

Figure 3.1 Schematic diagram of the kinetic rig used in these experiments

The Kinetic Hydrate Inhibitor (KHI) used was Luvicap EG, which consists of 40 mass% Poly (vinyl caprolactam) (PVCap) with molecular weight of 2000-8000 (g/mol) and 60 mass% ethylene glycol. Sodium bromide (NaBr) with a purity of 99.99%+ was supplied by Merck, 99%+ Potassium chloride (KCl) and 98% Magnesium chloride hexahydrate ($MgCl_2 \cdot 6H_2O$) were from Sigma Aldrich, and ($CaCl_2$) with a purity of 97%+ was purchased from Fluka. Deionised water was used in all tests. Natural gas (NG) was purchased from BOC, with its composition being determined by gas chromatography, as presented in Table 3.1.

Table 3.1. Test Natural Gas Composition

Component	Mole %
N_2	1.5
CO_2	1.16
C1	88.9
C2	6.14
C3	1.6
iC4	0.2
nC4	0.3
iC5	0.1
nC5	0.1

The experimental procedure used in all experiments was as follows. 150 ml of test liquid was first added to the cell, before remaining air was evacuated with a vacuum pump. The stirrer was then set to 500 rpm, the system cooled to the test temperature, and then natural gas was injected to achieve the desired starting pressure. Prior to starting each test/repeat run, the system was heated to 40 °C and left for at least 20 hours (with the aim of removing any hydrate memory).

Six salt components systems were investigated with the same ionic strength:

1. NG+ 2.5 mass % Luvicap EG solution (base case)
2. NG + 2.5 mass % Luvicap EG solution + 5.0 mass % NaCl
3. NG + 2.5 mass % Luvicap EG solution + 7.8 mass % NaBr
4. NG + 2.5 mass % Luvicap EG solution + 5.2 mass % KCl
5. NG + 2.5 mass % Luvicap EG solution + 4.6 mass % $MgCl_2$
6. NG + 2.5 mass % Luvicap EG solution + 5.9 mass % $CaCl_2$

In order to minimize the temperature and pressure effect (as described in Chapter 7), the concentrations of the salt systems were chosen to give equivalent phase boundaries to the water + NG system with the presence of 5 mass% NaCl. For each system, hydrate phase boundaries were predicted using the HWHYD model (version 1) assuming the PVCap polymer had negligible effect on stability. Figure 3.2 shows experimentally measured dissociation points for NG + water system with different salts together with the predicted hydrate phase boundary for NG with 5 mass% NaCl.

All the tests were carried out with a sub-cooling of 13 °C, P = 109.2 barg and 4 °C for the tests. This was achieved by modifying the salt concentration to attain similar subcooling conditions.

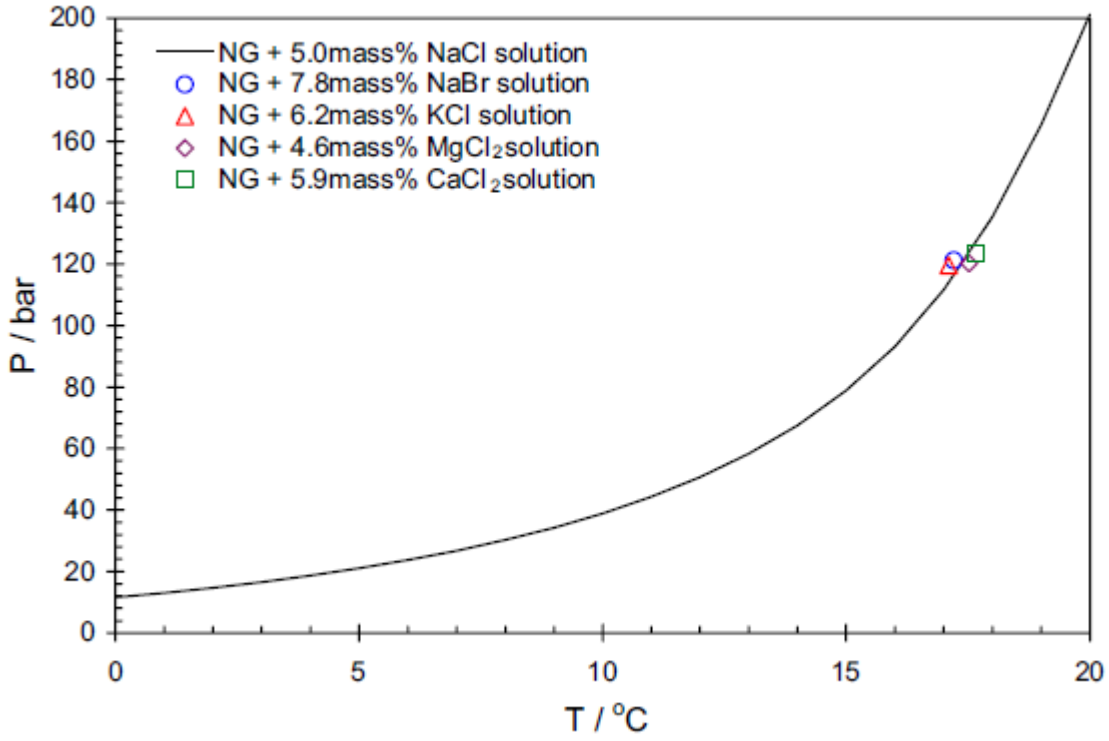

Figure 3.2 Solid line represent predicted (HWHYD version 1) hydrate phase boundary for NG + 5.0 mass % NaCl solution. Symbols are the dissociation points for NG +different salt solutions.

3.3 Results

Measured induction times are reported in Table 3.3 with the average values ($\overline{\Delta t}$). Table 3.4 is the baseline data for LuvicapEG in the absence of salt. Pressure drops as a function of time for different salts and repeat runs are plotted in Figures 3.3 through 3.9.

Table 3.3 Experimentally determined induction times (Δt) for investigated systems at ΔT = 13 °C and P = 109.2 barg and T = 4 °C.

System	Ionic Strength	Run #	Δt (hrs)	($\overline{\Delta t}$) (hrs)
NG + 2.5 mass% LuvicapEG + 5.0 mass% NaCl	0.9	1	2.66	21.70
		2	5.08	
		3	82.66	
		4	1.83	
		5	15.25	
NG + 2.5 mass% LuvicapEG + 7.8 mass% NaBr	0.85	1	5.17	8.40
		2	2.50	
		3	3.50	
		4	22.42	
NG + 2.5 mass% LuvicapEG + 5.2 mass% KCl	0.93	1	20.83	13.29
		2	2.75	
		3	23.83	
		4	5.75	
NG + 2.5 mass% LuvicapEG + 4.6 mass% $MgCl_2$	0.51/1.52	1	1.25	0.80
		2	0.83	
		3	0.67	
		4	0.67	
		5	0.58	
NG + 2.5 mass% LuvicapEG + 5.9 mass% $CaCl_2$	0.56/1.55	1	0.83	37.55
		2	0.92	
		3	4.09	
		4	39.32	
		5	142.0	

Table 3.4 Experimentally determined induction times (Δt) for NG + 2.5 mass % Luvicap EG at ΔT = 13 °C.

P (barg)	T (°C)	Run #	Δt (hrs)	($\overline{\Delta t}$) (hrs)
75.8	4.0	1	0.91	0.88
		2	1.16	
		3	0.58	
109.2	5.2	1	0.58	0.67
		2	0.50	
		3	0.92	

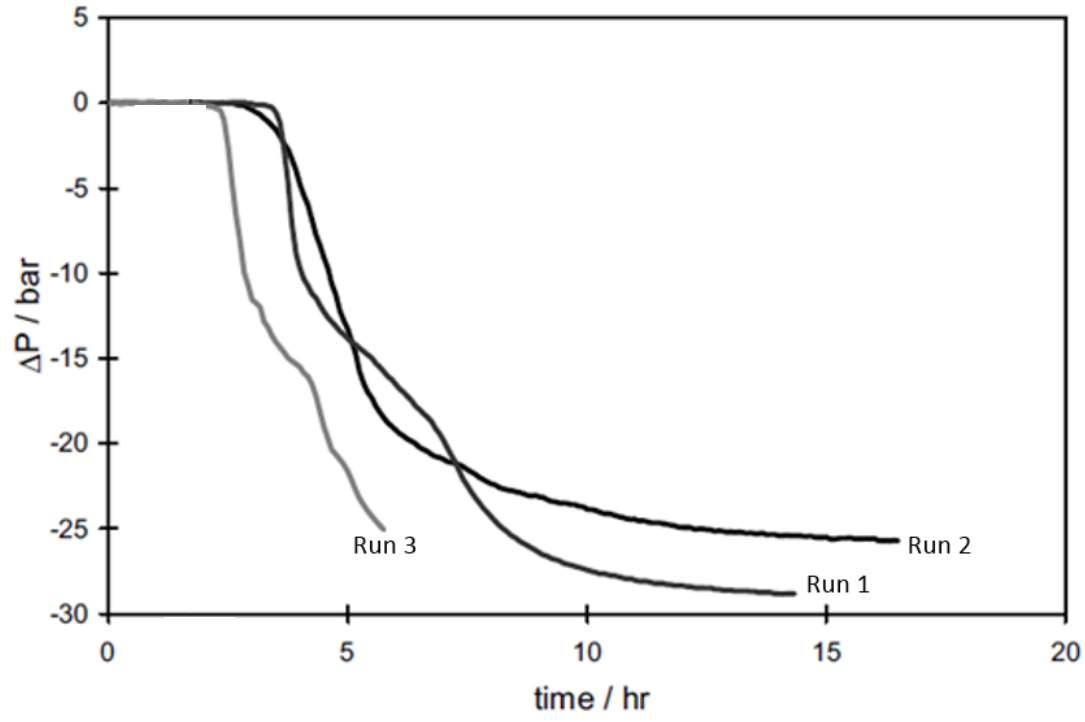

Figure 3.3 NG + 2.5 mass % Luvicap EG (75.8 barg)

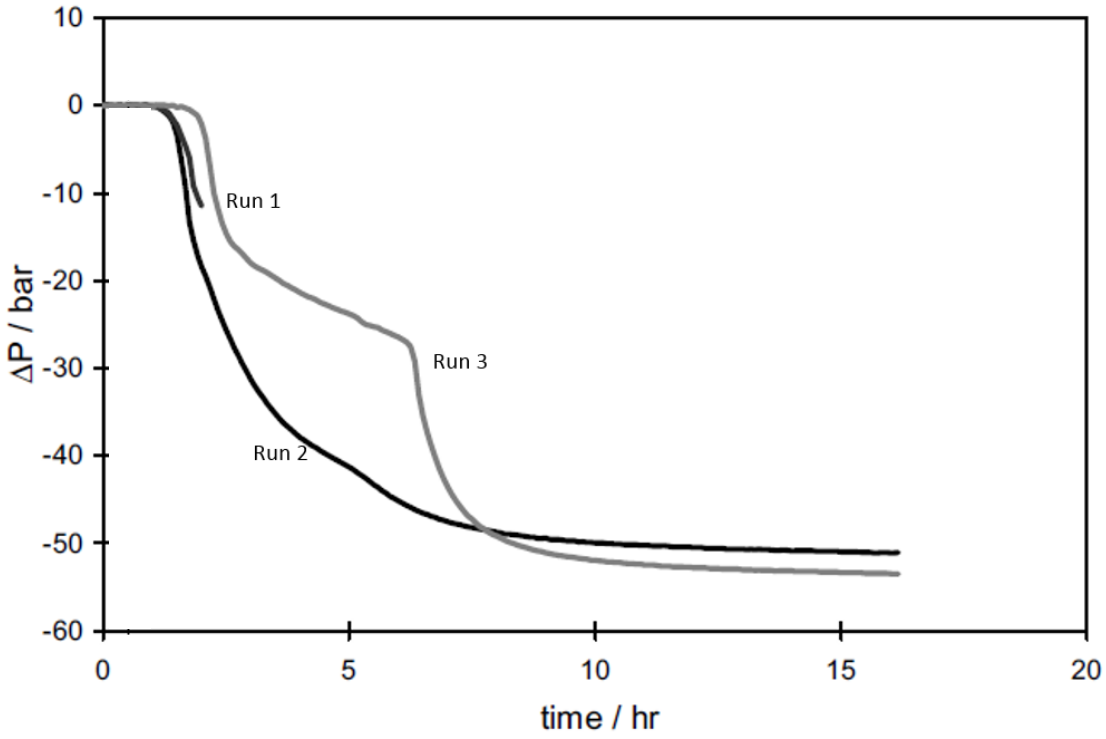

Figure 3.4 NG + 2.5 mass % Luvicap EG (109.2 barg)

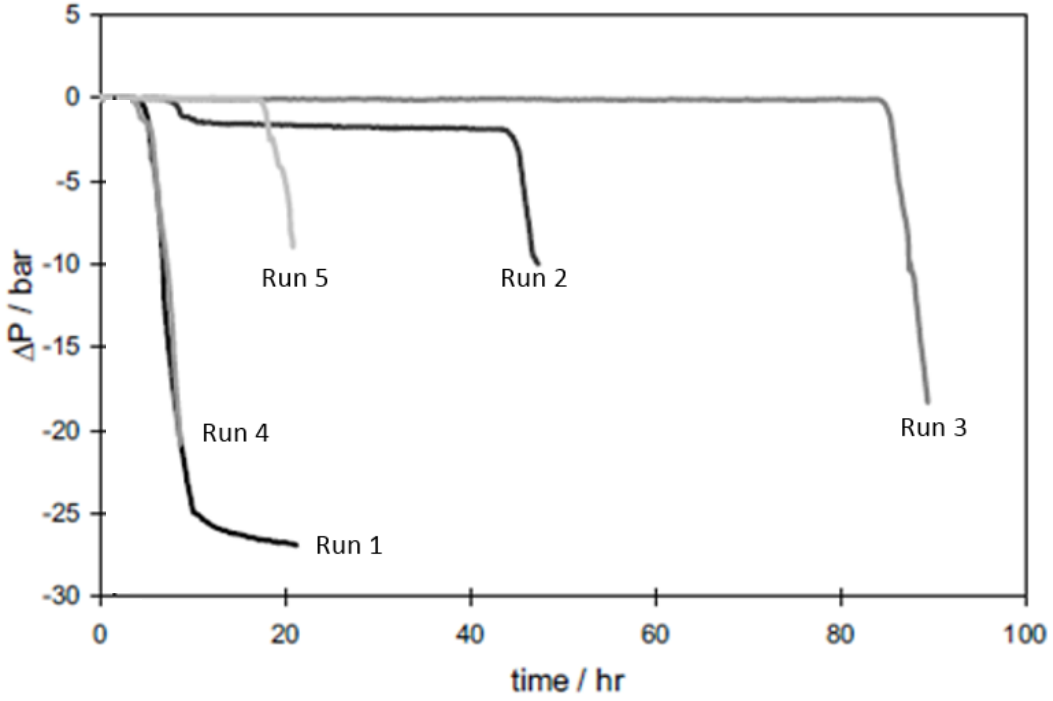

Figure 3.5 NG + 2.5 mass % Luvicap EG + 5 mass % NaCl

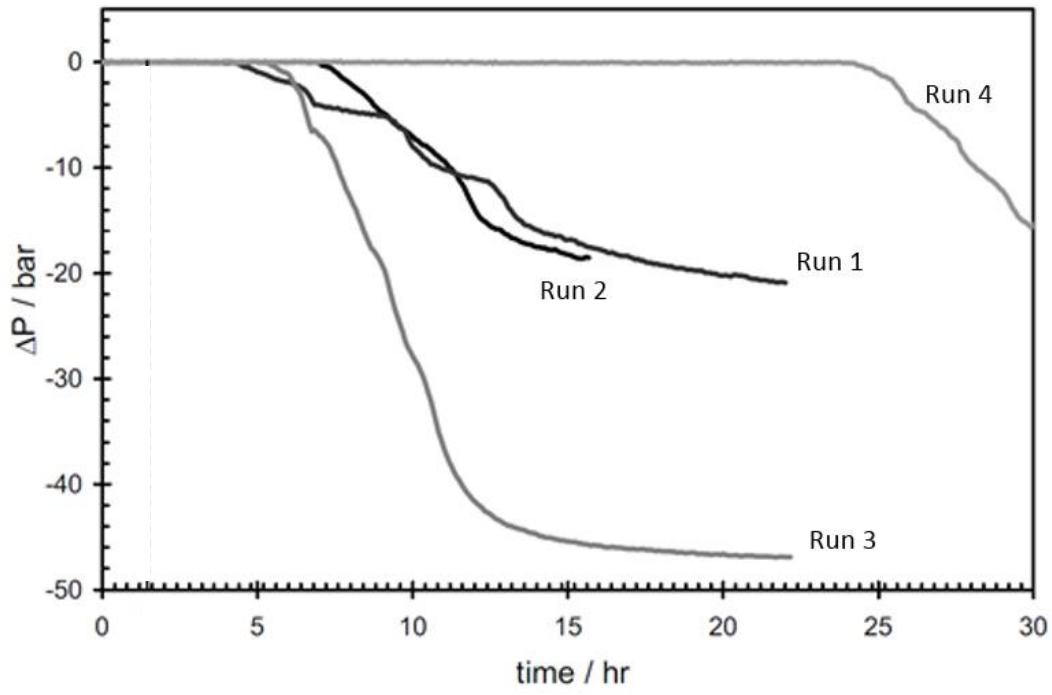

Figure 3.6 NG + 2.5 mass% Luvicap EG + 7.8 mass% NaBr

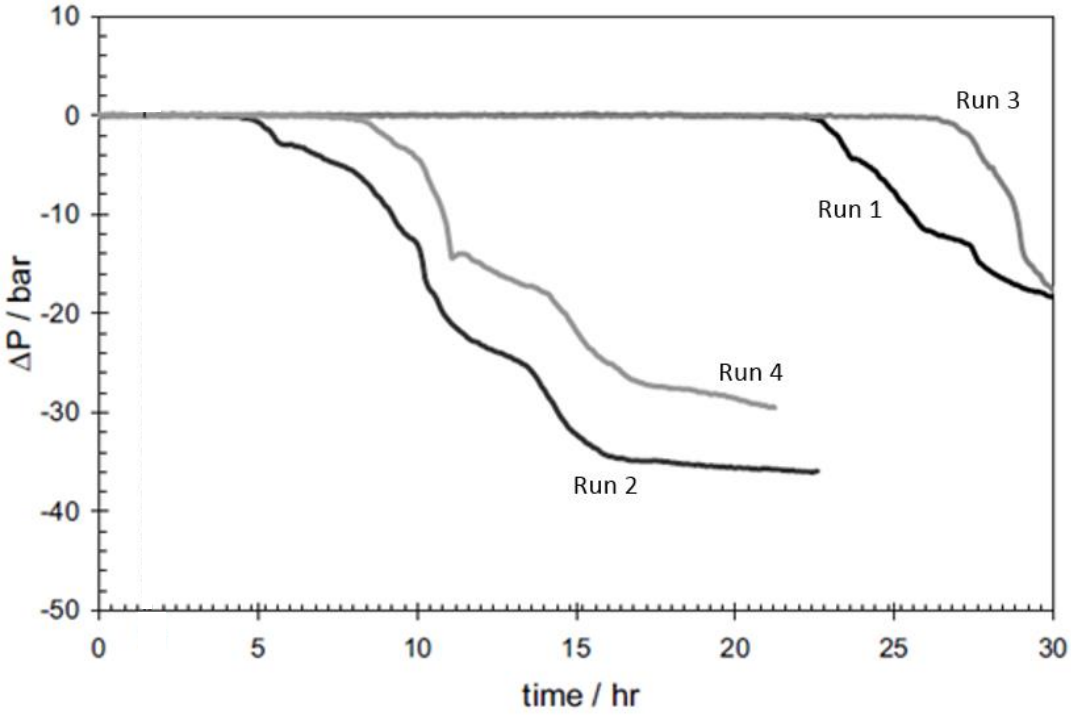

Figure 3.7 NG + 2.5 mass% Luvicap EG + 5.2 mass% KCl

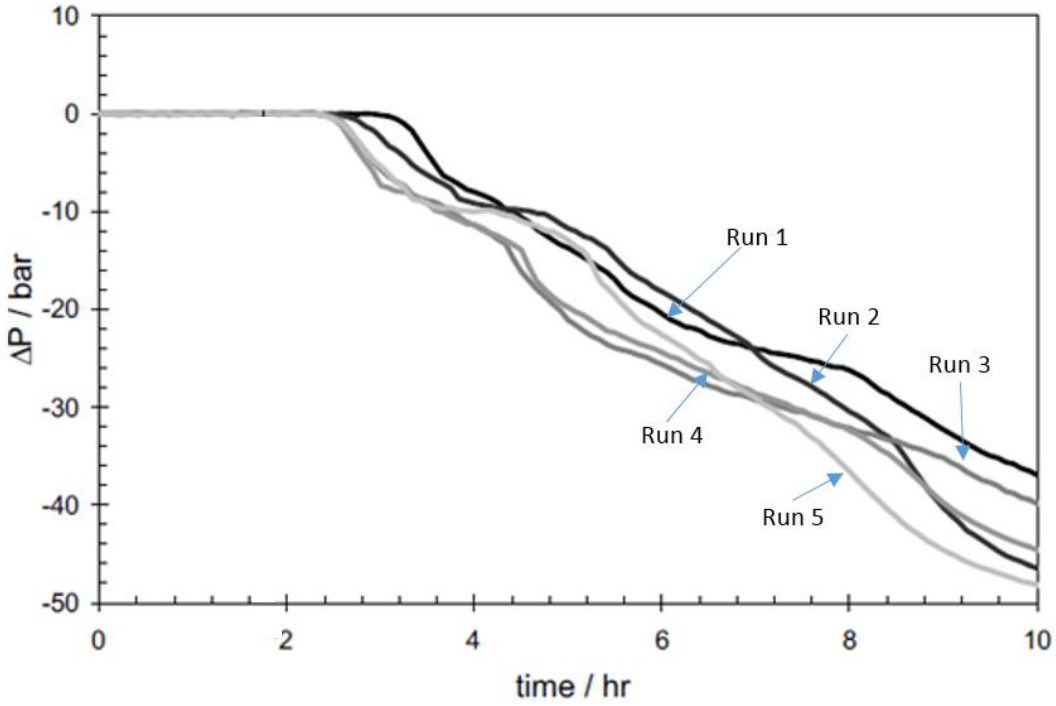

Figure 3.8 NG + 2.5 mass% Luvicap EG + 4.6 mass% $MgCl_2$

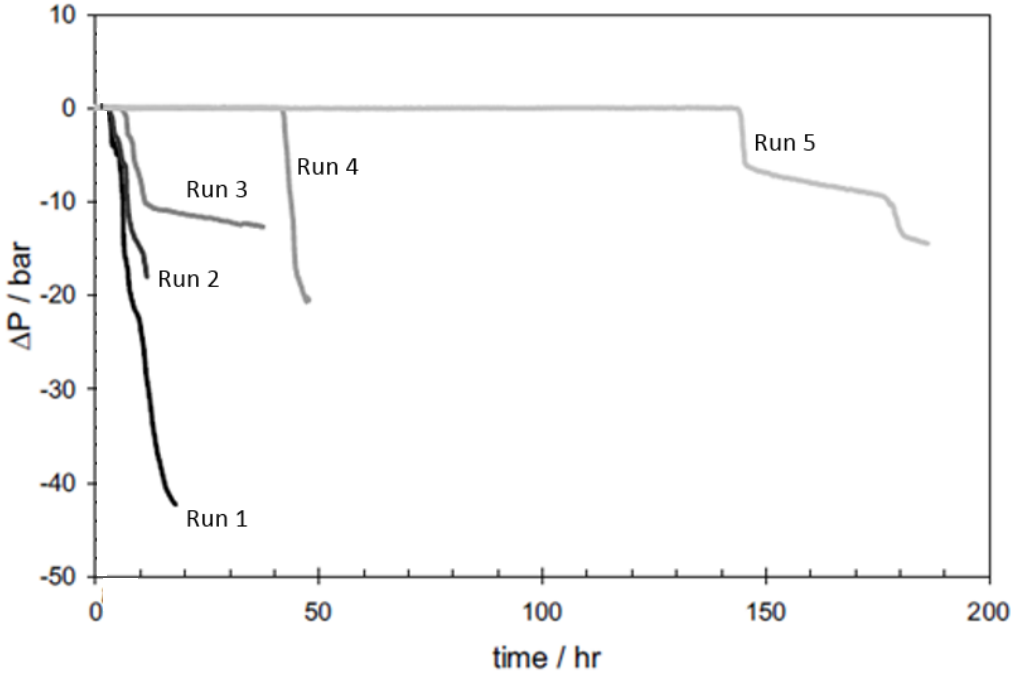

Figure 3.9 NG + 2.5 mass% Luvicap EG + 5.9 mass% $CaCl_2$

3.4 Results Discussion

The results presented have significant spread in the data, which is typical of the stochastic nature of hydrate nucleation. However, the data can be used to make a broad qualitative statement that the presence of salt seems to increase induction times prior to hydrate growth for natural gas PVCap systems. The increase in the ionic strength of the solution was calculated for each salt solution as shown in Table 3.3 and it demonstrates that the similar ionic strengths had no consistent impact to induction time, for example, $MgCl_2$ had negligible to no impact on performance unlike the other salts. The scatter in the results could be attributed to experimental scatter, however, general conclusions can be made that salts have a positive impact on PVCap performance.

The work presented by Sloan et al. (1998) seen in Figure 3.10 showed that mixed brine solutions had a negative or minimal effect on induction time at low concentrations and a positive effect at higher concentrations. The experiments conducted did not involve any experiments at low concentrations and the experimental data presented in this thesis is broadly in agreement with the previously reported work.

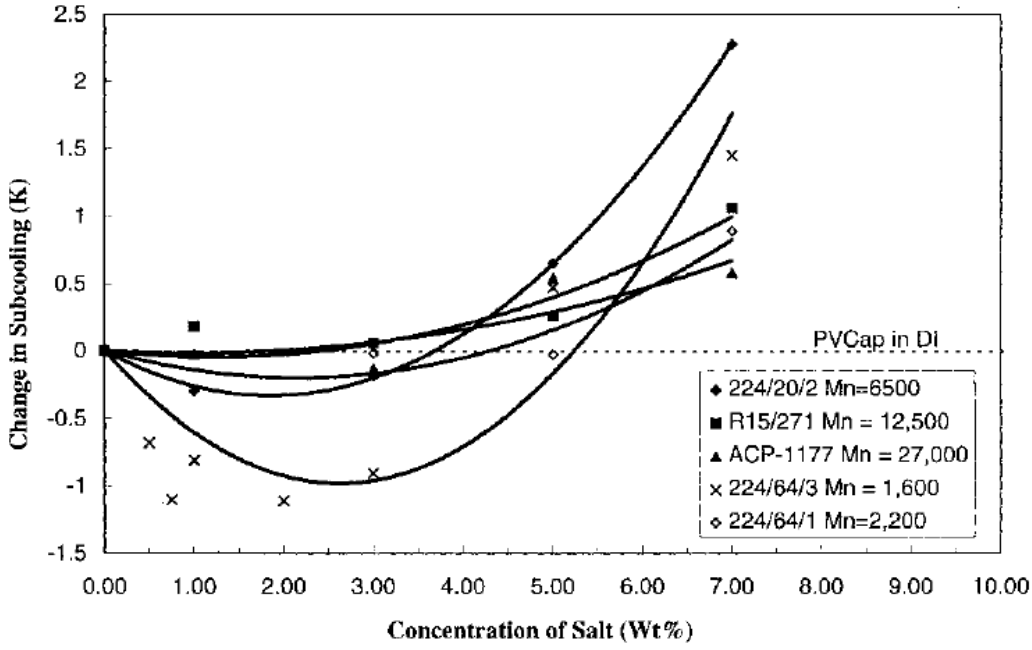

Figure 3.10. Impact of sea salt on varying lengths of PVCap polymers (Mn= molecular weight) from Sloan et al. (1998).

The data suggests that the mechanism of the synergy is due to salts increasing the polarity of the aqueous solution, which reduces the solubility of guest molecules to from hydrates. This is the opposite to methanol that increases the concentration of hydrate formers in the aqueous solution and could promote hydrate growth.

Figure 3.10 also shows data that investigated the impact of salt concentrations on the length of KHI polymer. The data suggests that salt does not impact the performance of longer polymer more than their shorter equivalents, which you would expect if the synergistic benefit is due to the salt impacting polymer conformance.

$MgCl_2$ did not have an impact on PVCap performance unlike the other salts. It remains unclear why $MgCl_2$ had no effect on induction time, it is possible that this could be due to the data quantity and the stochastic nature of the KHI induction time results from autoclave reactors. The rate of hydrate growth in the presence $MgCl_2$ is different to the growth for the other salts and unlike the other salts, there is no immediate rapid growth and it appears subdued. This could be indicative of impurities such as from impeller wear that could have resulted in seeds to accelerate hydrate nucleation, however the KHI was

impacting the growth. The use of the new technique by Anderson et al. (2011) where hydrate seeds are created prior to testing KHI growth is expected to eliminate this experimental scatter and it is proposed as further work.

Chapter 4: The Effect of 2-Butoxyethanol on the Performance of PVCap

The selection of a carrier fluid is a key decision of KHI suppliers. Traditionally this has been ethylene glycol, which is a good solvent for water soluble KHI polymers.

There are a great variety of chemicals that have claims attributed to have synergistic properties, including: corrosion inhibitors, quaternary ammonium salts, alcoholic and glycolic solvents (Kelland (2006)). The only published work discovered in regards to the "synergy" phenomenon is attributed to Cohen et al. (1997), which describes experimental work into the application of glycol ethers as synergists with vinylcaprolactam based polymers (PVCap, Gaffix VC-713®). Cohen et al. (1997) demonstrates that certain glycol ethers are effective synergists with these polymers, and concluded that the best chemical from this chemical family is 2-butoxyethanol also called Propylene Glycol Propyl Ether (for Gaffix VC-713®) and presents the idea of an optimum synergist concentration. Cohen et al. (1997) concludes with the hypothesis that the hydrophobicity of the alkoxy group on the ether may associate/interact with the dissolved polymer and alter the polymer's conformation in solution. This means that the glycol ether synergist keeps the polymer more open or unwound, and thus increases the surface area/active sites for inhibitor performance.

The 2-butoxyethanol molecular structure is shown in Figure 4.1. It is a molecule with a mixture of polar alcohol and alkoxy groups with non-polar alkane components.

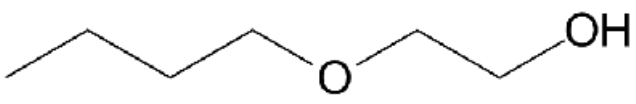

Figure 4.1. 2-Butoxyethanol molecular structure

4.1. Polymers in Dilute Solution

The conformation of a polymer in a solution depends on a variety of factors, including interactions between solvent and polymer molecules, conformational effects arising from the polarity and steric bulk of the substituent groups, and restricted rotation caused by resonance, for example, of the type common to polyamides. Soluble polymeric molecules such as the common kinetic inhibitors in dilute solutions can be considered to be distinct, and do not interfere or entangle with each other, due to the spatial area involved. The molecules can also be considered as approximate spheres or balls due to the tendency of the polymers to self-associate. This self-association is reduced if the polymer is in a better solvent or if the temperature is raised. This has been illustrated in Figure 4.2.

It follows that if the self-association is increased, the specific surface area of the polymer exposed to the solution is lowered. The implication for this in regards to hydrate inhibition is that with better solvents/synergists, more polymer can be exposed to actively inhibit hydrate formation. This implies that careful selection of solvents is required to optimise the overall performance of polymeric kinetic hydrate inhibitors.

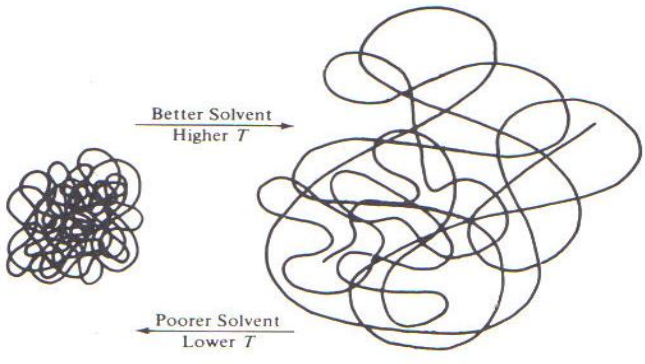

Figure 4.2. The effects of solvent strength and temperature on a polymer molecule in solution. (Rosen, 1993)

It follows that as the polymer length increases, this self-association is extenuated, because the longer polymer is able to twist on itself to a greater extent. From this theory it is hypothesized that the longer the polymer, the larger the change in inhibition performance due to a presence of a specified synergist concentration. This is due to the fact that

initially, the longer polymers will be self-associated to a greater extent than their shorter counterparts, and will be able to unwind to a larger extent in the presence of the synergist.

Based on this hypothesis; experimental work was conducted to examine the effect of a known synergist, on the kinetic inhibition performance of various lengths of a KHI.

4.2. Experimental Work

PVCap with 2-Butoxyethanol were selected for our inhibitor synergist mixture. This was based on experience of this system in previous studies at Heriot-Watt and published data by Cohen et al. (1998), and due to the availability of three different PVCap polymer lengths to test. The polymers used are described below:

- LUVICAP® (2000-8000 Daltons, dry polymer)
- LUVISKOL® (~100,000 Daltons, 40% active polymer based in ethanol)
- LUBASIN® (~1,000,000 Daltons, 40% active polymer based in ethanol).

To compare the polymers, it was required the remove the polymers from their commercial solvents to attain a dry polymer, as LUVISKOL®, LUBASIN® both are dissolved in ethanol that is a known antagonist of PVCap for hydrate inhibition. The polymers were separated from ethanol via drying in an open beaker in an autoclave at 80 °C for 2 days, then subsequent addition of water and a repeat of drying by heating at 90 °C for 2 days, then at 100 °C for 1 day. It was required to constantly break the surface of the polymer during drying, as the polymer created a crust. It was discovered that it was desirable to use flat large surface beakers for the drying to increase surface area for evaporation. LUVICAP® was supplied dry, and thus there was no requirement for separation. A concentration of 1 mass% active polymer (1.5 mass% Luvicap) with concentrations of 0%, 0.75% of 2-butoxyethanol, was made up with distilled water for the three different polymers.

The tests were conducted in a 200 ml, stirred, stainless steel, jacketed reactor. The reactor was charged with 100 ml of the specified solution and pressurised with natural gas. The vessel was then cooled, with the stirrer speed set to 600 rpm. To remove water history the temperature was raised to 32 °C for 20 hours for LUVICAP®, and 26-28 °C for 20 hours in regards to the heavier LUVISKOL® and LUBASIN®. This was done because deposition onto the metallic surfaces of the rig was witnessed in previous experiments (with LUVISKOL®).

Multiple tests were conducted to determine the maximum subcooling that the specified inhibitor solutions could delay the onset of hydrate growth and nucleation. Not all tests are presented, only the tests at conditions that the KHIs could provide a measurable induction time.

4.3 Results

Table 4.1. The results of the tests in a kinetic rig on natural gas-water system in the presence of different inhibitors /inhibitor and synergists.

LUVICAP® 1%- no synergist	Run	T (°C)	Pressure (bar)	Subcooling (°C)	Induction time (hrs)
	1	7.3	105.352	11.1	0
	2	7.9	106.041	11.2	0
	3	7.9	106.179	10.6	0 (slow formation)
	4	8.1	106.593	10.4	5.5

LUVICAP® 1% with 0.75% 2-butoxyethanol	Run	T (°C)	Pressure (bar)	Subcooling (°C)	Induction time (hrs)
	1	7.7	100.870	10.4	3
	2	6.7	100.112	11.4	0
	3	6.9	100.319	11.2	0
	4	7.5	100.663	10.6	5

LUVICAP® 1% with 1.5% 2-butoxyethanol	Run	T (°C)	Pressure (bar)	Subcooling (°C)	Induction time (hrs)
	1	7.4	100.663	10.7	0
	2	8.0	101.491	10.2	5.5
	3	8.0	101.215	10.2	5.5
	4	8.5	101.767	9.7	No formation

LUVISKOL® 1%- no synergist	Run	T (°C)	Pressure (bar)	Subcooling (°C)	Induction time (hrs)
	1	7.2	92.528	10.5	0
	2	7.1	91.976	10.5	0
	3	7.4	92.289	10.3	7
	4	8.0	92.597	10.1	No Formation

LUVISKOL® 1% with 0.75% 2-butoxyethanol	Run	T (°C)	Pressure (bar)	Subcooling (°C)	Induction time (hrs)
	1	5.6	89.218	11.9	0
	2	5.8	89.080	11.7	1
	3	5.8	89.218	11.7	1.5
	4	6.3	89.977	11.2	No Formation

LUBASIN® 1%- no synergist	Run	T (°C)	Pressure (bar)	Subcooling (°C)	Induction time (hrs)
	1	9.1	92.321	8.6	0
	2	9.0	92.252	8.7	0
	3	9.4	92.941	8.3	18
	4	9.5	92.941	8.2	No formation

LUBASIN® 1% with 0.75% 2-butoxyethanol	Run	T (°C)	Pressure (bar)	Subcooling (°C)	Induction time (hrs)
	1	8.3	99.216	9.7	0
	2	9.2	99.836	8.8	No formation
	3	8.9	99.629	9.2	0
	4	9.4	99.836	8.7	No formation

Table 4.1 shows the results of the experimental work carried out in the stirred autoclave reactors for the various inhibitors.

In Table 4.2 the summary of the results is shown with emphasis on the temperature at which the induction time disappears i.e. less than 120 minutes. This value of subcooling taken is the arithmetic average between a point of "no induction" (t_i<2 hours), and a point where there is a significant induction time (t_i>2 hours).

Table 4.2. Synergism effect of different concentrations of 2-butoxyethanol on different PVCap polymer lengths.

	Level of subcooling where no induction time present and % difference in performance					
	0% 2-butoxyethanol		0.75% 2-butoxyethanol		1.5% 2-butoxyethanol	
LUVICAP®	10.5 °C	-	10.9 °C	3.8%	10.1 °C	-3.7%
LUVISKOL®	10.4 °C	-	11.5 °C	10.6%	-	-
LUBASIN®	8.3 °C	-	9.0 °C	8.4%	-	-

4.4 Results Discussion

The benchmark for the analysis is the highest level of subcooling where the polymer is able to provide a measurable induction time to hydrate formation. The results show that there is an improvement in inhibitor performance in the presence of 0.75% 2-butoxyethanol for both of the longer polymers, with 10.6% and 8.4% improvement for LUVISKOL® and LUBASIN® respectively. There was a negligible improvement of 3.8% for the shorter LUVICAP® polymer in the presence of 0.75% 2-butoxyethanol. In the presence of 1.5% 2-butoxyethanol, the performance of LUVICAP® was reduced by 3.7%, which reduced performance but may still be within experimental accuracy.

The results have shown that the shorter length polymers are more effective at inhibition than their longer counterparts at similar mass%. This is attributed to the fact that the shorter polymer has a larger surface area exposed to the solution, for the same mass of polymer as it is expected that self agglomeration is more prevalent in the larger polymer.

The addition of the synergist had a greater positive effect on the longer polymers, which supports the proposed hypothesis that the synergist reduces self-agglomeration of the polymers, which is expected to be more significant in the larger polymers than their shorter counterparts, as longer polymers have potential to twist up on themselves to a greater degrees.

The increase of 2-butoxyethanol from 0.75 mass% to 1.5 mass% reduced the performance of the inhibitor. Cohen et al. (1998) describes the concept of an optimum inhibitor concentration, which may have already been passed in this case. This data suggests that too much of a solvent or synergist may become an antagonist to the inhibitors at higher concentrations.

It is unclear how 2-butoxyethanol impacts the conformation of a polymer. It is a compound with a mix of ionic and non-ionic components and could behave like a solvent. For example, the butane element of 2-butoxyethanol could associate with the polymer on its non-ionic components such as the aliphatic carbon ring or the carbon backbone, and the ionic alkoxy or alcohol groups of 2-butoxyethanol could associate with the water solution. This would effectively increase the polarity of the polymer, thus increasing solubility and prevent the level of self-agglomeration of the polymer. Further work is proposed to conduct molecular dynamic simulation with this system to better understand how the 2-butoxyethanol molecule interacts with the large PVCap polymers in aqueous solution.

Chapter 5: The Effect of Condensate on the Performance of KHI

The effect of various components present in reservoir fluids on the performance of kinetic hydrate inhibitors is of interest to KHI designers and suppliers. The performance of KHI in the presence of a condensate phase has not been investigated. Accordingly, this phenomenon is of concern to those using, developing and testing these inhibitors. The aim of the work detailed in this chapter is to test these conditions, with the intention of providing insight into ways of enhancing inhibitor performance/formulations.

There are several possible effects of condensate on KHI, which include:

- Dissolution of the polymer and/or synergist into the organic/condensate phase.

- The interface between hydrocarbon and water can be different from that of water and gas for mixed systems. This implication is that there may either be a larger or a smaller interface for mass transfer into the organic phase and/or a reduction of the inhibitor concentration on the interface due to a larger surface area (if inhibitor is surface active).

- Negative effect of dissolved component in the condensate including natural components or added components such as corrosion inhibitor. Due to the complex nature of the various components of a "real" condensate, this is not explored further in the thesis.

Two series of tests were carried to investigate the impact of a condensate on KHI. The first series of tests aimed to investigate the extent of dissolution of inhibitor components in the organic phase. This consisted of drying tests and GC tests to investigate the location of inhibitor components in the various phases of a condensate/water inhibited system.

The second series of tests aimed to investigate the difference in effect of natural condensate mixtures and synthetic condensates mixtures, to establish if the effect was due to natural components in the condensate or due to the alkane fraction of the condensate.

These tests involved a series of experiments in kinetic autoclave rigs to assess the performance of inhibited systems with a synthetic condensate.

5.1 Investigation of the Solubility of Inhibitor Components in the Various Phases

The location of inhibitor components undoubtedly plays an important role in the performance of KHI solutions. The dilution of either a polymer or synergist may have negative effects on inhibitor performance, and thus may lead to hydrate formation and the associated flow assurance problems. This work was designed to look at various KHIs to see if there is any loss of the inhibitor components from the aqueous phase to the organic phase.

5.1.1 PVCap Polymer and Ethylene Glycol Solubility

The first series of tests were conducted with the aim of identifying the phase location of the inhibitor components of Luvicap in a water and synthetic condensate system. 150 ml of an aqueous solution consisting of 2 mass% of PVCap and 3 mass% ethylene glycol was made up (5% Luvicap), 100 ml of this solution was added to 50 ml of chromatography grade n-heptane and two samples were taken from the remaining 50 ml. The resultant liquid was then mixed with a magnetic bar stirrer for 6 hours in a covered beaker. The mixture was then settled for 24 hours. 2 samples were taken from both phases and they were weighed. The samples were then heated at 110 °C for 24 hours to remove any water and heptane, and the samples were weighed once again. The samples were then heated to 200 °C for 48 hours to remove the ethylene glycol, and were once again weighed. The results for the test are shown in Table 5.1.

Table 5.1 Luvicap Solubility Test Result

	Unmixed Solution		Aqueous Phase		Organic Phase	
Test No.	1	2	1	2	1	2
Empty beaker (g)	41.43	40.60	43.61	41.37	40.71	40.59
Beaker & liquid (g)	106.52	115.34	114.07	110.68	83.59	80.22
Liquid (g)	65.09	74.74	70.46	69.31	42.88	39.63
Beaker & liquid @ 110 °C (g)	44.60	44.28	47.04	44.79	40.71	40.59
Beaker & liquid @ 200 °C (g)	42.64	41.99	44.93	42.68	40.71	40.59
Polymer & EG conc. (mass%)	4.87	4.92	4.86	4.94	0.00	0.00
Polymer conc. (mass%)	1.86	1.86	1.87	1.89	0.00	0.00
EG conc. (mass%)	3.01	3.06	2.99	3.05	0.00	0.00

The results show that after mixing, both the polymer and the synergist are only present in the aqueous phase. It was also visually observable that no components were present in the organic phase. Thus, any effect of a condensate on the performance of Luvicap cannot be explained via the theory that inhibitor components are lost to the organic phase.

5.1.2 Polymer Solubility Tests for Commercial Inhibitors

The tests to identify the phase solubility of PVCap and ethylene glycol is not sufficient to satisfactorily claim that all inhibitor components enter the aqueous phase, as other polymers and other carrier solvents and synergists are used in commercially available blends. Thus, the work was extended to include “real inhibitors”. The previous test procedure cannot be used for inhibitors with unknown solvents and polymers due to the unknown boiling points of the unknown inhibitor components, thus an alternate procedure was required to identify the phase concentration of the inhibitor components.

This procedure involved the mixing of 50 ml of n-heptane (Aldrich-GC grade) with 100 ml of the appropriate aqueous inhibitor solution in a beaker, the beaker was then covered with cellophane and vigorously mixed by a magnetic bar stirrer for 4 hours, and the solution was allowed to settle for a further 24 hours. Approximately 25 ml of the organic phase was weighed and then heated to 200 °C for 48 hours, and was then weighed

again. If no dry residual mass was left, the remainder of the sample was taken to be analysed via GC and compared to the chromatogram of the pure heptane. If residue remained it would not be possible to use the GC due to possible damage to the GC equipment.

5 inhibitors were tested as shown in Table 5.2. The drying of the organic phase resulted in no remaining residue for all the inhibitor solutions with the exception of KHI B. After the settling of KHI B, it could be seen that the hydrocarbon phase was cloudy, and after drying the hydrocarbon phase it could be seen that there was some orange residue similar to dried PVCap. From the weighing residue from the two phases, it was possible to calculate that the change in weight distribution of the polymer in solution after mixing, which was 13% in the hydrocarbon phase and 87% in the aqueous phase.

Table 5.2 Inhibitors Tested in Drying Tests

Inhibitor	Concentration in aqueous phase
Luvicap	2.5 mass%
Luvicap & 2-butoxyethanol	2.5 mass% Luvicap & 1.75 mass% 2-butoxyethanol
KHI A	5 vol%
KHI B	5 vol% (Not tested with GC)
KHI C	5 vol%

The results on the drying tests for all other polymers apart from KHI B implied that minimal polymer entered the hydrocarbon phase. This meant that all the hydrocarbon phases for the other inhibitors could be tested via GC. The tests with GC involved a simple comparison between GC analysis of the pure heptane, and the heptane contacted with the inhibitor solutions.

The results of the GC tests for Luvicap seen in Figure 5.1 showed that small traces of chemical components exist in the hydrocarbon phase (not seen in the pure heptane GC results). These are believed to be either remnants of components used in the polymerisation process and are in such small quantities that it is not believed that they can have any significant effect on inhibition. Similar impurities were seen for both KHI A and KHI C.

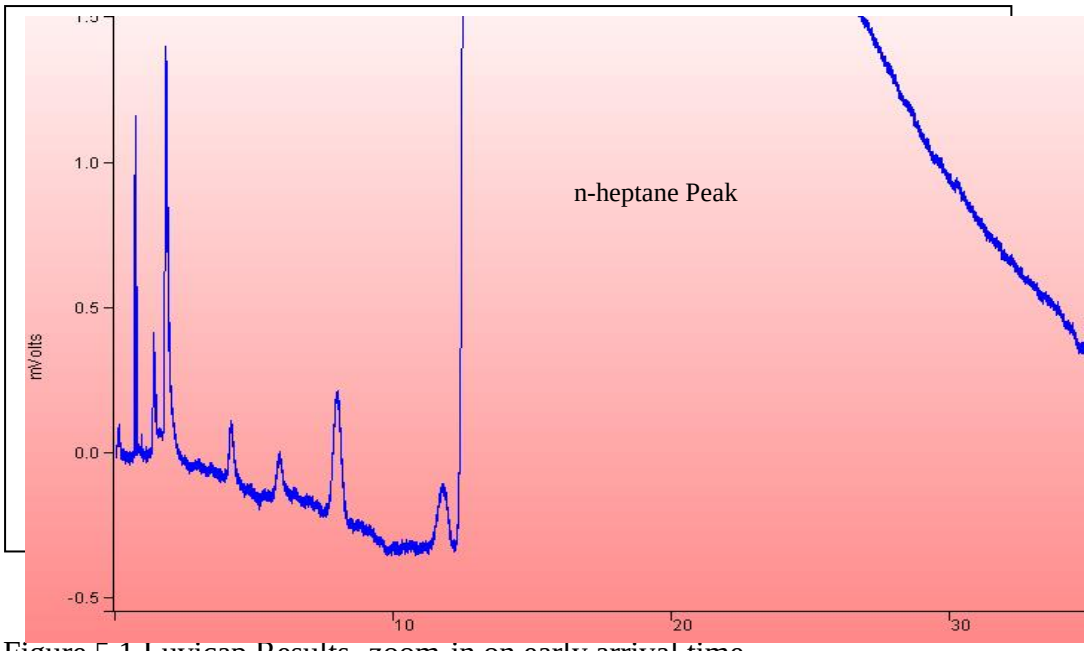

Figure 5.1 Luvicap Results- zoom-in on early arrival time.

The only test which resulted in significant quantities of material in the organic phase involved the testing of Luvicap & 2-butoxyethanol. The results can be seen in Figure 5.2 which showed that 2-butoxyethanol enters the hydrocarbon phase.

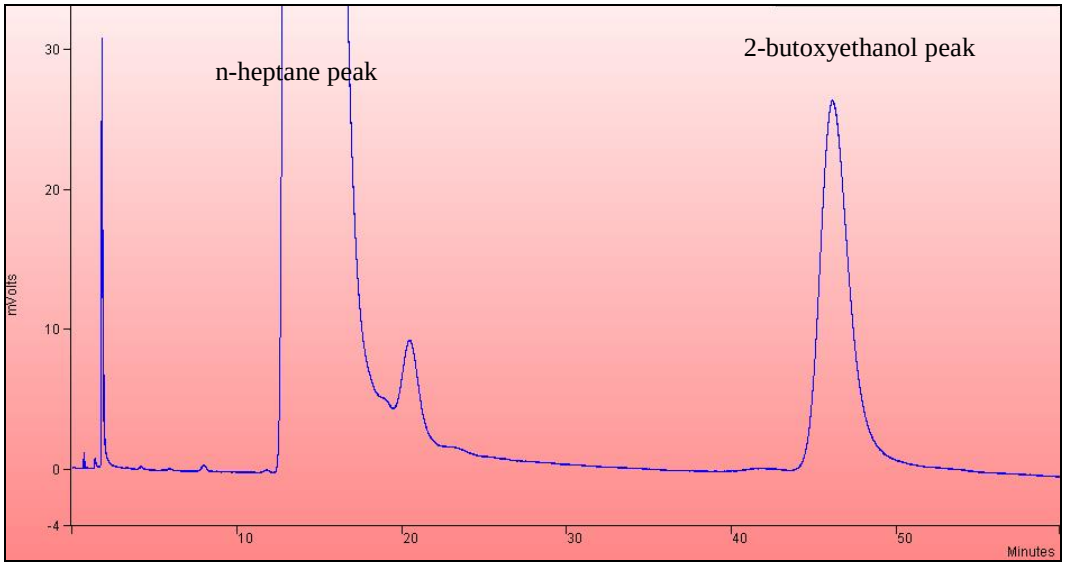

Figure 5.2 Luvicap & 2-butoxyethanol Results

Two further GC tests were conducted, one with a 50:50 vol mixture of 2-butoxyethanol and n-heptane (fully soluble), and another with a 50:50 vol mixture of ethylene glycol and n-heptane (immiscible). The aim of these tests was to determine if the solubility of the

components were significant in the organic phase, and the location of their indicative peaks. The results showed that the 2-butoxyethanol entered the hydrocarbon phase, whereas the ethylene glycol was completely insoluble in the heptane.

5.1.3 Solubility/GC Test Result Summary

The solubility tests and the GC tests showed that all of the inhibitors tested with the exception of one inhibitor (KHI B) remained in the aqueous phase, the results also showed that from the carrier solvents and synergist tested, only 2-butoxyethanol entered the hydrocarbon phase.

This work serves to highlight the importance of inhibitor and solvent location in inhibited solutions. The fact that 2-butoxyethanol enters the hydrocarbon phase may explain why it is not used as a carrier fluid in commercial KHI even though it is a proven synergist in the lab, whereas ethylene glycol stays in the aqueous phase.

5.2 Investigation of PVCap Performance with Synthetic Condensate Systems

Tests were conducted in a high pressure stirred autoclave to evaluate the effect of synthetic condensate on PVCap. It was decided to test PVCap with chromatography grade n-heptane (Aldrich).

5.2.1 Methodology

Tests were conducted in a 1200 ml high pressure stirred autoclave, with a liquid volume of 600 ml consisting of 300 ml condensate and 300 ml of aqueous solution consisting of 1% PVCap (2.5% Luvicap). A blank test of 600 ml of the aqueous solution was carried out for comparison. The rig was pressurised with the natural gas with a composition outlined in Table 2.1, and the rig was cooled to 4 °C and was stirred at 600 rpm for all tests.

5.2.2 Results

Table 5.2 represents the conditions for the tests carried out, including the temperature, pressure, the associated dissociation temperature, subcooling and induction time.

The calculation of the phase boundaries for the natural gas, heptane, and inhibitor solution was achieved by using HWHYD. Figure 5.3 illustrates the phase boundaries calculated using this software. For this calculation, it was necessary to calculate the molar composition of each phase, this was achieved by the use of Wichert and Aziz correlations and the Katz “standing chart” to attain a compressibility factor (Z) for the gas phase.

Table 5.2 Kinetic rig results for the effect of a condensate phase on the performance of PVCap.

600 ml of 2.5 wt% Luvicap aqueous solution.

Run	T (°C)	P (bar)	Dissociation Point (°C)	Dt (hours)	Subcooling (°C)
1	3.8	100	18.0	~35	14.2
2	3.7	100	18.0	>22	14.3
3	4.0	115	18.8	8	14.8
4	3.8	115	18.8	0	15.0

300 ml 2.5 wt% Luvicap aqueous solution and 300 ml n-heptane combined.

Run	T (°C)	P (bar)	Dissociation Point (°C)	Dt (hours)	Subcooling (°C)
1	3.7	114	14.9	6	11.2
2	4.0	113	14.8	6	10.8
3	3.8	113	14.8	3	11.0
4	4.2	109	14.6	18	10.4
5	4.4	111	14.7	15	10.3
6	4.5	112	14.7	18	10.2

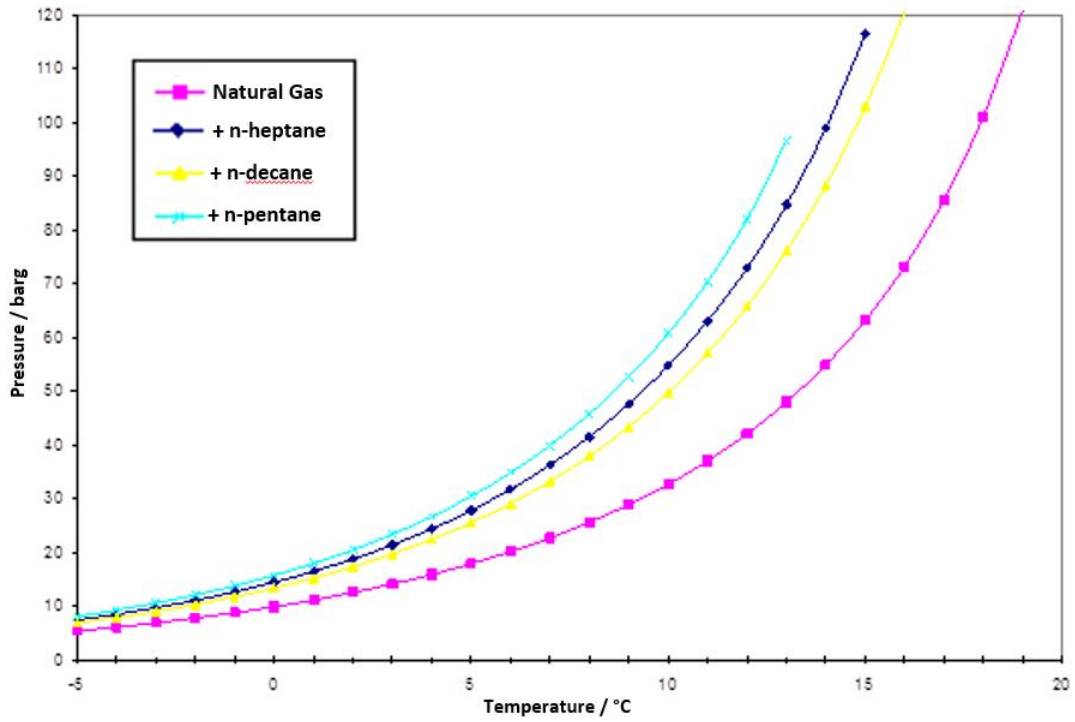

Figure 5.3. Hydrate Phase boundaries for a Natural Gas with different hydrocarbon phases calculated with HWHYD.

As can be seen from Figure 5.3, the phase boundary changes with added hydrocarbon phase. This is due to an appreciable solubility of the heavier hydrate forming gaseous components dissolving in the condensate phase which in turn means a lower concentration of the hydrate formers in the aqueous phase, and thus the phase boundary of the system changes.

5.2.3 Autoclave Tests Result Summary

The results show that there is a clear negative effect of an alkane phase on the performance of PVCap. The pure PVCap system can inhibit the formation of hydrates for 12 hours at a subcooling of 14.2 °C; whereas the addition of the n-heptane reduced the performance of the PVCap so that a subcooling of 10.4 °C or less is required to inhibit hydrates for more than 12 hours. The subcooling to which PVCap can inhibit hydrate formation seems high, though the data is comparable to other tests using PVCap in the same rig.

5.3 Discussion

The initial drying tests and GC tests suggest that the negative effect of the condensate phase is not due to components of the inhibitor entering the hydrocarbon phase as the tests proved that the majority of the KHI and solvents tested are water soluble.

The autoclave results demonstrate that the presence of hydrocarbon phase itself affects the performance of PVCap at similar level of subcooling. It is proposed that the effect may be due to either: an increase of the mass transfer of hydrate formers into the aqueous phase and the possible dilution of the KHI if it is surface active; or the dissolution of the heavier molecules such as n-butane that occupy the larger sII hydrate cage in the condensate resulting in the sI and sII hydrate phase boundaries being closer together, and then the subsequent failure of PVCap due to its inability to inhibit sI hydrate. These are discussed below.

The addition of a liquid hydrocarbon phase in a stirred autoclave has the potential to significantly alter the surface area between the aqueous phase and the hydrocarbon phase as illustrated in Figure 5.4. In (a) the autoclave does not have a liquid hydrocarbon phase

and the surface area for hydrate formers is restricted to the liquid gas interface. In (b) the addition of liquid hydrocarbon has the potential to significantly increase the contact area between the aqueous and hydrocarbon phase by the addition of the liquid hydrocarbon and water interface. This could increase the mass transfer of hydrate formers to the aqueous phase or reduce the concentration of the KHI if they are present at the aqueous interface. This area is significantly impacted by stirring rates in the autoclave.

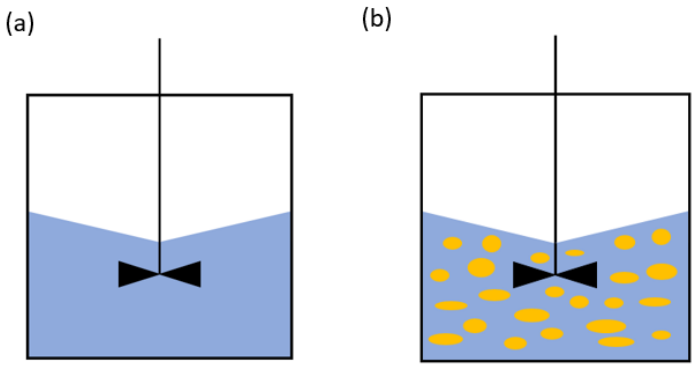

Figure 5.4. The impact of the addition of a hydrocarbon phase on the mass transfer interface in a stirred autoclave.

The addition of a hydrocarbon impacts the relative position of the sI and sII hydrate phase boundaries. This happens because the addition of a hydrocarbon phase dissolves heavier molecules such as n-butane that occupy the larger sII hydrate cage, which results in the sII hydrate phase boundary moving closer to the sI hydrate phase boundary, which mostly remains unchanged. This is important as the criteria used to evaluate KHI efficiency is the subcooling to the sII boundary and it is possible that hydrate formation may be due to the failure of KHI to inhibit sI hydrates; of which very few KHI effectively inhibit sI hydrates. This is illustrated in Figure 5.5 where a system of natural gas and natural gas plus condensate with an alkane phase are compared with similar sII hydrate levels of subcooling, where it can be seen that the sI hydrate subcooling is much higher for the system with the alkane phase in relation to the equivalent subcooling of the sII hydrate and that could result in the failure of the KHI.

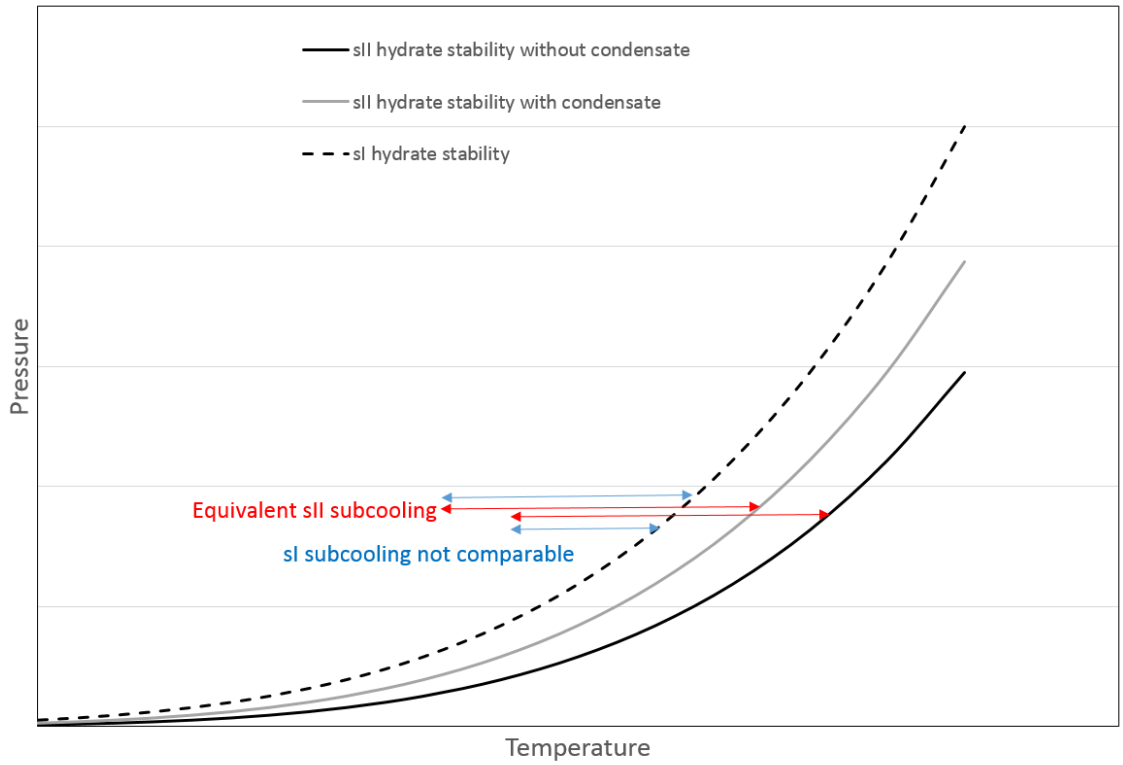

Figure 5.5. The relationship between sI and sII hydrate at comparable sII hydrate subcoolings in the presence and absence of an alkane phase.

Further work is proposed to validate the theory described above in relation to the sI hydrate curve. It is proposed to investigate this by repeating the tests with aqueous PVCap solution with and without n-heptane at the same pressure and temperature conditions. If similar KHI performance is evident between the two systems, it validates that PVCap's limitation to subcooling is at least in part due to an inability to prevent sI hydrates as previously discussed. The procedure described by Anderson et al. (2011) would also enhance the testing procedure and limit the scatter and uncertainty associated with the methodology used in the laboratory work.

Chapter 6: Molecular Dynamic Simulation to Investigate the Behaviour of Methanol and PVCap

The experimental work has shown that methanol has a negative effect on the performance of PVCap as a kinetic hydrate inhibitor. A proposed explanation for this phenomenon is that methanol alters the conformation of the polymer or associates to the polymer structure, and fundamentally altering the properties of the KHI. To independently verify this theory, molecular dynamic simulation has been carried out on a PVCap octamer in the presence and absence of methanol.

6.1 Molecular Dynamic Simulation

Molecular Simulation involves a series of techniques that are used to model or mimic the behaviour of molecules. The techniques are extensively used to investigate a wide variety of systems from large biological molecules such as enzymes, to relatively simple chemicals. Molecular simulation has been around since the 1950s, however the advent of the computer has made the process of simulation far more accessible to scientists, and has developed into a science it its own right (computational chemistry).

Molecular Simulation techniques are widely used to test specific theories, or to investigate rather general questions of fluid behaviour. One of the primary functions of molecular simulation is to act as a bridge between experiment and theory, where the computer simulation is used to test the theory independently. In practice, molecular systems generally consist of a vast number of particles, it is impossible to find the properties of such complex systems analytically; where molecular simulation circumvents this problem by using numerical methods.

In simple terms, the process of molecular simulation involves specifying the interactions of the molecules of interest and using various algorithms to calculate bulk properties, structure, and dynamics at the microscopic level. Two main categories of molecular simulation exist: Molecular Dynamic Simulation (MDS) and Monte Carlo simulation (MC).

MDS involves explicitly calculating the forces between the molecules, and then the motion of the molecules is computed using a suitable numerical integration method - essentially solving Newton's equations of motion (F=ma). Following Newton's laws and using the initial positions, velocities and forces, it is possible to calculate the positions and velocities of the atoms at a small time interval later. From these new positions, the forces are recalculated and a series of calculations over several time-steps are made. In a very crude sense, molecular modelling treats the molecules as a collection of weights connected with springs, where the weights represent the nuclei of the atoms and the springs represent the bonds.

MC simulation is used to calculate the bulk properties of a system by means of statistical mechanics. The method employs small random moves of the atoms in the system to generate sequences of atomic configurations, which is used in conjunction with a sampling algorithm to confine this “random walk” to thermodynamically meaningful configurations.

This study encompasses the use of molecular dynamic simulation. The main advantage that MDS offers over MC is that it offers time dependent properties of the molecules.

6.2. Summary of Simulation & DL_POLY

The MDS simulation was carried out by use of DL_POLY simulation package developed at Daresbury Laboratory by W. Smith, T.R. Forester and I.T. Todorov. The DL_POLY package requires the creation of three input files to run a simulation, which are called the FIELD, CONTROL and CONFIG files.

6.2.1 FIELD File

The FIELD file provides the input for the force field parameters which defines the interactions between the molecules. The values derived have a wide variety of analytical forms with some basis in chemical physics, which must be parameterised to give the correct energy and forces.

The energies included in the file are categorised into intramolecular and intermolecular forces. The intramolecular forces include: bond potentials, angle potentials, dihedral bond potentials. The intermolecular forces include the short ranged/van der Waals interactions and long ranged electrostatic/Coulombic potentials.

Bond Potentials

Bond potentials are used to define explicit bonds between specified atoms, and they are solely a function of the distance between atoms. These potentials ensure that the atoms of a molecule are at the correct spacing from each other.

Angle Potentials

The valence angle potentials describe the bond bending terms between the specified atoms. This makes it possible to model any set of molecules with a known bond angle. They require the specification of three atomic positions and are often called three body potentials. A classic example of this is water, where a non bonded pair of electrons ensures that the angle between the hydrogen bonds is 104.45°.

Dihedral Potentials

The dihedral angle potentials or torsion potentials describe the interaction arising from torsional forces in molecules. They require the specification of four atomic positions and are often called four body potentials. A classic example of a dihedral potential exists in ethane, this molecule consists of two carbon atoms and their three associated hydrogen atoms. The electron clouds of the hydrogen from both carbon molecules interact with each other and this in effect limits the freedom of the C-C bond to spin on its axis.

Short Range Interactions

The short-range interactions of a molecular system are dominated by van der Waals forces, which is a function of the effective size of an atom. These forces include both attractive and repulsive forces. These attractive forces involve the attraction between

temporarily induced dipoles in non-polar molecules as two non-bonded atoms are brought together and the van der Waals attraction between them increases (a decrease in energy). When the distance between them equals the sum of the van der Waals radii the attraction is at a maximum. If the atoms are brought still closer together there is strong van der Waals repulsion (a sharp increase in energy).

Long Range Interactions

The long-range interactions involve the Coulombic or electrostatic interactions between atoms with permanent charges.

For this simulation, the force field file used for the PVCap polymer was derived from Kvamme et al. (1997). In this simulation, the hydrogen atoms associated with the polymer have been consolidated to be included with their respective carbon atoms. In addition to this, the carbon ring has been considered to be a rigid body. Both these factors in the simulation are considered to be valid approximations due to the consolidation process and the inflexible nature of the carbon ring, and the need to significantly reduce simulation time. The unknown values and the intermolecular interactions were derived from AMBER (Assisted Model Building and Energy Refinement) software data files.

6.2.2 CONTROL file

The CONTROL defines the system control settings for the simulation. This includes: temperature settings, number of time-steps and equilibration time-steps, length of a time-step, ensemble used, the selection of various force algorithms used, and the selection of data recording.

For the simulations carried out, the target temperature was 280 K and a Nose-Hoover thermostat ensemble was used to control this temperature. The simulations included 100,000 equilibration steps and a further 300,000 steps, all of $1x10^{-3}$ picoseconds resulting in a total simulation time of 400 picoseconds. For the short term van der Waals interactions, a Lennard-Jones parameterisation system was used, with a cut off of 20 Angstroms. For the long-term Coulombic interactions, the Smooth Particle Mesh Ewald

(SPME) method was used. A radial distribution function (RDF) was calculated for all atoms with a sampling period of every 10 steps. Further information on the CONTROL file format can be found in Smith and Todorov (2006).

6.2.3 CONFIG file

The CONFIG file defines the initial location of the individual molecules. The initial shape and configuration of the polymer molecule was calculated by the use of the Cerius2 tool. The water and methanol boxes of suitable chemical composition were created by a programme developed in-house. A further in-house programme was used to add the polymer to the solvent box. To attain a feasible starting configuration for the polymer, it was necessary to continually build it up from a monomer, dimmer, tetramer and eventually into an octamer. The simulation with water contains one octamer PVCap molecule and 2154 molecules of water, which is equivalent to 2.8 mass% PVCap. The simulation with methanol contains one octamer PVCap molecule, 1672 molecules of water, and 288 molecules of methanol, which are equivalent to 2.8 mass% PVCap and 22.8 mass% MeOH.

The end points of the polymer backbone were labelled to allow the measurement of the hydrodynamic length of the polymer (distance between the first and eighth carbon on the octamer backbone).

6.3 MDS Results

Conformation of the Polymer

The conformation of the polymer was assessed via the use of a radial distribution (RDF), which gives the probability of finding the number of molecules at a specified distance from the other molecules.

The atoms at the end points of the polymer were marked and an RDF function was produced to evaluate the hydrodynamic length of the molecule. Hydrodynamic length is

indicative of the distance between the first and last carbon on the polymer; in the case of the octamer, it is the distance between C_1 and C_8 atoms.

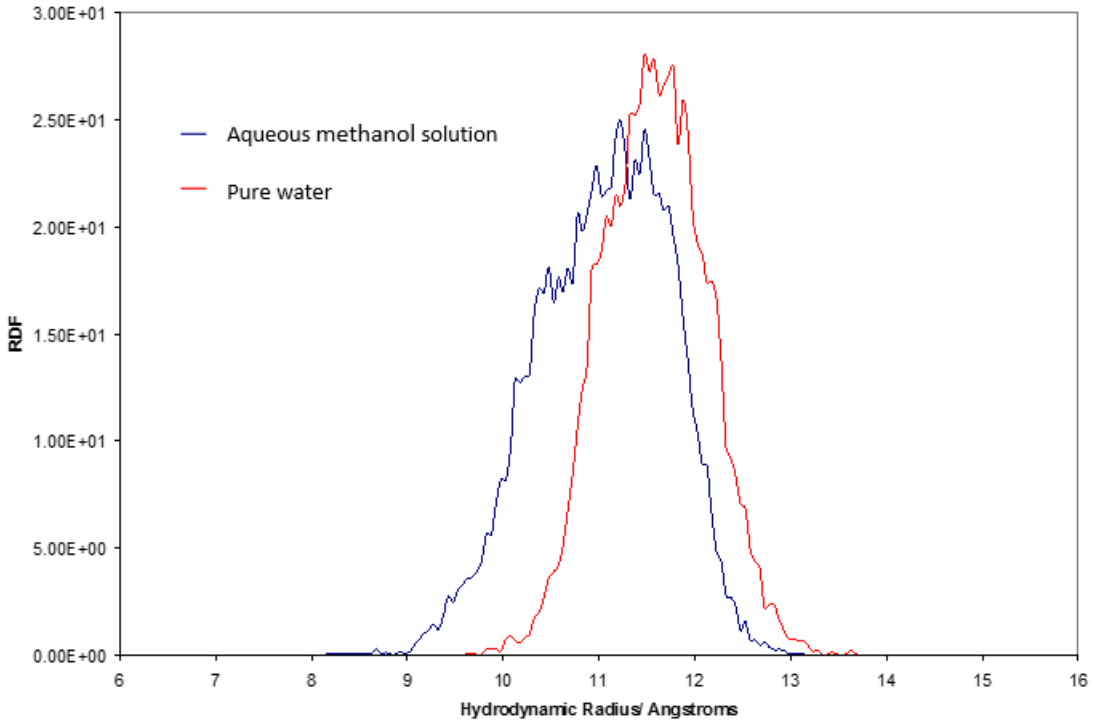

Figure 6.1. Hydrodynamic Length of the PVCap Octamer in pure water, and in 22.8 mass% aqueous methanol solution.

Figure 6.1 gives the comparison between the hydrodynamic length of the polymer in the pure water and the methanol solutions. As can be seen, the average hydrodynamic length of the polymer in pure water is 11 Å and 11.6 Å for the methanol solution. This suggests that methanol only marginally increases the solubility of the polymer. The impact of solubility on hydrodynamic length is illustrated in Figure 6.2.

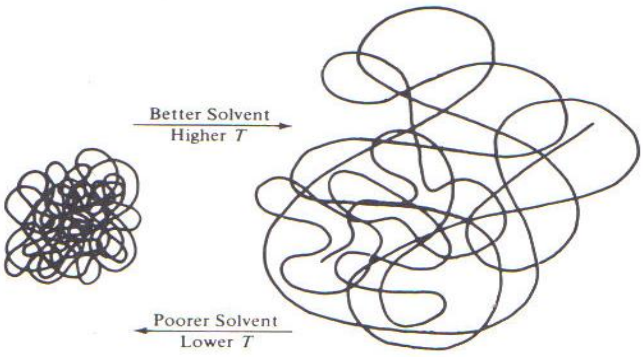

Figure 6.2. The effects of solvent strength and temperature on a polymer molecule in solution. (Rosen, 1993)

Association between the Methanol and the Polymer

The association between methanol and the polymer is evaluated by the use of radial distribution functions (RDF) in the same way as the conformation of the polymer. Initial investigation of the results involved looking at the interaction between the oxygen on the methanol atom (OM) and water (OW) in relation to the atoms on the polymer, i.e., the carbonyl oxygen group (OO), the nitrogen (NN), the carbonyl carbon (C1), and the aliphatic carbon atoms (C2). These are presented in Figures 6.3, 6.5, 6.7 and 6.8, respectively.

Figure 6.3 shows the radial distribution function between the oxygen on the PVCap structure (OO) to the oxygen atoms in the water (OW) and methanol (OM) molecules. As can be seen from the results, both the methanol and water hydrogen molecules associate to the oxygen in the PVCap ring by means of hydrogen bonding, which is indicated by the peaks at 2.5-3 Å; this molecular association is shown in Figure 6.4. Another interesting result is that the methanol concentration is considerably higher than water at distances >4 Å; this suggests that methanol is preferentially associating to the PVCap ring at another location. To find out how and why the methanol is associating to the polymer, various RDFs between the methanol/water and different atoms on the polymer are investigated.

Figure 6.5 shows the radial distribution function between the nitrogen on the PVCap structure (NN) to the oxygen atoms in the water (OW) and methanol (OM) molecules.

The results show that there is no hydrogen bonding between nitrogen and the solvent molecules, which is as expected. The results suggest that water and methanol associates to more or less the same degree to the nitrogen, although methanol does in fact have a marginally higher affinity. As can be seen once again, there is greater affinity for methanol than water at distances greater than 4 Å, which suggests that methanol is associating to the PVCap structure more than the water.

Figure 6.6 shows the radial distribution function between the carbonyl carbon on the PVCap structure (C1) to the oxygen atoms in the water (OW) and methanol (OM) molecules. From these results it can be seen that methanol does not preferentially associate to the carbonyl carbon on the group. There is some hydrogen bonding visible, which arises from the bonding through the associated oxygen.

Figure 6.7 shows the radial distribution function between the aliphatic carbon on the PVCap structure (C2) and the oxygen atoms on the water (OW) and methanol (OM) molecules, which shows that there is a preference for methanol to associate to the aliphatic carbon. Figure 6.8 shows the radial distribution function between the aliphatic carbon on the PVCap structure (C2) and the carbon atoms in the methanol (CM) molecules. This shows that the carbon on the methanol is clearly associating with the aliphatic carbons. The association between the methanol and the aliphatic carbon on the PVCap ring is illustrated in Figure 6.9. This behaviour is intuitive as the non-ionic species on the methanol will preferentially associate with the carbon on the PVCap, thus enabling the alcohol group will associate with the water molecules, both will serve to reduce the overall energy of the system.

Integrating the RDF functions can generate localised concentrations of methanol around the aliphatic carbons and is presented in Figure 6.10. The overall concentration of molecules within the water box is 17.2 mol% (excluding the polymer), however it is much higher within the 12 Å from the aliphatic carbons.

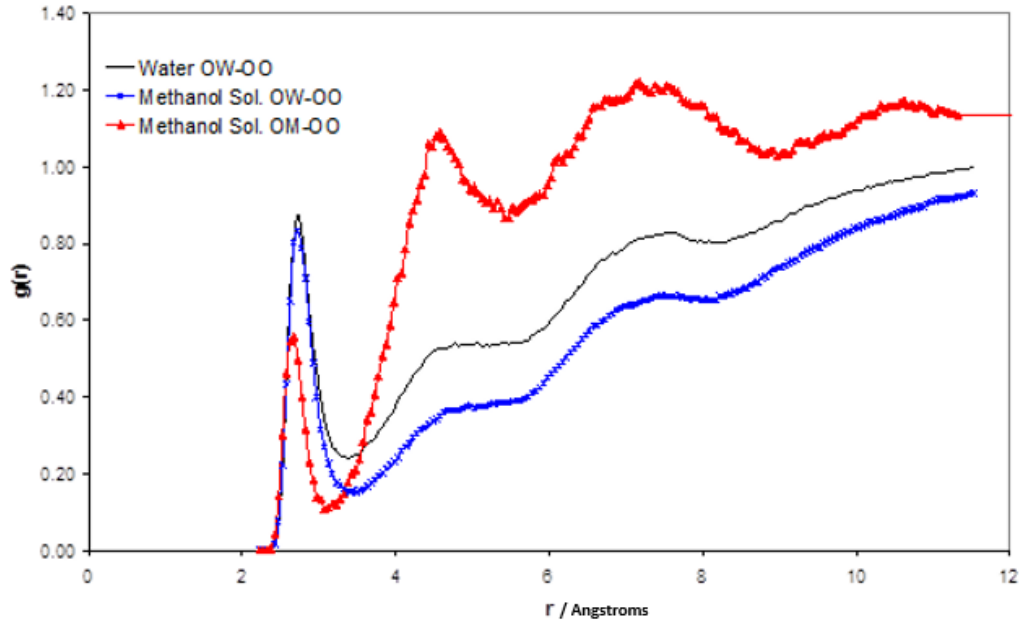

Figure 6.3 Radial Distribution Function between the oxygen atoms on the polymer (OO) to the oxygen atoms of the water (OW) and methanol (OM) molecules.

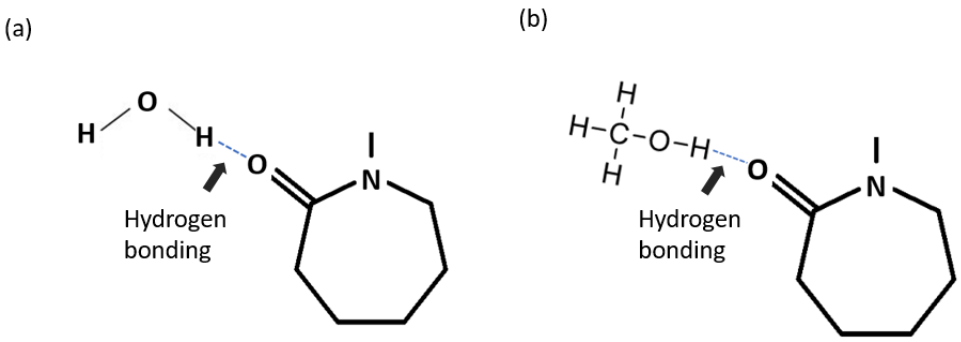

Figure 6.4 Hydrogen bonding between oxygen on the PVCap structure and (a) water and (b) methanol.

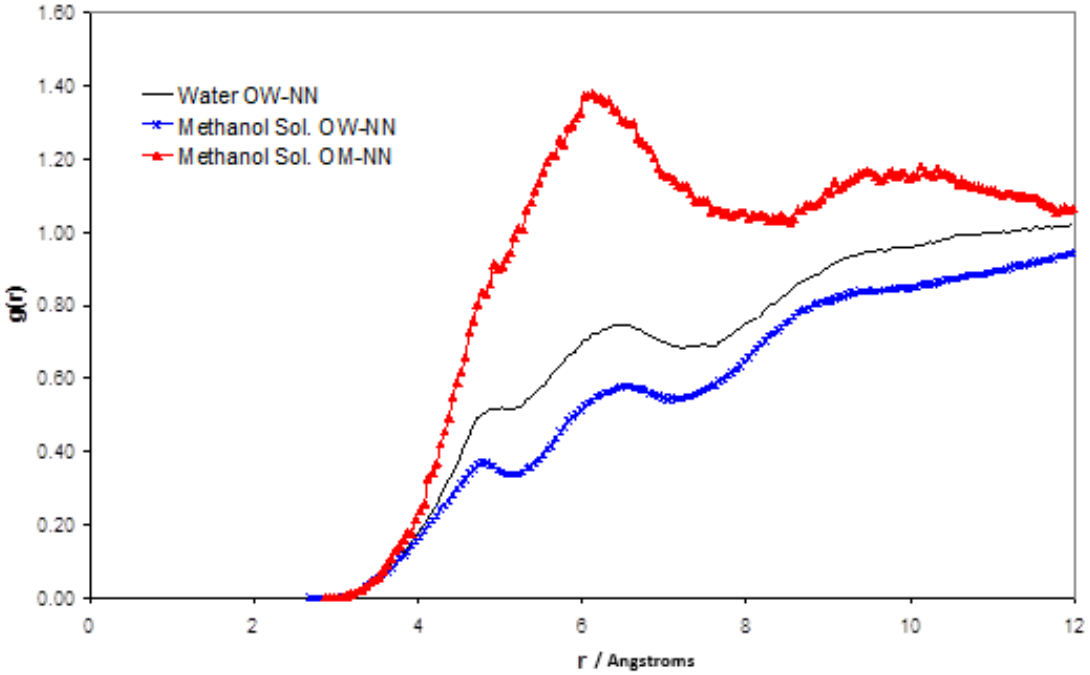

Figure 6.5 Radial Distribution Function between the nitrogen atoms on the polymer (NN) to the oxygen atoms of the water (OW) and methanol (OM) molecules.

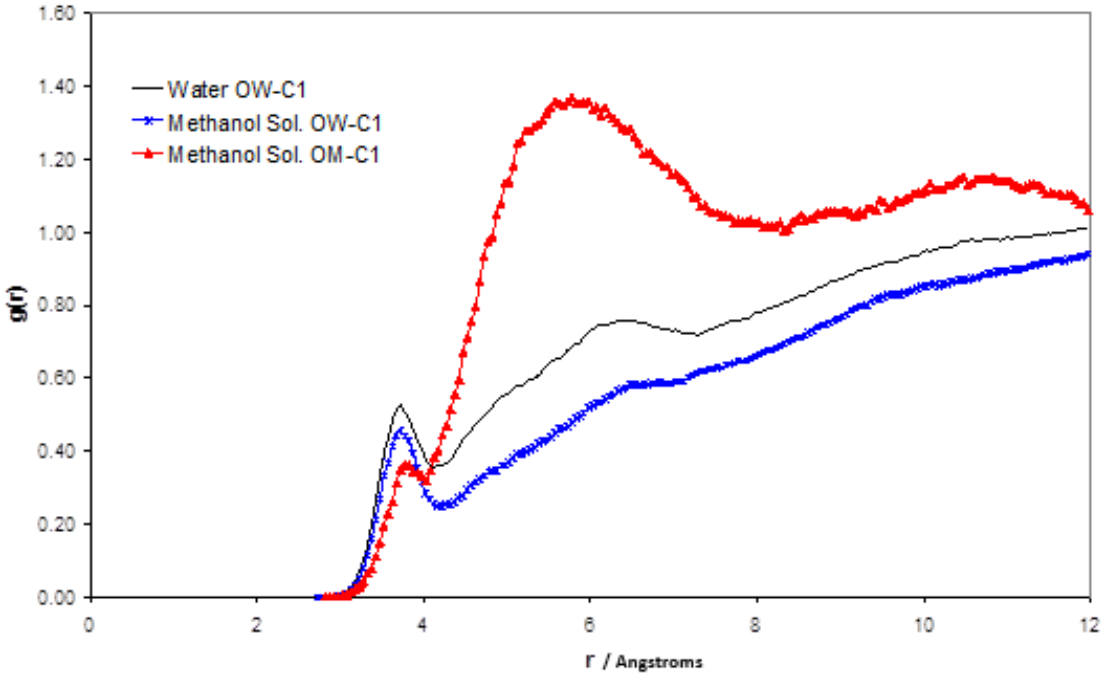

Figure 6.6 Radial Distribution Function between the carbonyl carbon atoms on the polymer (C1) to the oxygen atoms of the water (OW) and methanol (OM) molecules.

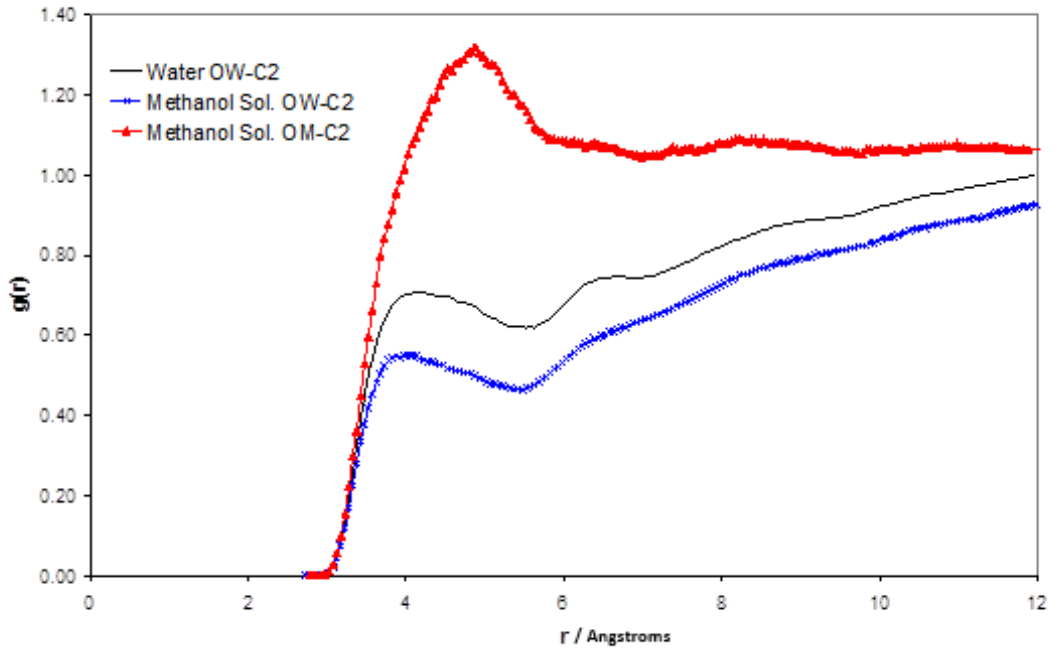

Figure 6.7 Radial Distribution Function between the aliphatic carbon atoms on the polymer (C2) to the oxygen atoms of the water (OW) and methanol (OM) molecules.

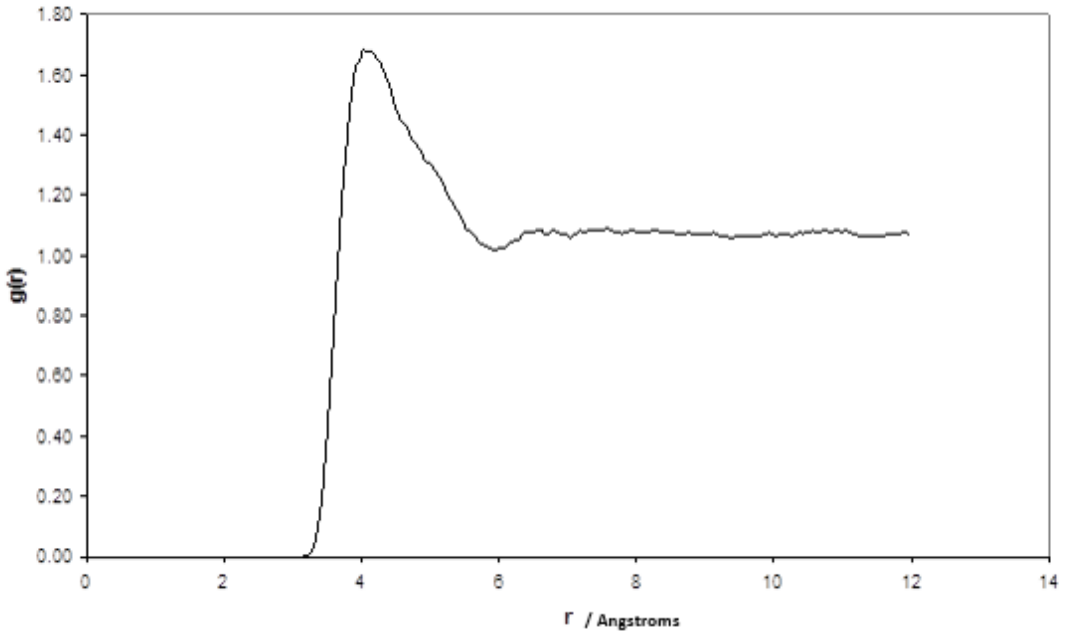

Figure 6.8 Radial Distribution Function between the aliphatic carbon atoms on the polymer (C2) to the carbon atoms in methanol (CM).

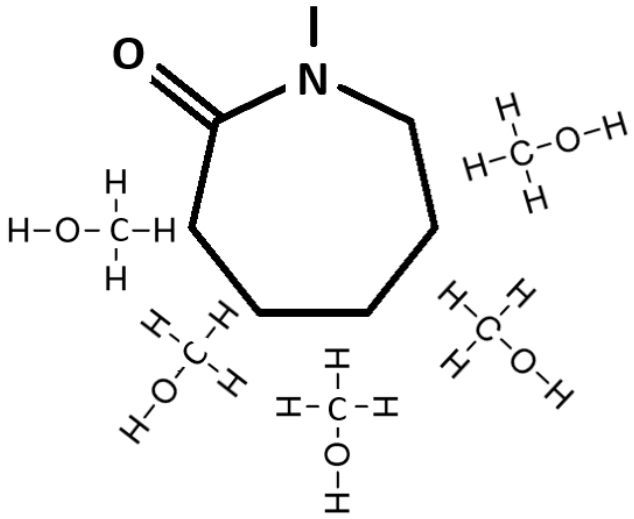

Figure 6.9 Association between the carbon and methanol and the aliphatic carbons on the PVCap ring.

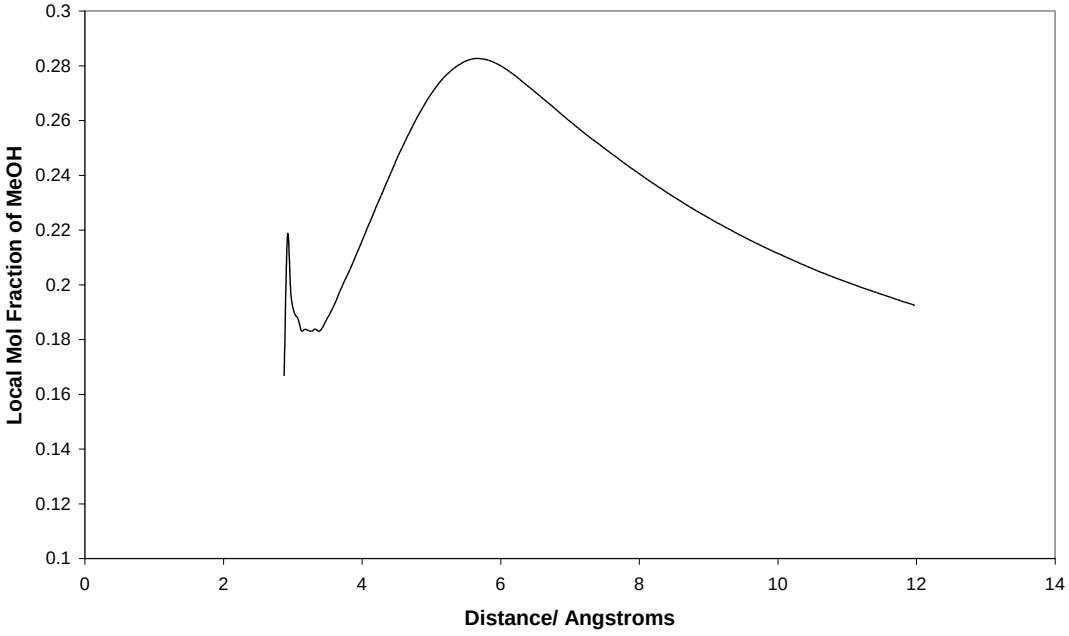

Figure 6.10 Localised MeOH molar concentration within a specified distance from the aliphatic carbon atoms on the PVCap polymer.

6.4 Results Discussion

The results discussion in Chapter 2 talks about the possible antagonistic mechanisms of methanol on PVCap. The molecular simulation suggests that the presence of methanol does have a small effect on the hydrodynamic length of PVCap, however, it is uncertain if this is enough to impact the performance of the KHI. Additionally, the association of methanol to the PVCap's ring structure seen in the results can potentially have two potential negative effects. Firstly, the adsorption of methanol may change the chemical and inhibition properties of PVCap; for example by hindering the active caprolactam sites. Secondly, the association may reduce the effective concentration of the methanol in the bulk of the liquid, which reduces the efficacy of methanol as a thermodynamic inhibitor.

The MDS conducted suggests that the methanol increases self-agglomeration and interfere with the active sites on PVCap. It is unclear how much of an impact this is to KHI performance, but it could have some impact.

Further work is proposed to conduct similar MDS on other chemicals that impact KHI performance, including: salts, ethylene glycol and 2-butoxyethanol. This information should provide additional insight into synergistic and antagonistic mechanism of these chemicals.

Chapter 7: Investigation into the Impact of Pressure and Temperature on: Hydrate Growth, KHI Performance, and the Stochastic Nature of KHI Performance

One of the obstacles in the development and application of Kinetic Hydrate Inhibitors (KHI) is the uncertainty and reliability involved with their testing and use. To improve confidence in the use of KHI there has been a desire to understand the stochastic nature they exhibit, and the testing method presented in Anderson et al. (2011) eliminated some of the uncertainty associated with KHI performance. Anderson et al. (2011) demonstrated that at higher levels of subcooling, the distribution of induction time was greater than at lower levels, which is still not well understood.

An additional issue in the testing of KHI is the use of subcooling as the parameter used to compare the performance of the inhibitors. It has been shown in Arjmandi et al. (2005) and in the results in Chapter 2 that different pressure reduces the performance of KHI at similar subcooling.

The Multi-Test-Tube Rocking Cell (MTTRC) developed by the Centre for Gas Hydrate Research provides an ability to produce large quantities of data at high pressure conditions, due to the number of tests that can be carried out simultaneously. This equipment provides an opportunity to investigate the stochastic nature of KHI, and the use of subcooling as the performance parameter for KHI.

The experimental work described in this chapter involves the generation of data in regards to the induction time versus subcooling of uninhibited and KHI inhibited systems. The two systems that were investigated included: natural gas and distilled water at various pressures and subcooling to investigate the impact of stochasticity of hydrate growth (in the absence of KHI), and a natural gas and aqueous PVCap solution at a fixed pressure to gain insight into the stochastic nature of KHI inhibition.

This work was published in Mali et al. (2017), which is found in Appendix A.

7.1 Methodology

The set-up used consisted of ten 10 ml high-pressure Hastelloy test-tube cells loaded with ball-bearings to aid in mixing. The cells all share the same heater/cooler jacket system, which is attached to a rocking system. Pressure transducers are present in each test tube cell to monitor hydrate growth and temperature is measured by temperature probes installed in the heater/cooler jacket system. A schematic of the MTTRC can be seen in Figure 7.1.

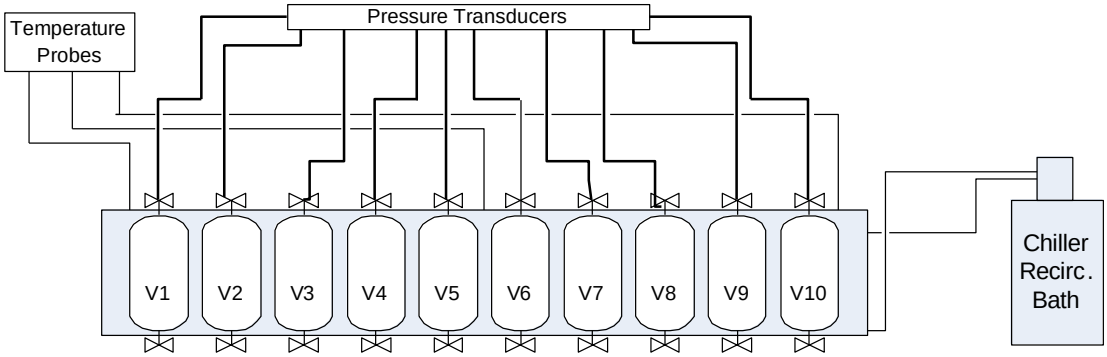

Figure 7.1. Schematic of the multi-test-tube rocking cell.

For all tests 5 ml of the respective liquid was introduced into the test-tube cells and pressurised with natural gas with the composition shown in table 7.1 to the specified pressure. The rocking system was then switched on, which rotates the cells 180° every 9 seconds. The pressure from each test tube, and the coolant temperature in the jacket were measured and logged on a PC. Multiple runs were conducted for each solution with heating of 30 °C for at least 1 day to remove hydrate history.

Two systems were investigated: 1 mass% aqueous PVCap (2.5 mass % Luvicap), and distilled water.

- The tests with distilled water were carried out at 6 different pressures of 17.2, 27.6, 62.1, 68.9, 103.4 and 172.3 bara with subcoolings from 3.2 °C to 8.0 °C.

- The tests with PVCap solution were conducted at 103.4 bara with subcoolings varying from 13.8 °C to 17.8 °C.

Table 7.1 Composition of test natural gas

Component	Mole%
N2	1.5
CO2	1.16
C1	88.9
C2	6.14
C3	1.6
iC4	0.2
nC4	0.3
iC5	0.1
nC5	0.1

The analysis of the data involves the use of two key parameters; the arithmetic mean (μ), and the standard deviation (σ). The arithmetic mean provides information on the most likely value to be encountered in a data set. In this case, the mean represents the most likely induction time that the inhibitor will fail. The standard deviation is a quantity used to help quantify the statistical dispersion of the results. The higher the standard deviation the higher the uncertainty in regards to the performance of hydrate inhibition. The equation for these terms can be seen below:

$$\mu = \frac{1}{N}\sum_{i=1}^{N} x_i$$

$$\sigma = \sqrt{\frac{1}{N}\sum_{i=1}^{N}\left(x_i - \mu\right)^2}$$

A normalised value for standard deviation ($\sigma_{normalized}$) is used to remove the magnitude associated with the standard deviation term, which allows comparison between the populated data at different subcooling.

$$\sigma_{normalised} = \frac{\sigma}{\mu}$$

7.2.1 Results- Distilled Water

The summary of the results of the tests with distilled water and natural gas is shown in Table 7.2; The G/RT driving force termed is described later in this section. Figure 7.2 shows the mean induction times for the different pressures at varying levels of subcooling. Figure 7.3 shows the mean induction times for the different pressures at varying levels of subcooling, with the lines of best fit.

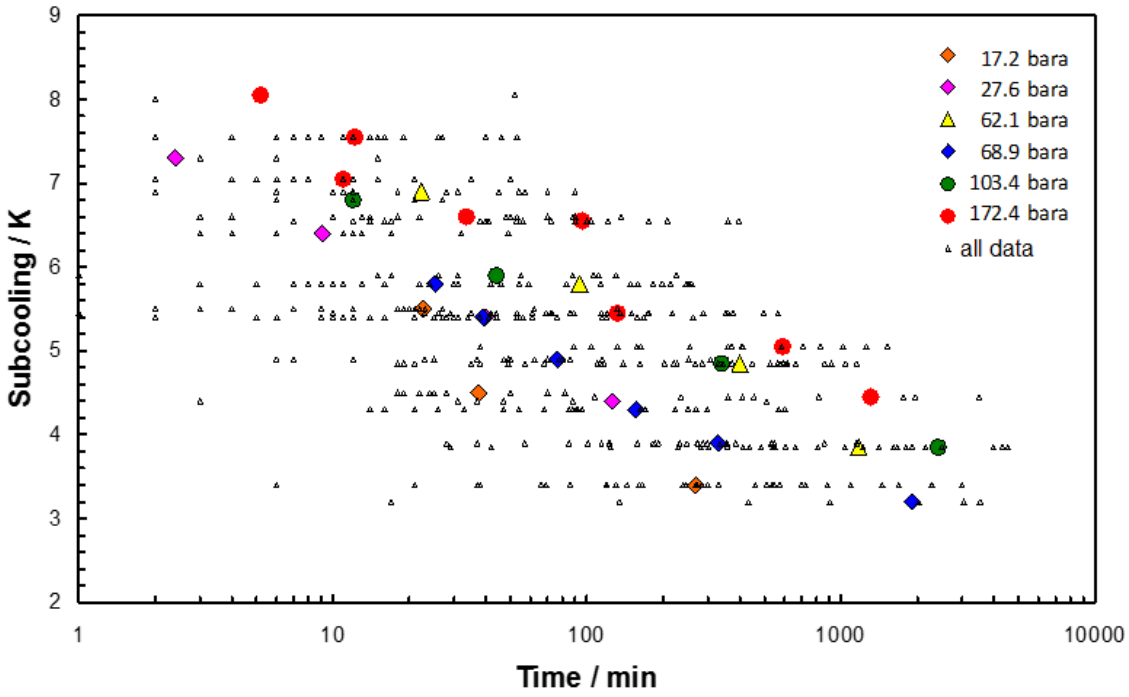

Figure 7.2. Mean induction time as a function of pressure and subcooling.

Table 7.2. Results of distilled water and natural gas to investigate impact of subcooling on arithmetic mean and standard deviation for the mean induction time.

T/ °C	Subcooling / °C	μ_{time} / min	σ_{time} / min	σ / μ	G/RT
17.2 bara					
273.4	5.5	23	30	1.33	0.575
274.4	4.5	38	23	0.61	0.462
275.5	3.4	268	192	0.72	0.337
27.6 bara					
275.5	7.3	2	5	2.08	0.759
276.4	6.4	9	12	1.32	0.659
277.4	5.4	40	54	1.35	0.548
278.4	4.4	126	193	1.53	0.438
62.1 bara					
282.1	6.9	22	26	1.17	0.705
283.2	5.8	94	90	0.96	0.588
284.2	4.85	400	329	0.82	0.482
285.2	3.85	1175	1234	1.05	0.376
68.9 bara					
283.9	5.8	25	48	1.9	0.592
284.3	5.4	39	56	1.43	0.550
284.8	4.9	77	80	1.04	0.497
285.4	4.3	156	163	1.05	0.434
285.8	3.9	328	298	0.91	0.394
286.3	3.4	954	931	0.98	0.343
286.5	3.2	1906	1570	0.82	0.323
103.4 bara					
285.4	6.8	12	12	1	0.710
286.3	5.9	44	60	1.36	0.621
287.4	4.85	339	311	0.92	0.515
288.4	3.85	2413	1792	0.74	0.424
172.4 bara					
286.8	8.05	5	16	3.08	0.865
287.3	7.55	12	14	1.15	0.819
287.8	7.05	11	14	1.27	0.774
288.3	6.6	34	36	1.07	0.731
288.3	6.55	96	109	1.14	0.731
289.4	5.45	132	146	1.11	0.641
289.8	5.05	589	466	0.79	0.611
290.4	4.45	1312	1246	0.95	0.569

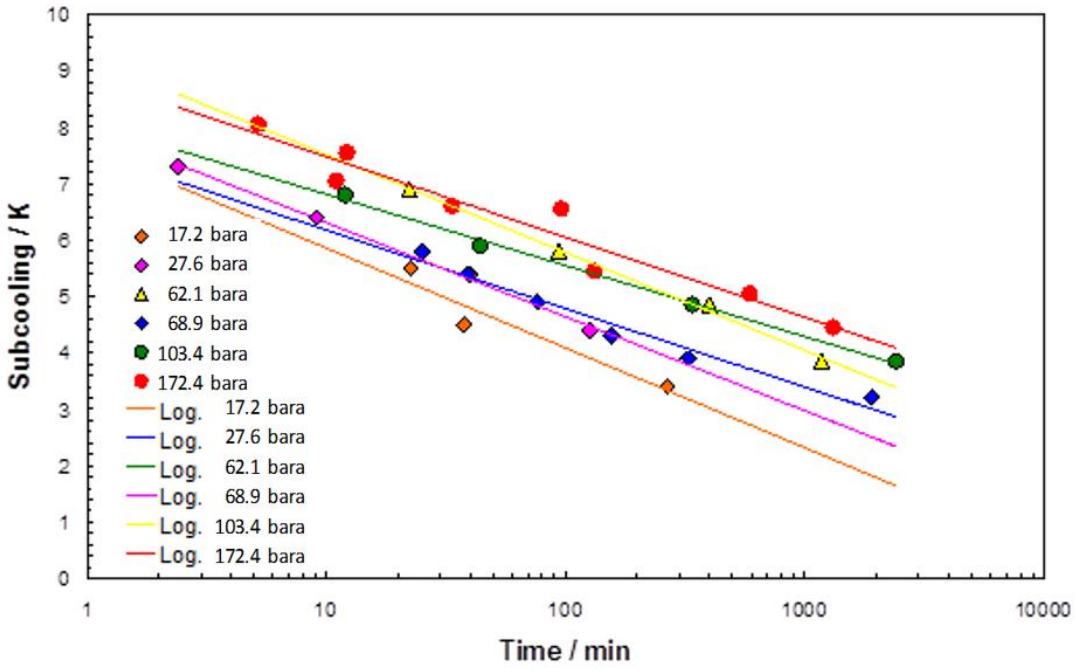

Figure 7.3. Mean induction time as a function of pressure and subcooling with lines of best fit.

The results of the mean values of the Figures 7.2 and 7.3 show that induction time reduces as subcooling increases, which is expected, due to the increase in thermodynamic driving force to form the hydrates. It appears that hydrates form quicker at lower pressures at the same level of subcooling. Although there is some scatter in the data, it appears that there is a clear difference between the results at 17.2 bara (orange) and 172.4 bara (red).

Figure 7.4 is a modified version of Figure 7.3 with the use of the straight line equation ($y=A\times\ln(x) + B$) with parallel lines (A constant) in a best fit relationship to the data.

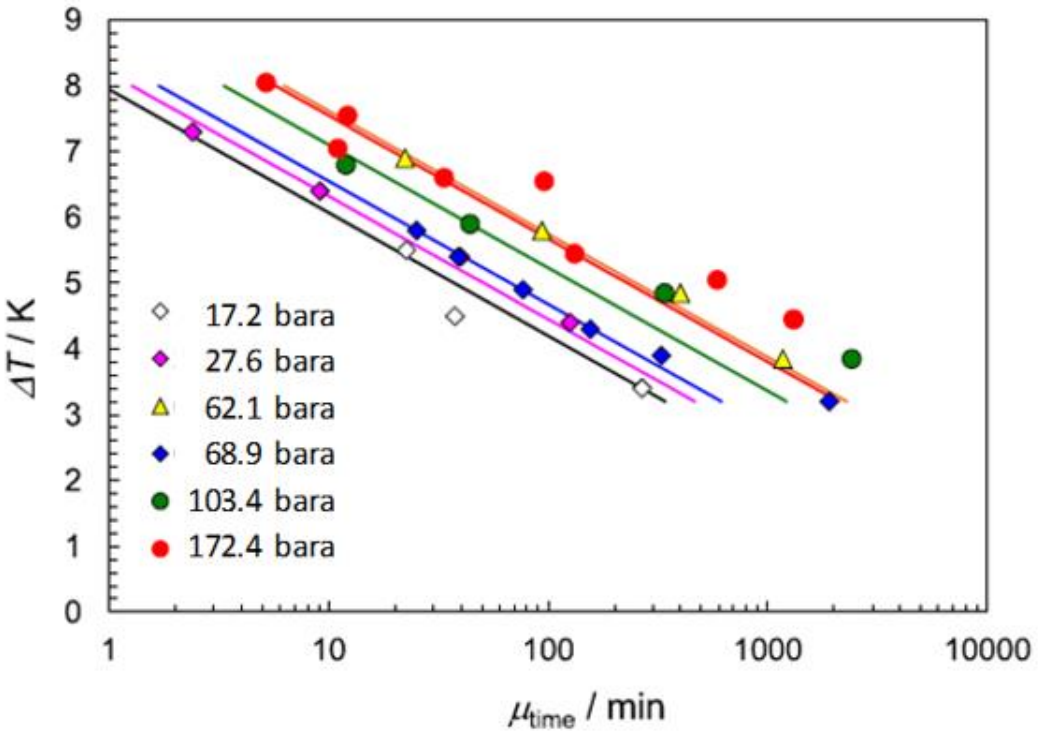

Figure 7.4. Data in the form of y=A×ln(x) + B with subcooling as driving force

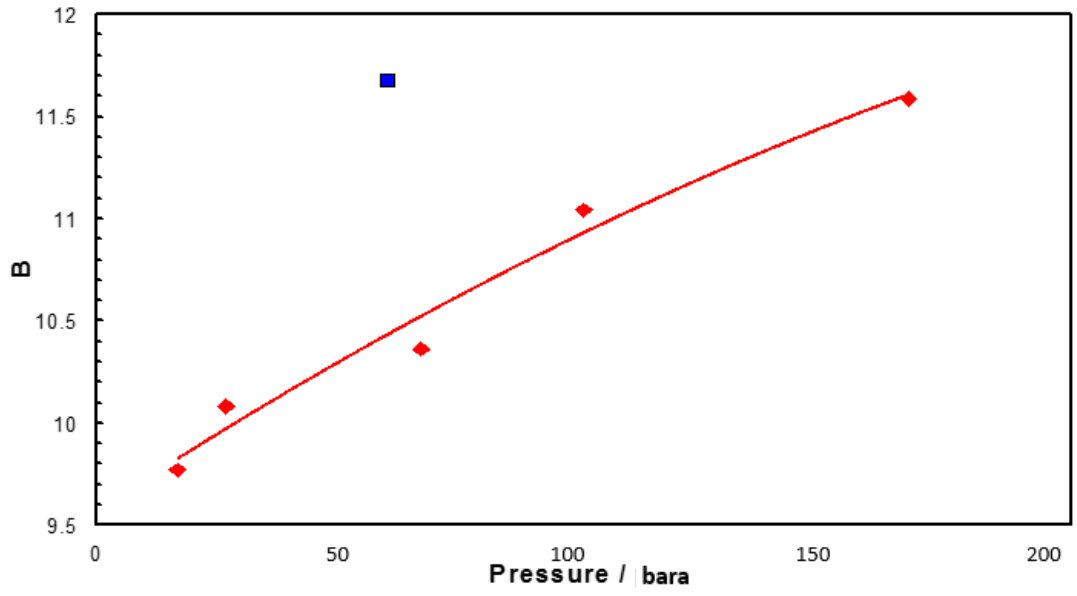

Figure 7.5. Subcooling intersection values of the parallel straight lines as a function of pressure. The blue point represents the intersect (B) at 62.1 bara, as explained below.

Figure 7.5 is a plot of the data gathered from Figure 7.4 in relation to the intersect B as a function of pressure. As can be seen there is a general trend with the intersect B increasing with increasing pressure. This suggests that increasing pressure has a near linear effect of increasing induction time. The exception to this data is the 62.1 bara data set, which does not follow the trend (blue on the figure). The results show that there can be up to approximately 25 times increase in the average induction time due to a change in pressure from 17.2 to 172.4 bara, at the same level of subcooling.

The use of subcooling as a driving force is discussed extensively in Arjmandi et al. (2005) and it demonstrates that the subcooling term cannot be directly used as a measurement of driving force in all conditions. Christiansen and Sloan (1995) or used the molar change in Gibbs free energy for hydrate formation (G/RT), which calculates the impact different pressures and temperatures has on driving force.

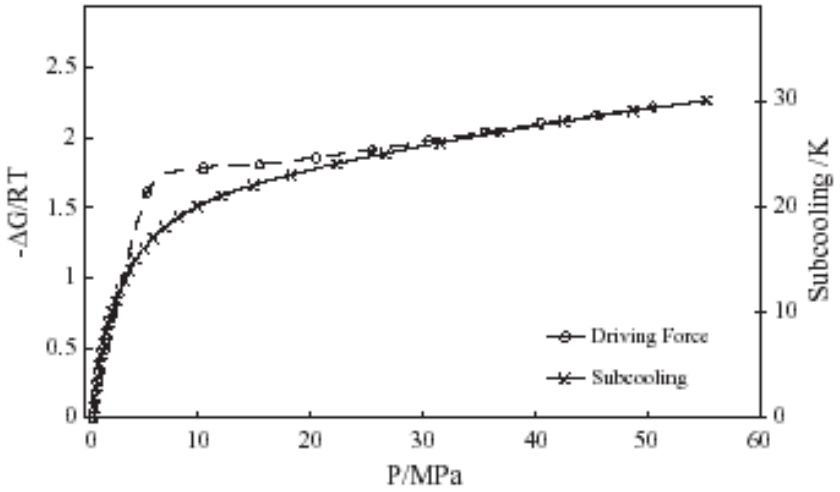

Figure 7.6. Comparison between driving force and subcooling for a natural gas as a function of pressure at constant temperature. (Christiansen and Sloan. 1995)

Figure 7.6 is taken from the work of Christiansen and Sloan (1995) and is the relationship between subcooling and driving force as a function of pressure resulting from calculations. The relationship shows that from 40-200 bara the subcooling can deviate from the calculated driving force using Gibbs free energy. The difference between the values of driving force and subcooling can potentially explains the phenomenon of higher induction time at same subcooling at higher pressures seen in the tests conducted.

To explore this, Figure 7.7 is a modified version of Figure 7.3 that uses the Gibbs free energy derived driving force methodology as an alternative to subcooling. The chart demonstrates that induction time is logarithmically related to Gibbs free energy, similar to subcooling.

Figures 7.8 and 7.9 are similar to Figures 7.4 and 7.5 but use Gibbs free energy instead of subcooling for driving force. The pressure still has an effect on induction time at comparative levels of Gibbs free energy, which implies that another physical parameter is impacting induction time at higher pressures. Figure 7.8 demonstrates that the perceived error on Figure 7.5 at 62.1 bara (blue square) is no longer present when using Gibbs free energy and is in trend with the other data, which is due to the use of Gibbs free energy as opposed to subcooling, which considers the impact of the pressure conditions that can affect driving force.

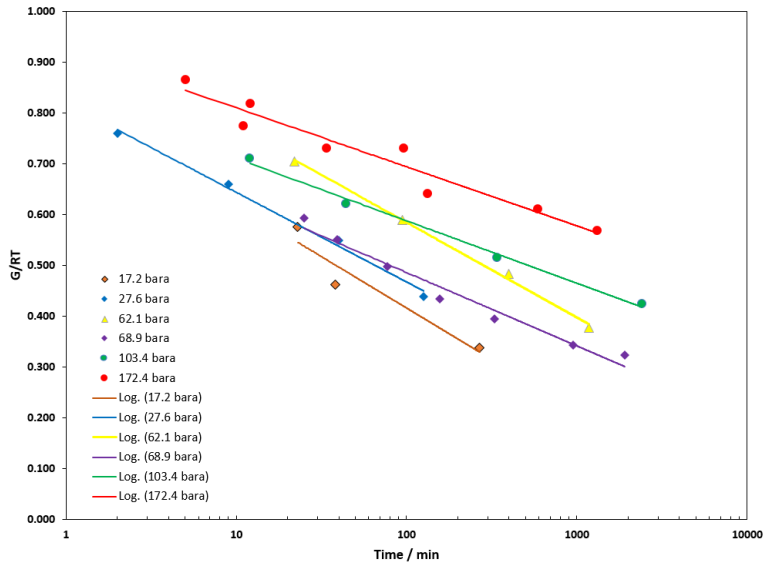

Figure 7.7. Mean induction time as a function of pressure and driving force with lines of best fit.

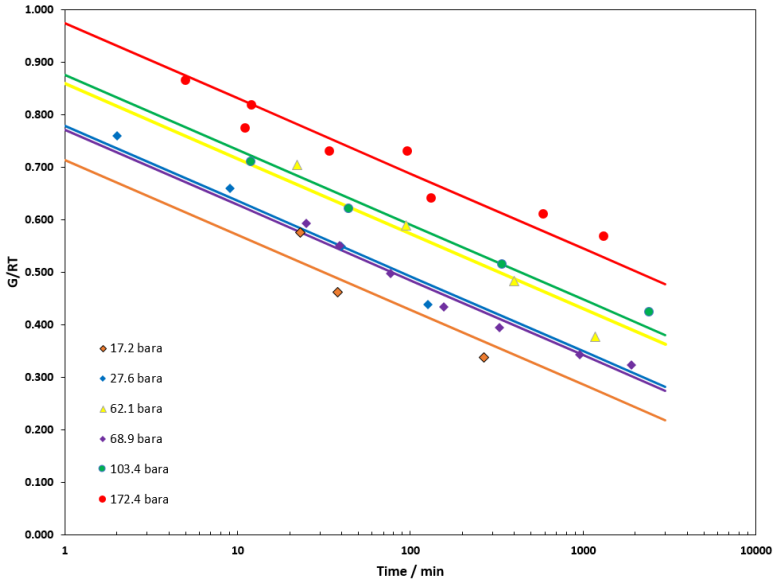

Figure 7.8 Data in the form of y=A×ln(x) + B with Gibbs free energy as driving force

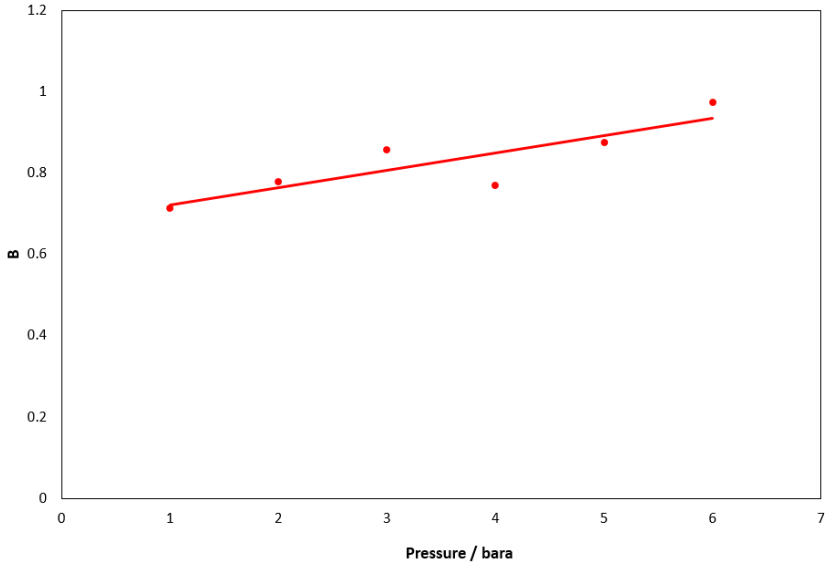

Figure 7.9. Gibbs free energy intersection values of the parallel straight lines as a function of pressure.

Figure 7.10 shows the normalised standard deviation for the different pressures at varying levels of subcooling. It is apparent from the data that the standard deviation (normalised) generally increases with subcooling. The implication is that there is more reproducibility of measured induction time and less stochasticity at lower subcooling. This is in agreement with Anderson et al. (2011) that demonstrates that at high subcooling

conditions, very small changes in temperature can result in a significant change in growth rate.

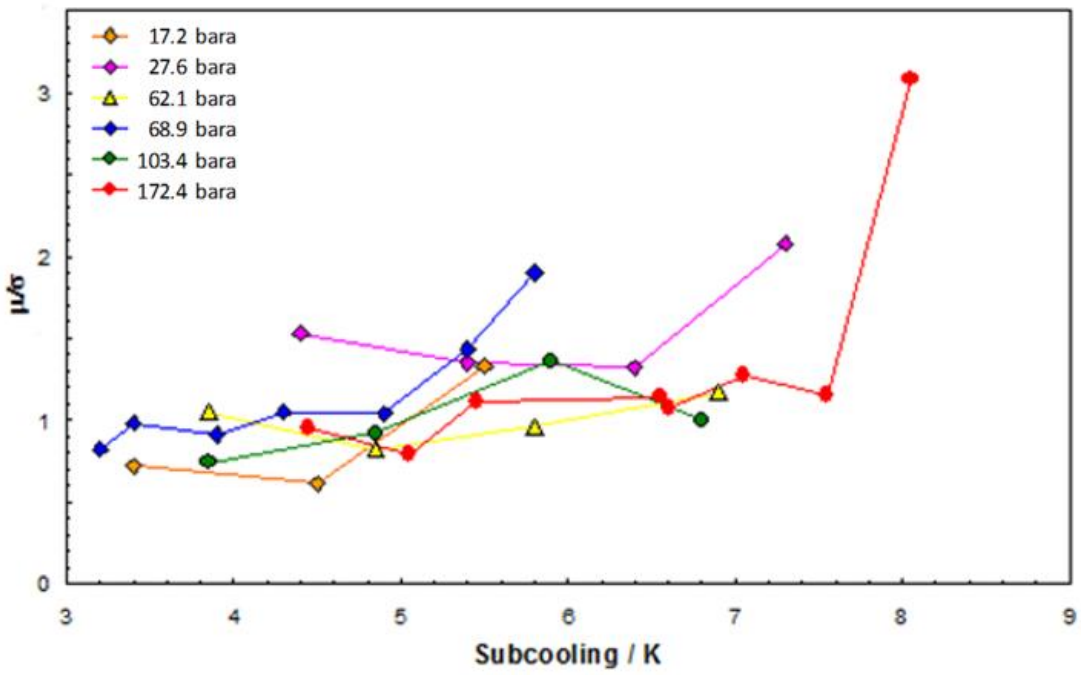

Figure 7.11. Normalised standard deviation versus subcooling

The figure shows that there is no clear relationship between the effects of pressure on standard deviation. This suggests that an increase or decrease in the system pressure does not have an effect on the stochasticity of the system of the uninhibited system.

7.2.2 Results- Aqueous PVCap Solution

The summary of the results of the tests with 1 mass% aqueous PVCap solution and natural gas is shown in Table 7.3. Figure 7.12 shows the mean induction times for the different pressures at varying levels of subcooling. Figure 7.13 shows the normalised standard deviation for the different pressures at varying levels of subcooling.

The results gathered for the aqueous PVCap solution had an inherent problem in the analysis of the data. Some of the runs had extremely long induction times until catastrophic growth, with slow pressure drop present indicative of some hydrate

formation. It became apparent that the slow growth of hydrate in the cell obstructed the free passage of the ball-bearing, which limited further mass transfer and significantly delayed the onset of critical growth. This made interpretation of the data very difficult and led to questions in defining induction time. It was decided to define induction time as the time until any slow growth or catastrophic growth was evident.

Figure 7.9 shows a similar relationship as encountered with natural gas with distilled water. The logarithmic relationship is evident once more.

Table 7.3 Results of 1 mass% aqueous PVCap solution and natural gas to investigate impact of subcooling on arithmetic mean and standard deviation for the mean induction time.

Tsystem/ °C	Subcooling/ °C	P/ bara	μ_{time} / min	σ_{time} / min	σ / μ
0.3	17.80	103.4	211	130	0.62
2.3	15.80	103.4	256	146	0.57
4.3	13.80	103.4	757	383	0.51
6.3	11.80	103.4	510	559	1.10

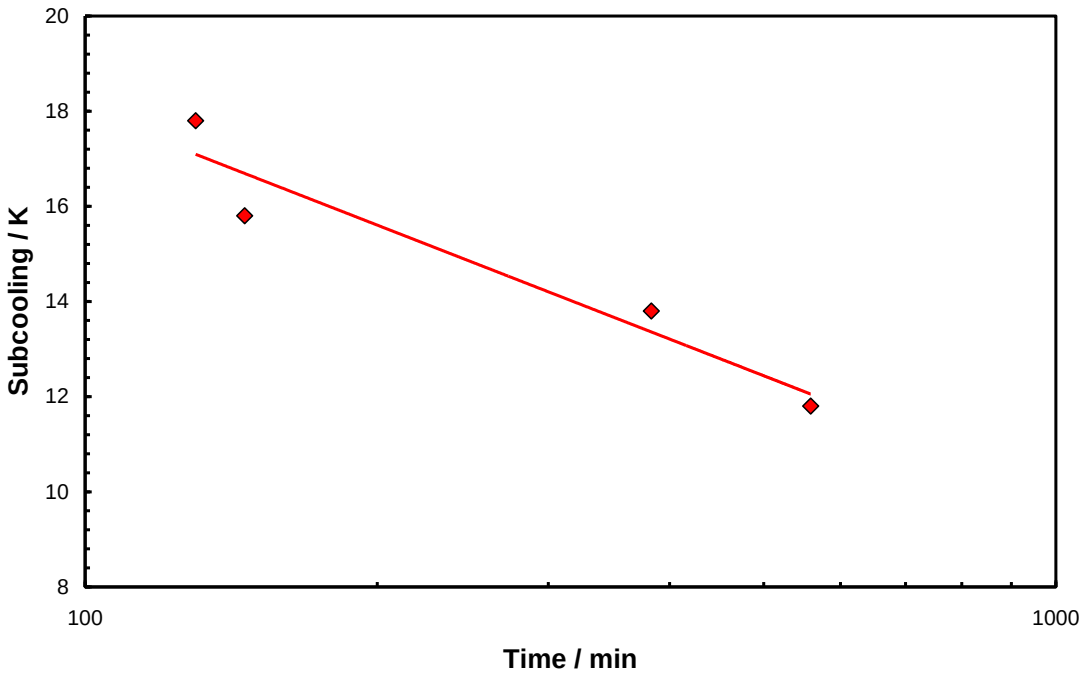

Figure 7.12. Mean induction time versus subcooling (semi-log chart)

Figure 7.13 shows the standard deviation versus subcooling for the solutions tested. It is apparent that there is no clear relationship; however, it is worth noting that magnitude of the deviation with PVCap is significantly less than those encountered with distilled water.

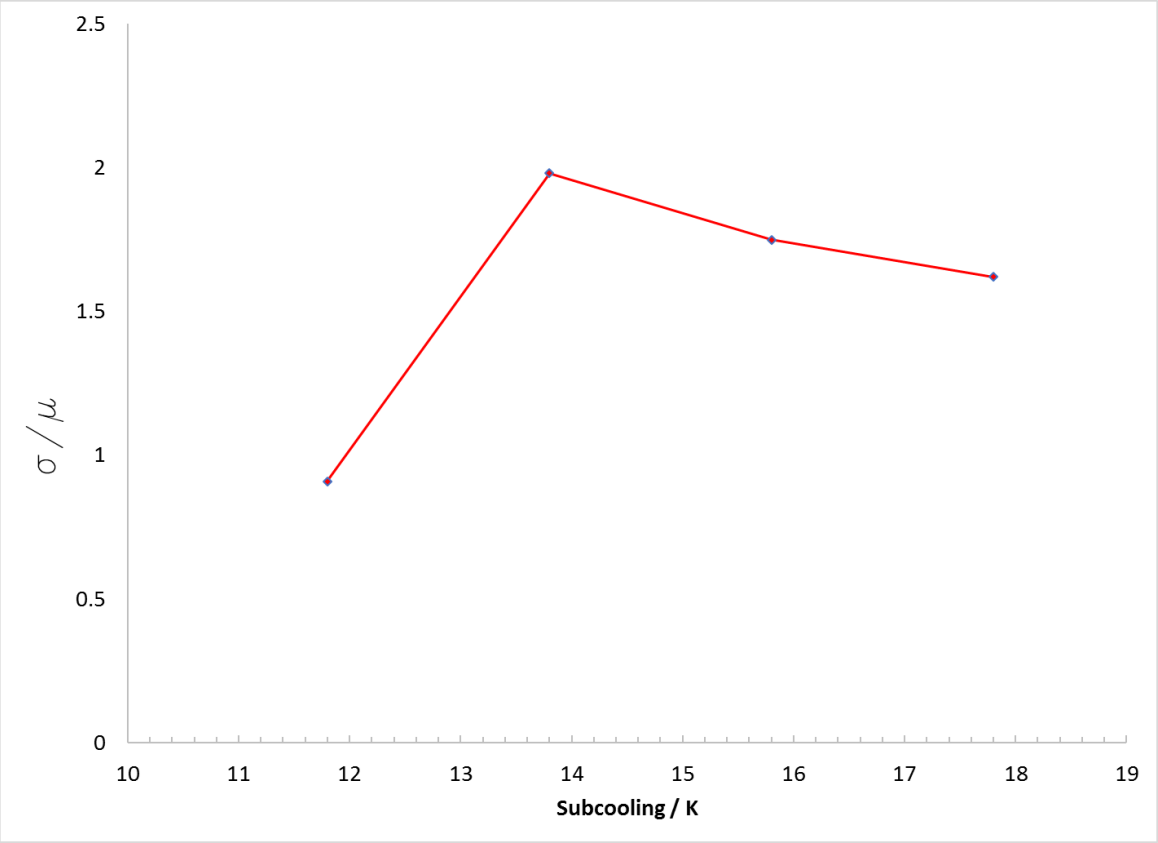

Figure 7.13. Normalised standard deviation versus subcooling.

7.3 Results Summary

The results demonstrate the value of the multi-test-tube rocking cell to gather statistical data on the stochastic properties of hydrate growth.

The data shows that subcooling is logarithmically related to induction time for both the inhibited and uninhibited systems.

The data also showed that an increase in pressure at the same subcooling increases the average induction time for the uninhibited system. The impact of pressure on the use of subcooling as a driving force term was explored by using Gibbs free energy developed by Christiansen and Sloan (1995) as an alternate driving force to subcooling. The analysis demonstrated that the impact of pressure on induction time was still present using the alternative method.

The results with distilled water and natural gas suggest that higher subcooling, increases the scatter in induction time. The results with aqueous PVCap solution showed that the scatter in results were greater than those seen with the uninhibited system (distilled water and natural gas).

Chapter 8: Thesis Conclusions and Recommendations

The thesis presented a series of laboratory testing and molecular dynamic simulations to investigate a wide variety of additives and factors that could impact the performance of KHI.

8.1 Impact of Salt and Alcohols on KHI Performance

Experimental work with stirred autoclave reactors has demonstrated that methanol and ethanol had a negative effect on the performance of PVCap and other commercially available KHI. In response to this, Molecular Dynamic Simulation was carried out for a PVCap octamer in aqueous methanol solution to better understand the interaction between methanol on PVCap. The results showed that there was a small difference in hydrodynamic length of the polymer in the presence of the alcohol which was indicative of an increase in self-agglomeration, and it was shown that the methanol molecules adsorb onto the PVCap molecule, which may impact inhibitor performance by a reduction of alcohol in the bulk aqueous phase, and/or sterically interfere with KHI active sites.

Experimental work in an autoclave reactor demonstrated that salt has a positive effect on PVCap performance. This supported previous published work by Sloan et al. (1998) who showed that sea salt had a positive performance with salts at concentrations greater than 6 mass%. Unusual results were evident with magnesium chloride, which did not have an impact on the KHI but it is possible that this could be attributed to experimental error.

There is no one proven explanation for the positive impact of salt and negative impact of methanol and ethanol on PVCap and several theories remain to explain this. However, the change to the polarity of the aqueous hydrate forming solution impacting the solubility of hydrate forming guest molecules is considered to be the simplest theory to explain the synergistic and antagonistic behaviours associated with salt and methanol respectively. However, the MDS does suggest that the alcohols may have additional impacts to PVCap performance relating to polymer conformance and interference with the active sites of the caprolactam ring.

8.2 Impact of 2-butoxyethanol on PVCap performance

A series of autoclave tests were conducted with 2-butoxyethanol on PVCap, which is a previously identified synergist in published literature. Tests were conducted on various lengths of PVCap polymer's KHI performance, which was designed this way to evaluate the theory that 2-butoxyethanol reduces self-association of the polymer, and the addition of the synergist would be more successful with longer polymers that naturally have the potential to self-associate to a greater extent. The data did show that 2-butoxyethanol increased KHI performance more in the longer polymers than their shorter counterparts. It remains unclear how these synergist components impact the inhibition mechanism, but a previously proposed theory of reducing self-association was supported by this work.

8.3 Impact of Alkane Phase on PVCap performance

A series of stirred autoclave reactor tests were conducted to investigate the impact of an alkane phase on PVCap. The tests demonstrated that the presence of a hydrocarbon phase has a negative impact on KHI performance at similar levels of subcooling. Further tests to identify the partitioning of the components demonstrated that the impact of inhibition is not due to the loss of inhibitor to the organic phase.

The proposed explanation of the reduction in PVCap performance is that the addition of a hydrocarbon phase will preferentially dissolve the heavier alkane components, which changes the sII hydrate phase boundary but keeps the sI hydrate phase boundary unchanged. If similar sII subcoolings are used for comparison for a system with and without an alkane phase, the degree of sI subcooling will be greater for the system with the alkane phase. It is also known that PVCap is a weak KHI for sI hydrates and that the failure is due to the creation of sI hydrates.

8.4 Statistical Analysis of Hydrate Growth in the Presence and Absence of PVCap

A novel mutli test tube rocking cell rig equipment was used to conduct a large number of tests to generate statistical data of hydrate formation of both PVCap inhibited and uninhibited natural gas systems. The results demonstrated that there is a logarithmic relationship between subcooling and induction time for both inhibited and uninhibited

systems. The results also showed that higher pressures increased induction time at comparative levels of subcooling. It was also seen that KHI inhibited systems had more scatter associated with hydrate formation.

8.5 Further Work

The thesis has revealed insight into the challenging process of designing, testing and application of kinetic inhibitors. The research into methods to evaluate and improve inhibitor performance is still very much ongoing in industry and academia.

Further work is proposed based on the research described in this thesis to further understand factors that influence inhibitor performance. The first recommendation for further work is to conduct the experimental work to investigate the impacts of thermodynamic inhibitors, salts and condensates with the novel method described by Anderson et al. (2011). This new evaluation method eliminates the uncertainty and data scatter of the testing by removing the stochasticity associated with nucleation and focuses on the impact that KHI have on crystal growth, which is the major source of the uncertainty with the experiments described in this thesis. This can be augmented by water sampling and gas chromatography to determine the composition of hydrate guest molecules in the aqueous phase prior to and during hydrate growth, which is potentially the key drivers for the changes in PVCap performance in salt and methanol.

To understand the impact of the alkane phase, further work should include the testing of similar PVCap solutions at similar temperatures and pressure in the presence and absence on an alkane phase to determine if the failure in the performance in the KHI is due to sI hydrate growth. This work could be enhanced by water and alkane phase sampling with the use of gas chromatography techniques to understand the impact of the failure of PVCap. If PVCap failure is proven to be due the inability to inhibit sI hydrate, it justifies additional research to identify and develop an sI inhibitor that could be combined with sII KHI as a mixture or copolymer to increase the efficacy of the sII KHI.

There is also value in additional molecular dynamic simulation of PVCap solutions with the other components experimentally evaluated for their impact on the performance on the inhibitor (salt, ethanol, ethylene glycol, and in particular 2-butoxyethanol). Further

investigation can reveal if the association of the components with the KHI polymer and impacting the self-assocaition of the polymer is shared with the various known antagonistic and synergistic chemicals.

The author sends his support and best wishes to the scientists and engineers working this field of research.

9.0 References

Adham, S., Gharfeh, S., Hussain, A., Minier-Matar, J., Janson, A, "Kinetic Hydrate Inhibitor Removal by Physical, Chemical and Biological Processes", Offshore Tecnology Conference Asia, Kuala Lumpur, 25-28 March (2014)

Anderson, R., Mozaffar, H., Tohidi, B., "Development of a Crystal Growth Inhibition Based Method for the Evaluation of Kinetic Hydrate Inhibitors", Proceedings of the 7th International Conference on Gas Hydrates, Edinburgh. 17-21 July (2011)

Argo, C. B., Blain, R. A., Osborne, C.G., Priestley, I. D., "Commercial Deployment of Low-Dosage Hydrate Inhibitors in a Southern North Sea 69 Km West-Gas Subsea Pipeline", Paper 37255 presented at the SPE International Symposium on Oilfield Chemistry, Houston, 18-21 February, (1997)

Arjmandi, M., Tohidi, B., Danesh, A., Todd, A. C., "Is Subcooling The Right Driving Force For Testing Low Dosage Hydrate Inhibitors?" Chemical Engineering Science, 60, 1313-1321, (2005)

Arjmandi, M., Description of experimental work as part of Flow Assurance: Micro and Macro-Scale Evaluation of Low Dosage Hydrate Inhibitors JIP (2005)

Bloys, B. and Lacey, C. "Laboratory testing and field trial of a new kinetic inhibitor" paper OTC 7772 presented at the Offshore Technology Conference, Houston, 1-4 May (1995)

Boyne, K., Horn, M., Bertrane, D., Fournie, F., Cooper, T., Quinn, P., Buchan, D., Allan, K., "Otter- A challenging marginal oil field development", SPE Paper 83975 presented at Offshore Europe, 2-5 September, (2003)

Budd, D., Hurd, D., Pakulski, M., Schaffer, T. D., "Enhanced Hydrate Inhibition in Alberta Gas Field" SPE Paper 90422, presented at the SPE Annual Technical Conference and Exhibition, Houston, 26-29 September, (2004)

Burgazli, C. R., World Patent Application WO 2004/111161 (2004)

Carver, T. J., Drew, M. G. B., Rodger, P. M., "Inhibition of Crystal Growth in Methane Hydrates", J. Chem. Soc. Faraday Trans, 91, (1995)

Carver, T. J., Drew, M. G. B., Rodger, P. M., "Characterisation of the {111} growth plane of a type II gas hydrate and study of the mechanism of kinetic inhibition by poly(vinylpyrrolidone)", J. Chem. Soc. Faraday Trans, 92(24), (1996)

Carver, T. J., Drew, M. G. B., Rodger, P. M., "Molecular dynamic calculations of N-methylpyrrolidone in liquid water", Phys. Chem. Chem. Phys, 1, 1807-1816 (1999)

Carver, T. J., Drew, M. G. B., Rodger, P. M., "Configuration-Biased Monte Carlo Simulations of Poly(vinylpyrrolidone)at a Gas Hydrate Crystal Surface", Annals of the New York Academy of Science 912, 658-668, (2000)

Christiansen, R.L., Sloan, E. D., "A compact model for hydrate formation", Proceedings of the 74th GPA Annual Convention, San Antonio, Texas, 15-21 March (1995)

Cohen, J. M., Wolf, P. F., Young, W. D., "Enhanced Hydrate Inhibitors: Powerful Synergism with Glycol Ethers" Energy and Fuels, 12, 216-218 (1998)

Colle, K. S., Costello, C. A., Talley, L.D., Longo, J. M., Oelfke, R. H., Berluche, WO Patent Application 96/08672 (1996[a])

Colle, K. S., Talley, L.D., Oelfke, R. H., Berluche, WO Patent Application 96/41784 (1996[b])

Colle, K. S., Costello, C. A., Talley, J. M., Oelfke, R. H., Berluche, WO Patent Application 96/41834 (1996[c])

Colle, K. S., Costello, C. A., Talley, Canadian Patent Application 96/2178371 (1996[d])

Colle, K. S., Costello, C. A., Talley, J. M., Oelfke, R. H., Berluche, WO Patent Application 96/08673 (1996[e])

Colle, K. S., Costello, C. A., Talley, J. M., Oelfke, R. H., Berluche, US Patent Application 6222083 (1996[f])

Colle, K. S., Costello, C. A., Talley, J. M., Oelfke, R. H., Berluche, WO Patent Application 96/41786 (1996[g])

Colle, K. T., Oelfke, R. H., "Method for inhibiting hydrate formation", US Patent No. 5,600,044 (1997)

Colle, K. T., Oelfke, R. H., Kelland M. A., US Patent No. 5,874,660 (1999)

Colle, K. S., Talley, L.D., Longo, J. M. WO Patent Application 2005/005567 (2005)

Corrigan, A., Duncum S. N., Edwards, A. R., Osborne, C. G., "Trials of Threshold Hydrate Inhibitors in the Ravenspurn to Cleeton Line", Paper 30696 presented at the SPE Annual Technical Conference and Exhibition, Dallas, 2-25 October. (1996)

Dzialowski, A., Patel, A., Nordbo, K., "The Development Of Kinetic Inhibitors To Suppress Gas Hydrates In Extreme Drilling Conditions" Offshore Mediterranean Conference and Exhibition, 28-30 March, Ravenna, Italy (2001)

Duncum, S. N., Edwards, A. R., Osborne, C. G., "Method for inhibiting hydrate formation", US Patent No. 5,331,105 (1994)

Duffy, D. M., Moon, C., Rodger, P. M., "Computer-assisted design of oil additives: hydrate and wax inhibitors", Molecular Physics, 20, Vol. 102, No. 2, 203-210, (2004)

Freer, E. M. and Sloan Jr., E. D. "An Engineering Approach to Kinetic Inhibitor Design Using Molecular Dynamic Simulations", Annals of the New York Academy of Science 912, 651-657, (2000)

Frostman, L.M., Crosby, D., In proceedings of the Deep Offshore Technology Conference, Marseille, 19-21 November (2003) cited from Kelland (2006)

Fu, B., Neff, S., Mathur, A., Bakeev, K., "Novel Low Dosage Hydrate Inhibitors for Deepwater Operations" SPE Paper 71472 presented at SPE Annual Technical Conference and Exhibition, New Orleans, (2001)

Fu, B., Houston, C., Spratt, T., "New Generation LDHI with an Improved Environmental Profile", Proceedings of the Fifth International on Gas Hydrates, Trondheim, May 12-16 (2005).

Glénat, P., Peytavy, J., Holland-Jones, N., Grainger, M., "South-Pars Phases 2 and 3: The Kinetic Inhibitor (KHI) Experience Applied at Field Start-up", SPE Paper 88751 presented at the 11th Abu Dhabi International Petroleum Exhibition, (2004)

Glenat, P., Anderson, R., Mozaffar, H., Tohidi, B., "Application of a New Crystal Inhibition Based KHI Evaluation Method for Commercial Formulation Assessment", Proceedings of the 7th International Conference on Gas Hydrates, Edinburgh. 17-21 July (2011)

Habetinova, E., Lund, A., Larsen, R., "Hydrate Dissociation Under the Influence of Low Dosage Kinetic Inhibitors", Proceedings of the 4th International Conference on Gas Hydrates, Yokohama, (2002)

Hawtin, R. W., Moon, C., Rodger, P. M., Grainger, N., Rogers, S. C., "Simulation of Hydrate Kinetic Inhibitors: The Next Level" Proceedings of the Fifth International on Gas Hydrates, Trondheim, May 13-16, page 118 (2005).

Hutter, J. L., King Jr., H. E., Lin, M. Y., "Polymeric Hydrate-Inhibitor Adsorption Measured by Neutron Scattering", Macromolecules, 33, 2670-2679 (2000)

Karaaslan, U., Parlaktuna, M., "PEO- A new hydrate inhibitor polymer", Energy & Fuels, 16 (6), 1387-1391, (2002)

Kelland, M. A., Klug, P. WO Patent Application 98/23843 (1998)

Kelland, M. A., Rodger, P. M., Namba, T,. US Patent No. 6319971

Kelland, M. A., “History of the Development of Low Dosage Hydrate Inhibitors”, Energy & Fuels, Volume 20, No.3, (2006)

Kim, J., Shin, K., Seo, Y., “Synergistic Hydrate Inhibition of Monoethylene Glycol with Poly(vinylcaprolactam) in Thermodynamically Underinhibited System”, J. Phys. Chem. B, 118 (30), 9065–9075 (2014)

King Jr., H. E., Hutter, J. L., Lin, M. Y., Sun, T., “Polymeric conformations of gas-hydrate kinetic inhibitors: A small-angle neutron scattering study”, Journal of Chemical Physics, 112 (5), 2523-2532, (2000)

Klomp, U. C., WO Patent Application 99/13197 (1999)

Koh, C. A., Westacott, R. E., Zhang, W., Hirachand, K., Creek, J. L., Soper, A. K., “Mechansims of gas hydrate formation and inhibition”, Fluid Phase Equilibria, 194-197 pages 143-151 (2002).

Kvamme, B., Huseby, G., Førrisdahl, O. K., “Molecular dynamic simulation of PVP kinetic inhibitor in liquid water and hydrate/liquid water systems”, Mol. Phys. 90(6), 979-991, (1997)

Kvamme, B. “Molecular dynamics simulations as a tool for the selection of candidates for kinetic hydrate inhibitors”, Proceedings of the eleventh international offshore and polar engineering conference, Vol. 1, 517-527 (2001)

Kvamme, B., Kuznetsova, T., Aasolden, K., “Molecular dynamics simulation for selection of kinetic hydrate inhibitors”, Journal of Molecular Graphics and Modelling 23, 524-536, (2005)

Larsen, R., Knight, C. A., Sloan Jr., E.,D., “Clathrate hydrate growth and inhibition”, Fluid Phase Equilibria, 150-15, 353-360, (1998)

Lederhos, J. P., Long, J. P., Sum, A., Christiansen R. L., Sloan Jr., E. D., “Effective kinetic inhibitors for natural gas hydrates”, Chem. Eng. Sci., 51 (8) 1221-1229 (1996)

Lee, J. D.; Englezos, P., “Enhancement of the performance of gas hydrate kinetic inhibitors with polyethylene oxide”, Chem. Eng. Sci. (60) 5323-5330 (2005)

Leporcher, E. M., Fourest J. M., Labes-Carrier, C., Lompre, M., “Multiphase Transportation: A Kinetic Inhibitor Replaces Methanol to Prevent Hydrates in a 12-inc. Pipeline”, Paper 50683 presented at the SPE European Petroleum Conference, The Hague, The Netherlands, 20-22 October, (1998)

Lovell, D. and Pakulski, M., “Hydrate Inhibition in Gas Wells Treated With Two Low Dosage Hydrate Inhibitors” SPE Paper 75668 presented at Gas Technology Symposium, Calgary, (2002).

Makogon, T. Y. and Sloan Jr., E. D. “Mechanism of Kinetic Hydrate Inhibitors”, Proceedings of the 4th International Conference on Gas Hydrates, Yokohama, (2002)

Mali, G. A., Chapoy A., Tohidi, B., “Investigation into the effect of subcooling on the kinetics of hydrate formation”, Journal of Chemical Thermodynamics (2017)

Matthews, P. N., Subramanian, S., Creek J., “high Impact, Poorly Understood Issues with Hydrates in Flow Assurance”, Proceedings of the 4th International Conference on Gas Hydrates, Yokohama, (2002)

Mehta, A. P., Hebert, P. B., Cadena, E. R., Weatherman, J.P., “Fulfilling the Promise of Low-Dosage Hydrate Inhibitors: Journey From Academic Curiosity to Successful Field Implementation”, SPE Paper 81927, presented at the Offshore Technology Conference, Houston, 6-9 May (2002)

Mitchell, G. F. and Talley, L. D., “Application of Kinetic Inhibitor in Black-Oil Flowlines”, Paper 56770 presented at the SPE Annual Technical Conference and Exhibition, Houston, 3-6 October, (1999)

Moon, C., Taylor, P. C., Rodger, P. M., “Clathrate nucleation and inhibition from a molecular perspective”, Can. J. Phys. 81, 451-457 (2003)

Moon, C., Hawtin, R. W., Rodger, P. M., “Direct Molecular Simulation of Hydrate Nucleation” Proceedings of the Fifth International on Gas Hydrates, Trondheim, May 13-16, page 317 (2005).

Notz, P. K., Bumgardener, B. D., Schaneman, B. D., Todd, J. L. “Application of kinetic inhibitors to gas hydrate problems” *SPE production and facilities*, 250, November (1996)

Pakulski, M., Prukop,, G, Mitchell, C., “Field testing and commercial application of high efficiency non-polymeric gas hydrate inhibitor in offshore platforms” paper 49210 presented at the SPE Annual Technical Conference and Exhibition, New Orleans, 27-30 September, (1998)

Pakulski, M., Qu, Q., Pearcy, R., “Gulf of Mexico Deepwater Completion with Hydrate Inhibitors” SPE International Symposium on Oilfield Chemistry, 2-4 February, The Woodlands, Texas, 92971 (2005)

Peiffer, D. G., Costello, C. A., Talley, L.D., Wright, P. J., “Method for Inhibiting Hydrate Formation” US Patent No. 6,194, 622 (2001).

Phillips, N.J., Grainger, M., “Development and Application of Kinetic Hydrate Inhibitors in the North Sea”, SPE Gas Technology Symposium, Calgary, 15-18 March, 40030 (1998)

Rithauddeen, M. A., Al-Adel, S., “The Challenges of Qualifying a Kinetic Hydrate Inhibitor for an Offshore Sour Lean Gas Field”, 9th North American Conference on Multiphase Technology, Banff, 11-13 June, BHR-2014-F1 (2014)

Rosen, S. L., “Fundamental Principles of Polymeric Materials”, Wiley (1993).

Sloan Jr., E.,D., “Method for controlling clathrate hydrates in fluid systems”, US Patent No. 5,420,370 (1995)

Sloan Jr., E.,D., Submaranian, S., Matthews, P. N., Lederhos, J. P., Khokhar, A. A., “Quantifying Hydrate Formation and Kinetic Inhibition”, Ind. Eng. Chem. Res., 37, 3124-3132, (1998)

Souza, W. F. and Freitas, A. M. “Dynamic Simulations on Inhibition of Methane Hydrate Formation- An Investigation of the Interaction between Individual Functionalities of Kinetic Inhibitors and a Single 51262 Cavity”, Proceedings of the Fourth International Conference on Gas Hydrates, Yokohama, May 19-23 (2002)

Storr, M. T. and Rodger, P. M. “A Molecular Dynamics Study of the Mechanism of Kinetic Inhibition”, Annals of the New York Academy of Science 912, 669-677, (2000)

Storr, M.T., Monfort, J-P., Taylor, P.C., Rodger, P. M., “Natural Gas hydrates Stability with Inhibitors”, Proceedings of the Fourth International on Gas Hydrates, May 19-23, Vol 1, 504-508 (2002).

Storr, M. T., Taylor, P. C., Monfort, J., Rodger, P. M., “Kinetic Inhibitor of Hydrate Crystallization”, J. Am. Chem. Soc., 126, 1569-1576 (2004)

Subramanian, S., Sloan, E. D., “Solubility Effects on Growth and Dissolution of Methane Hydrate Needles”, Proceeding of the Fourth International Conference on Gas Hydrates (2002)

Svartaas, T.M., Kelland, M.A., Dybvik, L., “Experiments Related to the Performance of Gas Hydrate Kinetic Inhibitors”, Annals of the New York Academy of Sciences 912, 744-752, (2000)

Szcymczak, S., Sanders, K., Pakulski, M., Higgins T., “Chemical Compromise: A Thermodynamic and Low-Dosage Hydrate-Inhibitor Solution for Hydrate in the Gulf of Mexico”, SPE Annual Technical Conference and Exhibition, 9-12 October, Dallas, Texas, Paper 96418 (2005)

Talley, L. D. and Mitchell, G. F. “Application of proprietary kinetic hydrate inhibitors in gas flowlines” paper OTC11036 presented at the Offshore Technology Conference, Houston, 3-6 May (1999)

Smith, W., Todorov, I.T. “A short description of DL POLY”, Mol. Sim. 32 (12), pages 935–943 (2006)

Wise, M., Chapoy, A., Burgass, R. “Solubility Measurement and Modeling of Methane in Methanol and Ethanol Aqueous Solutions”, J. Chem. Eng. Data 61 (9) (2016)

Yang, J., Description of experimental work as part of Flow Assurance: Micro and Macro-Scale Evaluation of Low Dosage Hydrate Inhibitors JIP (2005)

Yang, J., Tohidi, B., “Characterization of inhibition mechanisms of kinetic hydrate inhibitors using ultrasonic test technique” Chemical Engineering Science, Volume 66, Issue 3, 1 Pages 278–283 (2011)

Yousif, M. H., “The kinetics of hydrate formation”, SPE Paper 28479, presented at the 69th Annual Technical Conference, New Orleans, 25-28 September (1994)

Zeng, H., Walker, V. K., Ripmeester, J. A. “Examining the classification of low dosage hydrate inhibitors”, Proceedings of the Fifth International on Gas Hydrates, Trondheim, May 13-16, (2005)

Appendix A: Investigation into the effect of subcooling on the kinetics of hydrate formation

ARTICLE IN PRESS

J. Chem. Thermodynamics xxx (2017) xxx–xxx

Contents lists available at ScienceDirect

J. Chem. Thermodynamics

journal homepage: www.elsevier.com/locate/jct

Investigation into the effect of subcooling on the kinetics of hydrate formation

Gwyn Ardeshir Mali [a,b], Antonin Chapoy [b,c,*], Bahman Tohidi [b]

[a] Chevron North America Exploration & Production Company, United States
[b] Hydrates, Flow Assurance & Phase Equilibria Research Group, Institute of Petroleum Engineering, Heriot-Watt University, Edinburgh, Scotland, UK
[c] Mines Paristech, CTP – Centre Thermodynamique des procédés, 35 rue St Honoré, 77305 Fontainebleau, France

ARTICLE INFO

Article history:
Received 29 May 2017
Received in revised form 7 August 2017
Accepted 8 August 2017
Available online xxxx

Keywords:
Gas hydrates
Kinetics
Induction time

ABSTRACT

A novel multi-test tube rocking cell unit has been used to generate large amounts of data to investigate the relationship between gas hydrate formation induction time and subcooling. The experiments included tests to determine the induction time for a natural gas and water system at a wide range of pressures and subcooling. Over 500 induction times were measured at pressure ranging from 2 to 17 MPa. The statistical analysis of the results shows that the commencement of hydrate growth is logarithmically related to subcooling, and that the scatter of the onset of hydrate growth is greater at higher subcooling. It was also shown that the induction time for hydrate growth was lower at higher pressures at similar levels of subcooling.

1. Introduction

Gas hydrates or clathrate hydrates are ice like crystalline structures that are composed of hydrogen bonded water molecules in cage like structures, which contain guest molecules that occupy the cages, which stabilize the crystal structures [1]. In the petroleum industry, gas hydrates pose flow assurance issues to oil and gas pipelines as they can form in natural gas systems at typical temperatures and pressures encountered in many offshore and onshore pipelines. Clathrates of natural gas are also naturally present in permafrost and in the ocean and have been investigated for exploitation as an energy resource [2], or as a potential geohazard [3]. Other investigations have looked into the use of hydrates as a medium for use in water desalination [4], natural gas storage/-transportation [5], and carbon dioxide capture and sequestration [6,7].

The kinetics of hydrate nucleation and growth has been a subject of research that started in the beginning of the 1960s [8]. The most significant contribution to the area of research has been by Raj Bishnoi and his group, which was based on semi-batch continuous-state stirred reactors that measured the molar consumption of guest molecules [9–14]. The kinetics work identified three distinct regions; the first step called "dissolution" involves the dissolution of the gas with the guest molecules across the vapor-liquid water interface into the aqueous phase. The next step called the "induction period" involves a time period where the super-saturated aqueous phase has hydrate crystal structures forming and decomposing until a stable hydrate nuclei are formed. The last step is called "hydrate growth" where the previously formed nuclei grow, consuming the hydrate forming gases and increase the turbidity of the test solution due to the presence of solid hydrate crystals. The diffusion of hydrate formers to the aqueous phase is a key factor in the dissolution and hydrate growth stages of hydrate formation kinetics, which is itself a function of the interfacial area and mass transfer coefficient. Interfacial area and mass transfer coefficient are both strongly dependent on degree of agitation and the equipment used, as such, experimental equipment and operation impact the kinetic of hydrate formation, which makes it difficult to compare data between different research groups. Bishnoi's and several other groups [15–21] have subsequently conducted experimental tests and generated empirical based models for hydrate growth kinetics, all of which that have limitations to their use. An overview of the state of the art in hydrate kinetic modelling is comprehensively described by Ribeiro and Lage (2008) [22].

The major limitation into the prediction of hydrate kinetics is the stochastic nature of nucleation during the induction period, which requires large amounts of data to make any quantitative or qualitative conclusions, and studies to investigate the stochastic behaviour in the open literature is limited, particularly at high

* Corresponding author at: Hydrates, Flow Assurance & Phase Equilibria Research Group, Institute of Petroleum Engineering, Heriot-Watt University, Edinburgh, Scotland, UK.
E-mail address: a.chapoy@hw.ac.uk (A. Chapoy).

http://dx.doi.org/10.1016/j.jct.2017.08.014
0021-9614/

pressures. This study's objective is to investigate the statistical properties of the stochastic nature of gas hydrate induction. The investigation involves the measurement of the hydrate induction time for a natural gas with water over a wide range of pressures using a novel setup that enables the generation of large amounts of data.

2. Experimental

2.1. Experimental materials

The composition of the multi-component gas mixture as measured by GC is given in Table 1. Deionised water was used in all tests.

2.2. Equipment

A Multi Test Tube Rocking Cell (MTTRC) testing unit developed by Heriot Watt University was used for the experiments. Schematics of the set-up used for the solubility study is shown in Fig. 1.

The experimental set-up used consists of ten identical equilibrium cells, cryostat, rocking/pivot mechanism, and temperature/-pressure recording equipment controlled by a PC. The ten equilibrium cells are (maximum effective volume of 10 ml), titanium cylindrical pressure vessel with mixing ball. The cells are held into the same cooling/heating jacket, this jacket is mounted on a horizontal pivot with associated stand for pneumatic controlled rocking through 180 degrees. Rocking of the system, and the subsequent movement of the mixing ball within the equilibrium cells, ensures adequate mixing of the cell fluids. For the tests reported here, the cell was rocked through 180 degrees at a rate of 8 times per minute.

Table 1
Composition of test natural gas.

Component	X	U(x)
N2	0.015	0.0003
CO2	0.0116	0.0002
C1	0.8890	0.018
C2	0.0614	0.0012
C3	0.016	0.0003
iC4	0.002	0.0001
nC4	0.003	0.00015
iC5	0.001	0.00005
nC5	0.001	0.00005

The rig has a working temperature range of 253.15–323.15 K, with a maximum operating pressure of 40 MPa. System temperature is controlled by circulating coolant from a cryostat within a jacket surrounding the cell. The cryostat is capable of maintaining the cell temperature stability to within better than 0.05 °C. To achieve good temperature stability, the jacket is insulated with polystyrene board, while connecting pipe work is covered with plastic foam. The temperature is measured and monitored by means of three PRTs (Platinum Resistance Thermometers) located within the cooling jacket of the cell, which were calibrated regularly against a Prema 3040 precision thermometer. Cell temperature can be measured with an accuracy of 0.1 K. Ten pressure transducer with an accuracy of 0.01 MPa were used to monitor pressure of each individual cells. Temperatures and Pressures are monitored and recorded by the PC through an RS 232 serial port.

2.3. Procedures

For all tests, the cells were first cleaned and vacuumed at temperature well outside the predicted hydrate stability (303.15 K). 5 ml of distilled water was then introduced into each test-tube cell and pressurised with natural gas with the composition shown in Table 1 to the specified pressure. The rocking system was then switched on, which rotates the cells 180° every 9 s. The temperature of the thermostat bath is then set to the desired temperature. The pressure from each test tube, and the coolant temperature in the jacket were measured and logged on a PC. Multiple runs were conducted for each solution with heating of 303 K for at least 1 day to remove hydrate history. The onset of hydrate formation is detected by monitoring the change in the pressure.

Tests were conducted at 6 different pressures of 1.72, 2.76, 6.21, 6.89, 10.34 and 17.24 MPa (250, 400, 900, 1000, 1500 and 2500 psia) with subcoolings from 3.2 K to 8.0 K (Fig. 2). A total of 500 induction time run were carried out. The subcooling was calculated using our in-house thermodynamic package [23–25], the model was previously validated for similar natural gases [26,27]. The subcooling is defined at the difference in temperatures between the predicted three phase equilibrium temperature (the temperature on the hydrate phase boundary) and the temperature of hydrate

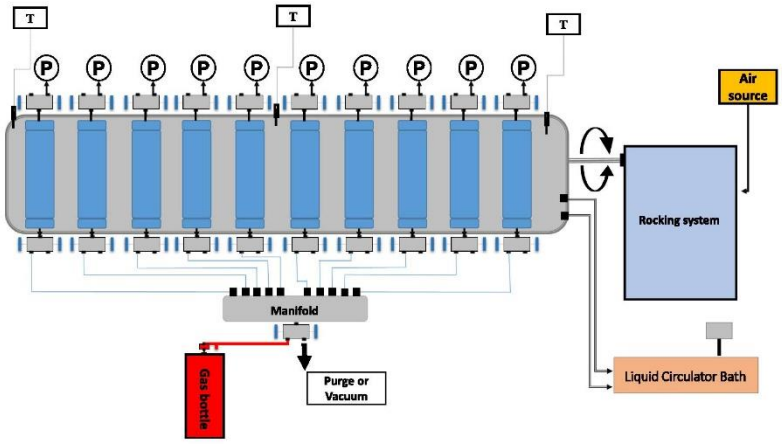

Fig. 1. Schematic of the multi-test-tube rocking cell.

Please cite this article in press as: G.A. Mali et al., J. Chem. Thermodyn. (2017), http://dx.doi.org/10.1016/j.jct.2017.08.014

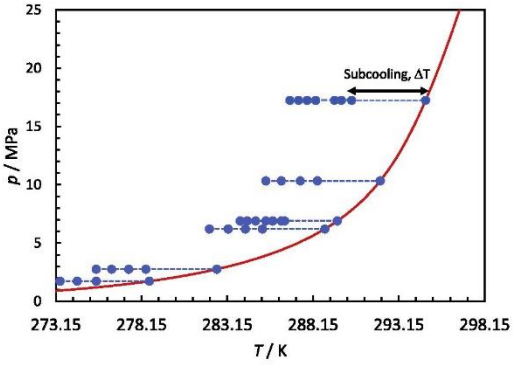

Fig. 2. Predicted hydrate stability zone (red lines) of the natural gas (composition given in Table 1). ●: test temperature and pressure. (For interpretation of the references to colour in this figure legend, the reader is referred to the web version of this article.)

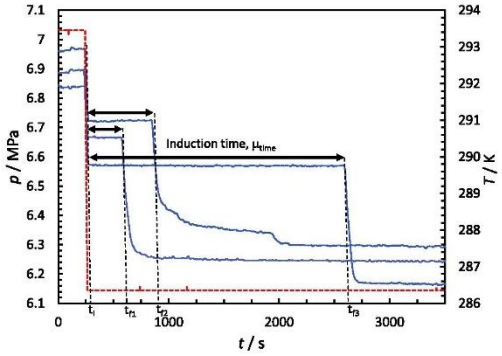

Fig. 3. Illustration of temperature, T, and pressure change in pressure (p) associated with hydrate formation as a function of time, t (blue traces: pressure; red dotted lines: temperature profile). Induction times in these experiments are determined as the period between the initial time, t_i, when system reach equilibrium for a given subcooling, and the time where hydrate formation is first observed, t_f, typically from a drop in system pressure (Δp).

onset, the set temperature. A typical run is shown in Fig. 3 for three test tubes. In this work the induction time is defined as the time difference between the time when the system reached equilibrium at the set temperature and the time when hydrate forms (if hydrates form before reaching the set temperature, the induction time is set to zero).

3. Results

The analysis of the results involves the use of two parameters; the arithmetic mean (μ), and the standard deviation (σ). A normalised value for standard deviation ($\sigma_{normalized}$) is also used to remove the magnitude associated with the standard deviation term, which allows comparison between the populated data at different subcooling. The equations for these terms can be seen below:

$$\mu = \frac{1}{N}\sum_{i=1}^{N} x_i$$

Table 2
Results of distilled water and natural gas to investigate impact of subcooling on arithmetic mean and standard deviation for the mean induction time.

T/K[a]	Subcooling ΔT/K	μ_{time}/min	σ_{time}/min	σ/μ
1.72 MPa (250 psia)				
273.4	5.50	23	30	1.33
274.4	4.50	38	23	0.61
275.5	3.40	268	192	0.72
2.76 MPa (400 psia)				
275.5	7.30	2	5	2.08
276.4	6.40	9	12	1.32
277.4	5.40	40	54	1.35
278.4	4.40	126	193	1.53
6.21 MPa (900 psia)				
282.1	6.90	22	26	1.17
283.2	5.80	94	90	0.96
284.2	4.85	400	329	0.82
285.2	3.85	1175	1234	1.05
6.89 MPa (1000 psia)				
283.9	5.80	25	48	1.90
284.3	5.40	39	56	1.43
284.8	4.90	77	80	1.04
285.4	4.30	156	163	1.05
285.8	3.90	328	298	0.91
286.3	3.40	954	931	0.98
286.5	3.20	1906	1570	0.82
10.34 MPa (1500 psia)				
285.4	6.80	12	12	1.00
286.3	5.90	44	60	1.36
287.4	4.85	339	311	0.92
288.4	3.85	2413	1792	0.74
17.24 MPa (2500 psia)				
286.8	8.05	5	16	3.08
287.3	7.55	12	14	1.15
287.8	7.05	11	14	1.27
288.3	6.60	34	36	1.07
288.3	6.55	96	109	1.14
289.4	5.45	132	146	1.11
289.8	5.05	589	466	0.79
290.4	4.45	1312	1246	0.95

[a] u(T) = 0.1 K.
[b] u(P) = 0.01 MPa.

$$\sigma = \sqrt{\frac{1}{N}\sum_{i=1}^{N}(x_i - \mu)}$$

$$\sigma_{normalised} = \frac{\sigma}{\mu}$$

The summary of the results of the tests with distilled water and natural gas is shown in Table 2. Fig. 4 shows the mean induction times for the different pressures at varying levels of subcooling. Fig. 5 shows the mean induction times for the different pressures at varying levels of subcooling, with the lines of best fit.

4. Discussion

4.1. Subcooling

The raw experimental data is presented in Fig. 4 and the results show that the induction time for the natural gas and water system tested is very stochastic, which is aligned with previously reported experience by other researchers.

The cumulative distribution and the probability density curve of the data with similar subcooling is presented in Figs. 5 and 6 respectively. The results demonstrate that the scatter in induction time is higher at lower levels of subcooling than at higher levels of subcooling. Fig. 7 shows data representing the 90%, 95% and 98%

Please cite this article in press as: G.A. Mali et al., J. Chem. Thermodyn. (2017), http://dx.doi.org/10.1016/j.jct.2017.08.014

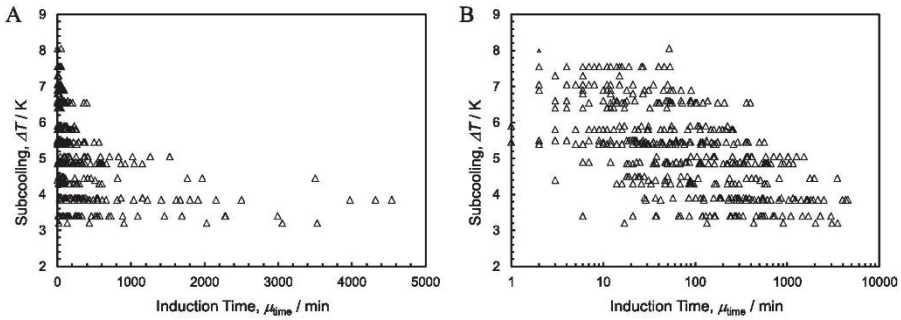

Fig. 4. All experimental induction time, μ_{time} of Natural Gas and water system.

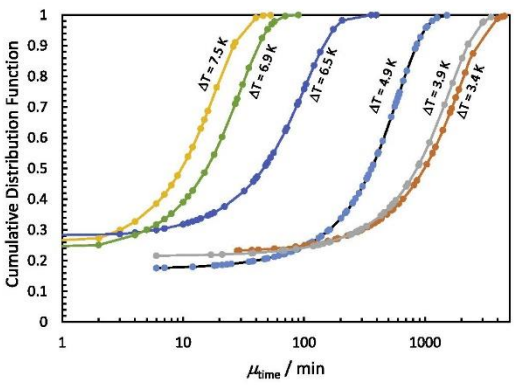

Fig. 5. Induction time μ_{time} cumulative distribution function.

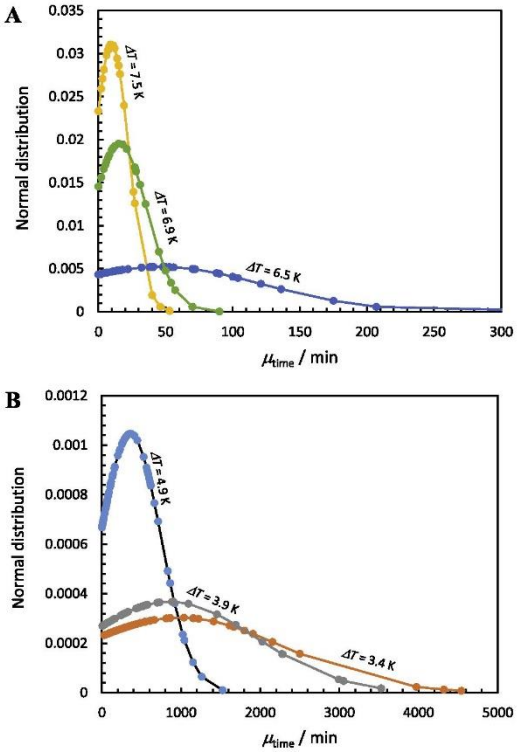

Fig. 6. Induction time probability density function.

induction times (i.e. induction time when 90%, 95% and 98% of the samples have formed hydrates), for the three probability the induction clearly follow an exponential behaviour with the subcooling. Fig. 8 is a plot of the data with the addition of the mean induction times for the tests with similar pressure, and Fig. 9 presents the lines of best fit of the data. The results demonstrate that under the same pressures, induction time is logarithmically related to subcooling.

4.2. Pressure

As seen in Fig. 9, the mean values of induction time reduces as the subcooling increased due to the greater thermodynamic driving force to form the hydrates. Although there is some scatter in the data, it is also apparent that the hydrates also form quicker at lower pressures at the same level of subcooling. The results show that there can be up to approximately 25 times increase in the average induction time due to a change in pressure from 1.72 to 172 MPa at the same level of subcooling.

To further explore the impact of pressure on induction time, Fig. 9 was created with the use of a straight line equation ($y = A \times \ln(x) + B$) with parallel lines (A constant) in a best fit relationship to the data. Fig. 11 is a plot of the data gathered from Fig. 10 in relation to the intersect B as a function of pressure. As can be seen there is a general trend with the intersect B increasing with increasing pressure. This suggests that increasing pressure has a near linear effect of increasing induction time. The exception to this data is the 6.21 MPa (900 psia) data set, which does not follow the trend (blue on the figure). This may be attributable to experimental method, such as the presence of nucleus forming particles in that test sample.

The results presented align with the findings of Arjmandi et al. (2005) [28] that demonstrated that a change in pressure impacts induction time with similar subcooling. One of the conclusions of the work was that the Gibbs free energy term or $-G/RT$ should be used in comparing kinetic studies at different pressure conditions.

Please cite this article in press as: G.A. Mali et al., J. Chem. Thermodyn. (2017), http://dx.doi.org/10.1016/j.jct.2017.08.014

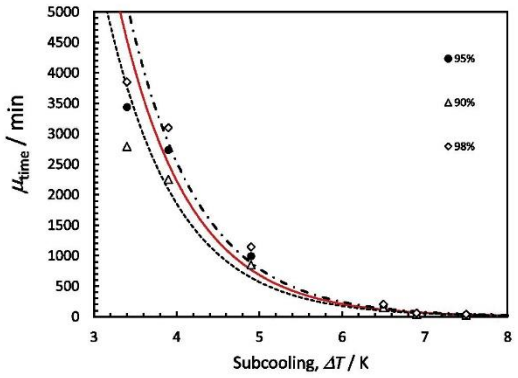

Fig. 7. 90, 95 and 98% induction time vs subcooling.

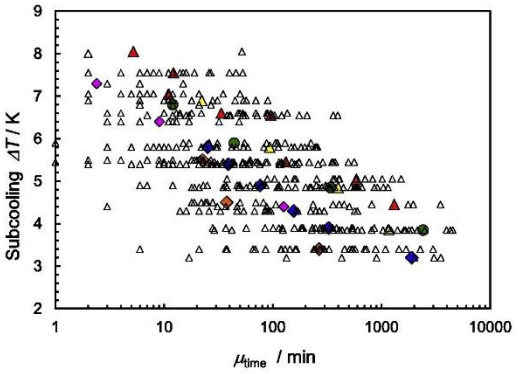

Fig. 8. Mean induction time, μ_{time} as a function of pressure and subcooling, ΔT (Δ: all data; ◆: mean induction at 1.72 MPa, ◆: at 2.76 MPa, ▲: 6.21 MPa, ◆: 6.89 MPa, ●: 10.34 MPa and ▲ 17.24 MPa) (Note: 0 min induction time forming systems (systems forming hydrates before reaching the target temperature) are not shown on the figure).

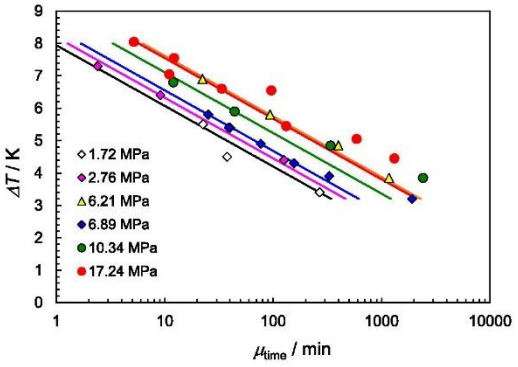

Fig. 9. Mean induction time, μ_{time} as a function of pressure and subcooling. (Data were correlated in the form of $\Delta T = A \times \ln(\mu_{time}) + B$).

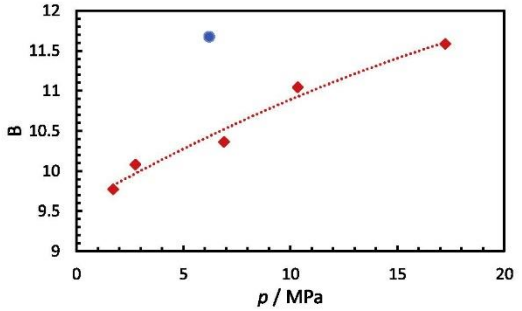

Fig. 10. Intersection values of the parallel straight lines as a function of pressure.

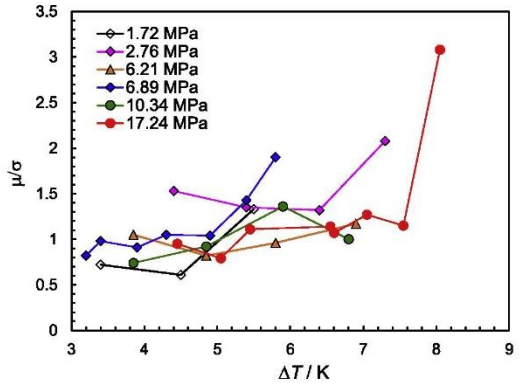

Fig. 11. Normalised standard deviation versus subcooling.

Fig. 11 shows the normalised standard deviation for the different pressures at varying levels of subcooling. It is apparent from the data that the standard deviation (normalised) generally increases with subcooling. The implication is that there is more reproducibility of measured induction time and less stochasticity at higher subcooling, and less so at lower subcooling.

5. Conclusions

The nature of the tests carried out with the multi test tube rocking cell lends itself to the generation of large volumes of data, enabling researchers to make statistical analyses and make meaningful conclusions with a reasonable degree of certainty.

The results presented show that induction time is logarithmically related to subcooling for a natural gas and distilled water system. The results also showed that an increase in pressure at the same subcooling increases the average induction time, which is broadly in agreement with previously published work [28]. Additionally, the results show that the scatter in induction time is smaller at higher levels of subcooling.

The impact of pressure on induction time at similar subcooling is attributed to the relative subcooling change not being equivalent to the relative driving force change. The result of this conclusion is that the driving force term and not subcooling should be used for comparing kinetic tests at different pressures.

Please cite this article in press as: G.A. Mali et al., J. Chem. Thermodyn. (2017), http://dx.doi.org/10.1016/j.jct.2017.08.014

References

[1] E.D. Sloan, C.A. Koh, Clathrate Hydrates of Natural Gases, third ed., CRC Press, 2007.
[2] Y.F. Makogon, Natural gas hydrates – a promising source of energy, J. Nat. Gas Sci. Eng. 2 (1) (2010) 49–59.
[3] M. Maslin, M. Owen, R. Betts, S. Day, T.D. Jones, A. Ridgwell, Gas hydrates: past and future geohazard?, Philos Trans. R. Soc. A 368 (1919) 2010.
[4] J.S. Sangwai, R.S. Patel, P. Mekala, D. Mech, M. Busch, Desalination of Seawater using Gas Hydrate Technology- Current Status and Future Direction, in: Proceedings of Hydro 2013 Internationsl, IIT Madras, Chennai, 2013, pp. 4–6.
[5] F. Ahmadloo, G. Mali, A. Chapoy, B. Tohidi, Gas Separation and Storage using Semi-Clathrate Hydrates, in: Proceedings of the 6th International Conference on Gas Hydrates (ICGH 2008), Vancouver, July 6–10 (2008).
[6] P. Linga, A. Adeyemo, P. Englezos, Medium-pressure clathrate hydrate/membrane hybrid process for post combustion capture of carbon dioxide, Environ. Sci. Technol. 42 (2007) 315–320.
[7] B. Castellani, M. Filipponi, A. Nicolini, F. Cotana, F. Rossi, Carbon dioxide capture using gas hydrate technology, J Energy Power Eng. 7 (2013) 883–890.
[8] K. Levkam, P. Ruoff, Kinetics and mechanism of methane hydrate formation and decomposition in liquid water Description of hysteresis, J. Cryst. Growth 179 (1997) 618–624.
[9] A. Vysniauskas, P.R. Bishnoi, A kinetic study of methane hydrate formation, Chem. Eng. Sci. 38 (1983) 1061.
[10] A. Vysniauskas, P.R. Bishnoi, Kinetics of ethane hydrate formation, Chem. Eng. Sci. 40 (2) (1985) 299.
[11] P. Englezos, N. Kalogerakis, P.D. Dholabhai, P.R. Bishnoi, Kinetics of Formation of Methane and Ethane Gas Hydrates, Chem. Eng. Sci. 42 (1987) 2647.
[12] V. Natarajan, P.R. Bishnoi, N. Kalogerakis, Induction Phenomena in Gas Hydrate Nucleation, Chem. Eng. Sci. 49 (1994) 2075.
[13] P.R. Bishnoi, N. Kalogerakis, Induction phenomena in gas hydrate nucleation, Chem. Eng. Sci. 49 (1994) 2075–2087.
[14] J.S. Parent, P.R. Bishnoi, Investigations into the nucleation behaviour of natural gas hydrates, Chem. Eng. Commun. (CEC) 144 (1996) 51–64.
[15] P. Skovborg, P. Rasmussen, A mass transport limited model for the growth of methane and ethane gas hydrates, Chem. Eng. Sci. 49 (8) (1994) 1131–1143.
[16] M. Mork, J.S. Gudmundsson, Hydrate Formation Rate in a Continuous Stirred Tank Reactor: Experimental Results and Bubble-to-Crystal Model, in: Proceedings of the Fourth International Conference on Gas Hydrates, Yokohama, 813–818 (2002).
[17] S. Hashemi, A. Macchi, P. Servio, Dynamic Simulation of Gas Hydrate Formation in an Agitated Three-Phase Slurry Reactor, in: 2007 ECI Conference on The 12th International Conference on Fluidization - New Horizons in Fluidization Engineering, Vancouver, pp. 329–336. (2007).
[18] S. Hashemi, A. Macchi, P. Servio, Gas hydrate growth model in a semibatch stirred tank reactor, Ind. Eng. Chem. Res. 46 (2007) 5907–5912.
[19] M.H. Yousif, "The kinetics of hydrate formation", SPE Paper 28479, presented at the 69th Annual Technical Conference, New Orleans, 25-28 September (1994).
[20] R.L. Christiansen, E.D. Sloan, "A compact model for hydrate formation", in: Proceedings of the 74th GPA Annual Convention, San Antonio, Texas, 15–21 March (1995).
[21] R.L. Christiansen, V. Bansal, E.D. Sloan, "Avoiding Hydrates in the Petroleum Industry: Kinetics of Formation", in: SPE Paper 27994, University of Tulsa Centennial Petroleum Engineering Symposium, Tulsa, 29-31 August, (1994).
[22] C.P. Ribeiro, P. Lage, Modelling of hydrate formation kinetics: State-of-the-art and future directions, Chem. Eng. Sci. 63 (8) (2008) 2007–2034.
[23] A. Chapoy, H. Haghighi, R. Burgass, B. Tohidi, On the phase behaviour of the (carbon dioxide+water) systems at low temperatures: experimental and modelling, J. Chem. Thermodyn. 47 (2012) 6–12.
[24] A. Chapoy, M. Nazeri, M. Kapateh, R. Burgass, C. Coquelet, B. Tohidi, Effect of impurities on thermophysical properties and phase behaviour of a CO 2-rich system in CCS, Int. J. Greenhouse Gas Control 19 (2013) 92–100.
[25] H. Haghighi, A. Chapoy, R. Burgess, B. Tohidi, Experimental and thermodynamic modelling of systems containing water and ethylene glycol: Application to flow assurance and gas processing, Fluid Phase Equilib. 276 (1) (2009) 24–30.
[26] A. Chapoy, B. Tohidi, Hydrates in high inhibitor concentration systems, GPA Res. Rep. 205 (2010).
[27] H. Najibi, A. Chapoy, B. Tohidi, Methane/natural gas storage and delivered capacity for activated carbons in dry and wet conditions, Fuel 87 (May) (2008) 7–13.
[28] M. Arjmandi, B. Tohidi, A. Danesh, A.C. Todd, Is subcooling the right driving force for testing low dosage hydrate inhibitors?, Chem Eng. Sci. 60 (2005) 1313–1321.

JCT 17-453

Please cite this article in press as: G.A. Mali et al., J. Chem. Thermodyn. (2017), http://dx.doi.org/10.1016/j.jct.2017.08.014